

A DIRECT APPROACH TO FREQUENCY
SAMPLING FILTER DESIGN

By

B. N. SURESHBABU

Bachelor of Engineering
Bangalore University
Bangalore, India
1970

Master of Engineering
Bangalore University
Bangalore, India
1972

Submitted to the Faculty of the Graduate College
of the Oklahoma State University
in partial fulfillment of the requirements
for the Degree of
DOCTOR OF PHILOSOPHY
May, 1978

Thesis
1978 D
S96/d
cop. 2



A DIRECT APPROACH TO FREQUENCY
SAMPLING FILTER DESIGN

Thesis Approved:

Nav yanlayedee

Thesis Adviser

Craig S. Sims

P. P. P. Potes

J. P. Chandler

Bennett Basore

Norman N. Durham

Dean of the Graduate College

1016643

ACKNOWLEDGMENTS

I wish to express my sincere thanks and gratitude to Dr. Rao Yarlagadda, my thesis adviser and chairman of my doctoral committee, for his interest, guidance and encouragement during the entire phase of my graduate study. His dedicated approach to scientific problems and numerous suggestions was instrumental in writing this thesis. The interest and comments offered by Dr. R. P. Rhoten, Dr. C. S. Sims, and Dr. J. P. Chandler, members of my doctoral committee, are appreciated.

Special thanks are due to Dr. J. P. Chandler for his advice and help with regard to the computer programs. The financial support from the School of Electrical Engineering, Oklahoma State University, is acknowledged. I am grateful to Ms. Charlene Fries for her excellent typing of this thesis.

Finally, I want to dedicate this thesis to my parents for making it all possible.

TABLE OF CONTENTS

Chapter	Page
I. INTRODUCTION	1
1.1 Statement of the Problem	1
1.2 Review of the Literature	3
1.3 Organization of the Thesis	9
II. THE APPLICATION OF FFT TO THE SOLUTION OF A SYSTEM OF TOEPLITZ NORMAL EQUATIONS	10
2.1 Introduction	10
2.2 Normal Equations Using Symmetric Circulants	19
2.3 Digital Filter Design by Discrete Convolution and by the Frequency Sampling Technique-- a Relationship	23
2.4 Summary	26
III. A DIRECT APPROACH TO THE FREQUENCY SAMPLING FILTER DESIGN	28
3.1 Introduction	28
3.2 Basic FIR Design Problem	28
3.3 Method of Design	30
3.4 Direct Approach to the Frequency Sampling Filter Design With Two and Three Transition Samples	59
3.5 Bandpass Filter Design	86
3.6 Ripple Reduction in the Passband	95
3.7 High-Pass Filter Design	100
3.8 Summary	107
IV. SUMMARY AND SUGGESTIONS FOR FURTHER STUDY	109
4.1 Summary	109
4.2 Suggestions for Further Study	111
BIBLIOGRAPHY	113
APPENDIX A - COMPUTATION OF FREQUENCY RESPONSE OF FIR FILTERS	118
APPENDIX B - COMPUTATION OF TRANSITION SAMPLE VALUES	125

LIST OF TABLES

Table	Page
I. Transition Sample Values	45
II. Optimum Transition Sample Values	49
III. One Transition Sample Values	54
IV. Two Transition Sample Values	67
V. Modified "Transition Sample Values"	71
VI. Three Transition Sample Values	81
VII. Band Pass Filter Design--One Transition Sample Values . . .	90
VIII. Band Pass Filter Design--Two Transition Sample Values . . .	91
IX. Band Pass Filter Design--Three Transition Sample Values . .	93
X. Transition Sample Values (Pass Band)	101
XI. High-Pass Filter Design (One Transition Sample Values) . . .	107

LIST OF FIGURES

Figure	Page
1. Specifications for a Low-Pass Filter	32
2. Variation of Stopband Frequency Response as a Function of Transition Sample $H_{\ell-1}^{(1)}$ (Enlarged Scale)	34
3(a). Ripple Reduction in the Stopband When Transition Sample is Optimum	39
3(b). Stopband Response When Transition Sample is One	40
3(c). Stopband Response When Transition Sample is One (to an Enlarged Scale, N-Even)	41
3(d). Stopband Response for N-Even, $M = 1$, and for $N/4 < BW < N/2$ (Enlarged Scale)	42
4. Plot of $\beta(t)$ Around a Step Discontinuity	47
5. Two Cases of Linear Phase Filters	55
6. Frequency Response of a Low-Pass Filter for Values of $H_{\ell-1}^{(0)}$ and $H_{\ell-1}^{(R)}$	57
7(a). Frequency Response for Two Transition Samples	61
7(b). Stopband Response for Two Transition Samples (Enlarged Scale)	62
7(c). Stopband Response for Two Transition Samples (to an Enlarged Scale, N-Even)	63
8(a). Stopband Frequency Response for Three Transition Samples Derived From Figure 1	73
8(b). Stopband Response for Three Transition Samples (Enlarged Scale)	74
8(c). Stopband Response for Three Transition Samples (to an Enlarged Scale, N-Even)	75
9. Frequency Response of a Low-Pass Filter	79

Figure	Page
10. Typical Specifications of a Digital Bandpass Filter.	87
11. Frequency Response of a Bandpass Filter.	96
12. Variation of Passband Response as a Function of Transition Sample.	98
13. Frequency Response of a High-Pass Filter	103
14. Variation of Stopband Response of a High-Pass Filter as a Function of Transition Sample.	104

CHAPTER I

INTRODUCTION

1.1 Statement of the Problem

A digital filter in broad terms is any device which accepts a sequence of numbers as its input and operates on them to produce another sequence as its output. Because of the above generality, digital filters have been used, and shall continue to be in use, in a wide variety of disciplines. Historically, the digital filter theory was developed in the 1940s in connection with the sampled-data control systems. With the advent of digital computers digital filter theory gained added importance. In recent years the special purpose digital computers are used to do digital spectral shaping, wave form synthesis and to perform digital filtering operations. With the development of integrated circuit technology, the digital hardware can be designed in integrated form with low cost and high speed of operation. Recently, the digital filters are being used in many applications, where analog filters have been used traditionally.

Some of the advantages of the digital filters over the analog filters are the following:

1. The analog components cannot be easily made to a tolerance of less than about one percent. The inaccuracies of digital filters, which are due to rounding errors in the computer arithmetic, can be made small.
2. A digital filter can be implemented by programming on a computer

to meet the desired characteristics. The alteration of a digital filter design involves, at most, rewriting of a section of a program code or often merely the reading-in of a different set of filter coefficients as data.

3. The characteristics of a digital computer program remain the same each time it is run, regardless of variations in main supply voltage, ambient temperature, and so on. Analog components suffer from aging. The effects of drift in analog components can appear as spurious signals.

4. Digital filters can be time shared.

Among the disadvantages of digital circuits are that they use finite-precision arithmetic, which in turn induces noise by quantization and computation round-off.

Basically, there are two types of digital filters, recursive and nonrecursive. A nonrecursive filter has no feedback paths. The unit impulse response of a nonrecursive filter is of finite duration and is usually referred to as finite impulse response filter (FIR filter). On the other hand, a recursive filter has feedback structure and usually has infinite impulse response.

Tapped delay line filters are used extensively in radar, in digital radio communications, and in telephony. With the advancement of surface wave technology, transversal filters can be designed using low-dispersion acoustic delay lines (1).

Recently, there has been a good deal of interest in FIR filters as they can always be realized and are always stable. In addition, they can be designed such that they have linear phase characteristics. The problem of instability due to coefficient truncation cannot arise in FIR

filters. Also, the effect of spurious input such as switching transient disappears completely after a finite length of time. Long sequences are sometimes necessary to achieve sharp cutoff filters. With the advent of fast Fourier transform (FFT), such filters have become very attractive and computationally efficient, and are even comparable to the design of infinite-duration impulse response (IIR) elliptic filters. The insight gained in the design of FIR filters can be applied to other related topics such as phased array antenna patterns, spectral estimation, etc.

Basically, recursive filters are designed using classical analog filter approximations, such as Butterworth, Chebyshev, elliptic filter approximations. This thesis is mainly concerned with FIR filters and therefore the recursive filters are not discussed further.

Comparatively, the FIR filter design is more indirect. However, research is being done at the present time to obtain simple and direct techniques for designing FIR filters. The FIR filters have a significant role in the area of deconvolution also. The deconvolution problem, in general, requires the solution of a set of Toeplitz normal equations of the form

$$A_{\text{Toe}}x = y \quad (1.1)$$

where A_{Toe} is a symmetric Toeplitz matrix.

This thesis presents a direct approach to the FIR filter design problem along with the solution of Toeplitz normal equations using fast Fourier transforms.

1.2 Review of the Literature

There are various techniques available for solving a system of normal equations given in Equation (1.1). Levinson (2) presented an

elegant recursive algorithm to solve a system of normal equations. The same problem was reformulated by others (3). Another method which is twice as fast as that of Levinson's is that by Durbin (4). Recently, Trench (5) has presented some interesting results on the inversion of Toeplitz matrices. In some cases the formulas for the first row and column of the inverse of the Toeplitz matrices are given. There are other special cases where the inverse can be given explicitly (6) (7) (8). In addition to these, there are other works which include some detailed survey articles (9) through (12). A tutorial discussion on this subject can be found in Reference (13). Wang and Treitel (14) discussed the solution of a system of normal equations using gradient methods. More recently, Rino (15) proposed an inversion scheme for scalar covariance matrices, which in turn can be considered as a special case of Toeplitz forms. Ekstrom (16) used an iterative improvement method to find an approximate solution of vector Toeplitz systems. The above method uses the special structure of Toeplitz matrices.

The design of FIR filters involves the selection of $h(kT)$, the filter weights, in the z-domain transfer function

$$H(z) = \sum_{k=0}^{N-1} h(kT)z^{-k} \quad (1.2)$$

such that $H(z)\Big|_{z=e^{j\omega T}} = H(e^{j\omega T})$ satisfies the given magnitude and/or phase specifications. Hereafter, $T = 1$ for simplicity. Noting the periodicity of $H(e^{j\omega})$, one method of design is to expand the given filter specifications by Fourier series and truncate the series to a desired length (17) through (20). This method creates problems when approximating functions which have discontinuities. This problem is referred to in the

literature as the Gibbs phenomenon (21). A better way of obtaining FIR filters is to modify the Fourier coefficients by using a finite weighting sequence called a window. There are various types of windows available. These include Fejer window (22), Hamming window (22), Kaiser window (17), Dolph-Chebyshev window (18), etc. Each one has its own advantages and disadvantages. The window design is an analytical method and does not involve any iterative techniques. In the window function design, the tradeoff between ripple suppression and a transition bandwidth for a given N in Equation (1.2) is an important parameter. At the present time, Kaiser window and Dolph-Chebyshev window are perhaps the most popular windows. This is due to the fact that the designer can have control over both the transition width and the ripple amplitudes. One of the basic problems with window techniques is smearing (23). Other problems are that the closed form expression for $h(kT)$ in Equation (1.2) may not be available.

A second method of design of FIR filter is the frequency sampling technique (23 through 32). Gold and Jordan (26) first proposed this method and it was later developed by Rabiner et al. (27). The frequency sampling method is based on the idea that a desired frequency response can be approximated by sampling it at N equally spaced points, and then obtaining an interpolated frequency response that passes through the frequency sampled points. For filters with smooth frequency responses the interpolation error is small. The frequency samples which occur in passbands and stopbands are set to a specified value and those in the transition bands are unspecified and to be determined to satisfy the specifications. These unspecified values are usually chosen by an optimization algorithm which minimizes the weighted approximation error

over the frequency range of interest. Mini-max approximation is normally desired. These methods, in general, are not efficient, when there are more than four transition samples. Recently, linear programming has been used and found that it overcomes some of these difficulties (33) (34).

A third technique for designing FIR filters is first proposed by Herrmann (35). The filter response is assumed to be equiripple both in the passband and stopband. Also, the number of ripples in both passbands and stopbands are fixed a priori. The design is carried out by constraining the equiripple frequency characteristic by means of a set of nonlinear equations. The unknown quantities are the filter coefficients and the frequencies at which the extrema occur. When N is odd, for example, the unknown quantities are the $(\frac{N+1}{2})$ filter coefficients and $(\frac{N-3}{2})$ set of frequencies at which extrema of the approximation error occur. By imposing constraints on the extrema and on the derivatives, a system of $(N-1)$ nonlinear equations will result with $(N-1)$ unknowns and these are solved using an iterative descent method. Owing to the numerical difficulties of solving nonlinear equations, the maximum length of the filter that has been solved is limited to 40. Even though this method gives the narrowest transition region for a given order of the filter, the choice of cutoff frequency is still a problem.

The above method is extended by Hofstetter et al. (36) (37). In this method an iterative technique is used to derive a trigonometric polynomial which has the extrema at the desired frequencies. The classical Lagrange interpolation method is used to derive the coefficients of the polynomial at each iteration. It has been shown that the method converges to an equiripple approximation (36). The main drawback of this method is that it is not possible to specify the location of the

passband, stopband and transition band edges a priori. It has been shown that the filters designed by the above approach are of extraripple type (24).

In order to get a precise control over the locations of the edges of the passband and stopband for a given size of the filter, it is well known that the passband ripple and the stopband attenuation has to be a free design parameter. Parks and McClellan (38) have shown that the low-pass filter design can be formulated over disjoint sets as a Chebyshev approximation problem. Also, they have shown that the necessary and sufficient conditions for the best Chebyshev approximations can be obtained from the alternation theorem. The filter coefficients are derived using the Remez exchange algorithm. This work has further been extended to design filters which have linear phase characteristics (39).

Recently, linear programming techniques are used to obtain the best Chebyshev approximation (33) (34). Compared to Remez exchange algorithm, the computational time required to derive the optimal filter is slower. Thus, the length of the filter that could be designed by the above method is limited. The method is more flexible with regard to constraints. Both time domain and frequency domain constraints can be used in deriving FIR filters. The filters designed by the above two methods are optimal and the solution is unique.

The transformed Chebyshev functions have also been used to design nonrecursive digital filters that have equiripple characteristics (40). The interesting aspect of this method is that it does not make use of any optimization methods, but makes use of a transformation to arrive at an analytical solution. The drawback of this method is that it leads to higher order solutions when compared to other methods to meet the same

filter specifications.

The weighted least squares approach has also been used in designing an FIR filter (41). If the number of samples is small, then the filter could be designed easily using a matrix inversion routine. On the other hand, if the number of samples is large, then successive approximations using discrete equivalent of Neumann series is employed. This method is inferior to a mini-max filter as it requires 15 percent more normalized transition band width to obtain the same stopband specifications. Constrained ripple design techniques have also been used in designing non-recursive filters (42). By this method filters are designed such that the magnitude response falls between specified upper and lower bounds. It uses the tangency condition to arrive at a desired filter. The algorithm converges to a cosine polynomial meeting the tangency condition. Some of these results are extended to FIR filters which have nonlinear phase (43).

Other methods of design include the statistical approach in which the FIR filter is treated as an estimator structure (44) (45). The criteria used minimizes the mean square error of the estimate of the design signal imbedded in a random noise sequence. By treating the signal noise covariance as design parameters, FIR filters can be designed with spectral responses that approximate the power spectral density of the design signal. Efficient methods for inverting Toeplitz matrices are needed for this technique. For higher-order filters, the computer storage required to invert the matrix is exceedingly high.

Several other design techniques in the area of FIR filter design can be found in Theory and Application of Digital Signal Processing (23).

1.3 Organization of the Thesis

Chapter II presents an approach to the solution of a system of Toeplitz normal equations. The solution is based on using iterative techniques, circulant matrices, and the fast Fourier transform. Also, a relationship between the filter design by frequency sampling and the discrete convolution is established.

Chapter III presents a direct approach to the frequency sampling filter design. The direct method is based on using the ideas of smoothing techniques and a direct solution. This new approach has been applied successfully to the design of low-pass, bandpass, and high-pass filters. The results are compared with other existing techniques and the computed transition values are tabulated.

Chapter IV presents a summary and suggestions for further study.

Appendices A and B, respectively, present the computer listings for determining the frequency responses of FIR filters and for computing the transition sample values.

CHAPTER II

THE APPLICATION OF FFT TO THE SOLUTION OF A SYSTEM OF TOEPLITZ NORMAL EQUATIONS

2.1 Introduction

In the deconvolution problem there is a need for solving a set of Toeplitz normal equations of the form,

$$\underline{y} = A_{\text{Toe}} \underline{x}$$

where A_{Toe} is a symmetric Toeplitz matrix of order ℓ and \underline{x} and \underline{y} are ℓ dimensional vectors. A Toeplitz matrix $A_{\text{Toe}} = (\alpha_{k,j})$ has the property that (13)

$$\alpha_{k,j} = \alpha_{k-j} \quad (2.1)$$

These matrices appear in the study of covariance matrices of weakly stochastic time series. Also, the matrix representation of linear time invariant discrete time filters is of Toeplitz type (13). There are numerous applications of these matrices in mathematics (46), physics (47), signal processing and applied estimation theory (48). In the area of communication theory, usually an input vector is known which is the sum of a data vector \underline{x} and a noise vector \underline{w} . The object, for example, is to design a filter in such a way as to minimize the expected value of the mean square error between \underline{x} and the estimate of \underline{x} , $\hat{\underline{x}}$. This is the classic problem of Wiener filtering (3).

In compact form, Equation (2.4a) and (2.4b) can be written as

$$\underline{y} = A_{\text{con}} \underline{x} \quad (2.5a)$$

and

$$\underline{y} = X_{\text{con}} \underline{a} \quad (2.5b)$$

In section 2.3, Equation (2.5a) is used extensively. In the following the above equations are used in the deconvolution problem.

In the deconvolution problem, the input vector and the desired output vector $\underline{d} = (d_0, \dots, d_{m+\ell})$ are known a priori. It is required to determine the filter weights $a_i, i = 0, \dots, \ell$ such that when the known input is applied to the filter, the resulting output $y_t, t = 0, \dots, (m + \ell)$ should be as close as possible to the desired output vector $\underline{d} = (d_0, \dots, d_{(m+\ell)})$ in the least squares sense. The above operation is expressed as

$$\underline{d} = X_{\text{con}} \underline{a} \quad (2.6)$$

which is an overdetermined system. The error is expressed by

$$\underline{e} = (\underline{y} - \underline{d}) \quad (2.7)$$

The filter weights $a_k, k = 0, 1, \dots, n$ are obtained by using the method of least squares (50), i.e., minimize the mean square error with respect to each of these parameters. This results in a set of normal equations of the form (3)

$$X_{\text{con}}^T X_{\text{con}} \underline{a} = X_{\text{con}}^T \underline{d} \quad (2.8)$$

where $(X_{\text{con}}^T X_{\text{con}})$ is a symmetric Toeplitz matrix. From Equation (2.8) it is clear that the inverse of symmetric Toeplitz matrices is required to obtain the filter weights.

Thus, from the above discussion it can be observed that the standard formulation of the discrete single-channel Wiener filter problem will result in a system of Toeplitz normal equations, which can be written as

$$A_{\text{Toe}} \underline{a} = \underline{y} \quad (2.9)$$

where A_{Toe} is a symmetric positive definite matrix of the Toeplitz type, and can be explicitly written as

$$A_{\text{Toe}} = \begin{bmatrix} \alpha_0 & \alpha_1 & \alpha_2 & \cdot & \cdot & \cdot & \alpha_{\ell-1} \\ \alpha_1 & \alpha_0 & \alpha_1 & \cdot & \cdot & \cdot & \alpha_{\ell-2} \\ \alpha_2 & \alpha_1 & \alpha_0 & \cdot & \cdot & \cdot & \alpha_{\ell-3} \\ \cdot & \cdot & \cdot & \cdot & \cdot & \cdot & \cdot \\ \cdot & \cdot & \cdot & \cdot & \cdot & \cdot & \cdot \\ \cdot & \cdot & \cdot & \cdot & \cdot & \cdot & \cdot \\ \alpha_{\ell-1} & \alpha_{\ell-2} & \alpha_{\ell-3} & \cdot & \cdot & \cdot & \alpha_0 \end{bmatrix} \quad (2.10)$$

In practice, the system in Equation (2.9) is solved by using Levinson's algorithm (2), which uses the special structure of Toeplitz matrices. Levinson's solution is exact except for round-off errors. However, it cannot be programmed efficiently for special purpose hardware. Sometimes an approximate solution to Equation (2.9) is good enough. In such cases, gradient methods are employed (14). Gradient methods have the advantage that they can be implemented effectively on special purpose floating point hardware. Gradient methods are based on the principle that the successive approximations to solution vector \underline{a} minimizes the magnitude of the specified error function. In seismic signal processing there is a need for solving a new set of normal equations of like order for successive traces of seismic record. A similar situation exists in time-adaptive Wiener filtering (51). In order to save computer time,

Levinson's algorithm and the gradient method can be combined to arrive at a solution. For the first trace of data, the system of normal equations can be solved by using Levinson's algorithm. It is assumed that for different traces, the solution for each will not vary drastically. The exact solution determined for the first trace can be used to arrive at a solution for the second set of normal equations using gradient methods. The successive solutions can be obtained by using gradient methods with the initial solution from the previous known solution (14).

In a recent article Wang and Treitel discussed the solution of Equation (2.9) using gradient methods (14). The computational requirements of these have been compared with the classical Levinson's algorithm. Based on their comparison, it appears that gradient methods play an important role in the area of seismic signal processing. Furthermore, other avenues should be investigated to reduce the computational requirements. The method presented here uses some of these ideas and the computational requirements are reduced by making use of the classical fast Fourier transform (FFT) algorithm (52). For easy reference a brief summary of conjugate gradient method (53) is presented in the following.

2.1.1 Conjugate Gradient Method

The solution of Equation (2.9) can be obtained in ℓ steps where ℓ corresponds to the number of equations in Equation (2.9). The solution is obtained by using the following procedure:

- (1) First, assume an arbitrary solution for \underline{a} , \underline{a}_0 .
- (2) Compute $\underline{p}_0 = \underline{r}_0 = \underline{y} - A_{Toe} \underline{a}_0$.
- (3) Compute successively at the k th step:

$$\begin{aligned}
b_k &= \|r_k\|^2 (p_k, A_{\text{Toe}} p_k)^{-1} \\
a_{k+1} &= a_k + b_k p_k \\
r_{k+1} &= r_k - b_k A_{\text{Toe}} p_k \\
d_k &= \|r_{k+1}\|^2 \|r_k\|^{-2} \\
p_{k+1} &= r_{k+1} + d_k p_k
\end{aligned}$$

The solution for Equation (2.9) is given by

$$\bar{a} = \sum_{k=0}^{\ell-1} (p_k, y) (A_{\text{Toe}} p_k, p_k)^{-1} p_k \quad (2.10)$$

The above algorithm requires

$$2\ell^2 + 8\ell - 3 \quad (2.11)$$

multiplications and additions (MADs) for each iteration step. Most of these MADs (ℓ^2 MADs) are required for the computation of

$$Q_k = A_{\text{Toe}} p_k \quad (2.12)$$

In the following an interesting procedure is presented which uses FFT algorithm to compute Equation (2.12). The approach is based upon relating the Toeplitz matrices to circulant matrices. In the following a brief summary on the circulant matrices is presented (54).

2.1.2 Circulant Matrices

A circulant matrix of order p has the same elements $\{c_v\}$ arranged in cyclic order in each row and column in the following way:

$$A_{\text{cir}} = \begin{bmatrix} c_0 & c_1 & c_2 & \cdot & \cdot & \cdot & c_{p-1} \\ c_{p-1} & c_0 & c_1 & \cdot & \cdot & \cdot & c_{p-2} \\ \cdot & \cdot & \cdot & \cdot & \cdot & \cdot & \cdot \\ \cdot & \cdot & \cdot & \cdot & \cdot & \cdot & \cdot \\ \cdot & \cdot & \cdot & \cdot & \cdot & \cdot & \cdot \\ c_1 & c_2 & c_3 & \cdot & \cdot & \cdot & c_0 \end{bmatrix} \quad (2.13)$$

with

$$c_{k-j} = c_{p+(k-j)} \quad \text{for } k - j < 0 \quad (2.14)$$

For convenience let A_{cir} be expressed by

$$A_{\text{cir}} = (\underline{B}_0, \underline{B}_1, \cdot \cdot \cdot, \underline{B}_{p-1}) \quad (2.15)$$

where

$$\underline{B}_{j-1} = (c_{j-1}, c_{j-2}, \cdot \cdot \cdot, c_{j-p})^T \quad (2.16)$$

Next, the relationship between the circulant matrices and the discrete Fourier transform is discussed. One of the most important properties of circulant matrices is that (13)

$$A_{\text{cir}} = \left[\left(\frac{1}{\sqrt{p}} \right) A_{\text{DFT}} \right] \Lambda \left[\left(\frac{1}{\sqrt{p}} \right) A_{\text{DFT}}^* \right] \quad (2.17)$$

where A_{DFT} is the discrete Fourier transform matrix in which

$$a(kj) = e^{-i \frac{2\pi}{p} (k-1)(j-1)} \quad (2.18)$$

The entries on the diagonal matrix $\Lambda = \text{dia}(\lambda_1, \lambda_2, \cdot \cdot \cdot, \lambda_p)$ can be obtained from

$$[\lambda_1, \lambda_2, \cdot \cdot \cdot, \lambda_p] = [c_0, c_1, \cdot \cdot \cdot, c_{p-1}] A_{\text{DFT}}^T \quad (2.19)$$

where $[c_0, c_1, \dots, c_{p-1}]$ is the first row of A_{cir} .

Interestingly, A_{cir} can also be expressed by

$$A_{\text{cir}} = [(1/\sqrt{p})A_{\text{DFT}}^*] D [(1/\sqrt{p})A_{\text{DFT}}] \quad (2.20)$$

with

$$D = \text{dia}(d_1, d_2, \dots, d_p) = A_{\text{DFT}} B_0 \quad (2.21)$$

Note that Equations (2.17) and (2.20) are different. Equation (2.21) is pointed out in Reference (16). However, Equation (2.21) is not given before. In the following, two proofs are presented to show the equality in Equation (2.20). The first proof is direct and is different from what is given in Reference (13). The second proof uses Equation (2.17) explicitly. Now the first proof is given below.

Noting that $(1/\sqrt{p})A_{\text{DFT}}$ is a unitary matrix, it suffices to show that $\beta = \gamma$ where

$$\beta = (\beta_{kj}) = A_{\text{DFT}} A_{\text{cir}}$$

$$\gamma = (\gamma_{kj}) = D A_{\text{DFT}}$$

Now,

$$\beta_{kj} = \sum_{\ell=1}^p c_{j-\ell} e^{-i \frac{2\pi}{p} (k-1)(\ell-1)} \quad (2.22)$$

and

$$\gamma_{kj} = d_k e^{-i \frac{2\pi}{p} (k-1)(j-1)} \quad (2.23)$$

We need to show that $\beta_{kj} = \gamma_{kj}$ or $\alpha_k = d_k$, where

$$\begin{aligned}\alpha_k &= \beta_{kj} e^{i \frac{2\pi}{p} (k-1)(j-1)} \\ &= \sum_{\ell=1}^p c_{j-\ell} e^{-i \frac{2\pi}{p} (k-1)(\ell-j)}\end{aligned}$$

Defining $(j-\ell) = 1-r$, we have

$$\begin{aligned}\alpha_k &= \sum_{r=2-k}^{p+1-k} c_{1-r} e^{-i \frac{2\pi}{p} (k-1)(r-1)} \\ &= c_{k-1} e^{i \frac{2\pi}{p} (k-1)} + c_{k-2} e^{i \frac{2\pi}{p} (k-1)(k-2)} \\ &\quad + \dots + c_1 e^{-i \frac{2\pi}{p} (k-1)^2} + c_0 \\ &\quad + c_{p-1} e^{-i \frac{2\pi}{p} (k-1)} \\ &\quad + c_{p-2} e^{-i \frac{2\pi}{p} (k-1)^2} \\ &\quad + \dots + c_k e^{-i \frac{2\pi}{p} (k-1)(p-k)}\end{aligned}$$

where we have used the relation $c_{-j} = c_{p-j}$. Noting that

$$e^{i \frac{2\pi}{p} (k-1)j} = e^{-i \frac{2\pi}{p} (k-1)(p-j)}$$

we have the desired relation

$$\alpha_k = d_k$$

Since j is not restricted to any particular value, it follows that

$$\beta_{kj} = \gamma_{kj}$$

and Equation (2.20) follows.

Equation (2.20) can also be shown by starting with the transpose of the original circulant matrix (which is also a circulant matrix). From Equation (2.17)

$$A_{\text{cir}}^T = E = \frac{1}{p} A_{\text{DFT}}^* \Lambda A_{\text{DFT}} \quad (2.24)$$

where we have used the fact that $(A_{\text{DFT}}^*)^T = A_{\text{DFT}}^*$. It is clear that Equation (2.24) is applicable to any circulant matrix E and the diagonal entries in Λ are obtained by taking the A_{DFT} of the first column of E . Thus, applying Equation (2.24) to A_{cir} , we have

$$A_{\text{cir}} = \frac{1}{p} A_{\text{DFT}}^* D A_{\text{DFT}}$$

where the entries in the diagonal matrices D are given by Equation (2.21), and the equality in Equation (2.20) is proven.

The above decomposition of circulant matrices allow for the use of discrete Fourier transforms in solving a system of Toeplitz normal equations. This is discussed in the following section.

2.2 Normal Equations Using Symmetric Circulants

The coefficient matrix A_{Toe} in Equation (2.9) is, in general, not a circulant matrix. However, a symmetric circulant matrix is a symmetric Toeplitz matrix. This aspect can be used in our solution and is discussed in the following.

First, a new set of equations is formed using Equation (2.9), and is

$$\begin{bmatrix} y \\ y_1 \end{bmatrix} = A_{\text{cir}} \begin{bmatrix} x \\ 0 \end{bmatrix} \quad (2.25)$$

where

$$A_{\text{cir}} = \begin{bmatrix} a_0 & a_1 & \cdots & a_{\ell-1} & a_{\ell} & \cdots & a_{N-1} \\ a_1 & a_0 & \cdots & a_{\ell-2} & a_{\ell-1} & \cdots & a_{N-2} \\ \vdots & \vdots & \cdots & \vdots & \vdots & \cdots & \vdots \\ \vdots & \vdots & \cdots & \vdots & \vdots & \cdots & \vdots \\ \vdots & \vdots & \cdots & \vdots & \vdots & \cdots & \vdots \\ a_{N-1} & a_{N-2} & \cdots & \vdots & \vdots & \cdots & a_0 \end{bmatrix} \quad (2.26)$$

and

$$N = 2^{\nu} = 2(\ell-1) + 1 + \beta \quad (2.27)$$

where β is the smallest integer which satisfies Equation (2.27). The first principal submatrix of order ℓ is the given Toeplitz matrix in Equation (2.9). The other a_i 's are selected such that

$$\begin{aligned} a_{N-k} &= a_k, & k &= 0, \dots, \ell-1 \\ a_k &= 0, & \ell &\leq k \leq N - \ell \end{aligned} \quad (2.28)$$

Using the property of circulants, Equation (2.12) is rewritten as

$$\begin{bmatrix} \underline{Q}_k \\ \underline{Q}'_k \end{bmatrix} = A_{\text{cir}} \begin{bmatrix} \underline{P}_k \\ \underline{0} \end{bmatrix} \quad (2.29)$$

By using Equation (2.20) in Equation (2.29), we have

$$\begin{bmatrix} \underline{Q}_k \\ \underline{Q}'_k \end{bmatrix} = \frac{1}{N} A_{\text{DFT}}^* D A_{\text{DFT}} \begin{bmatrix} \underline{P}_k \\ \underline{0} \end{bmatrix} \quad (2.30)$$

Since our approach is based on using FFT algorithm to compute Equation (2.30), the number of computations required in the worst case will be

$$2N \log_2 N + N \quad (2.31)$$

MADs. Note that the computation of D is not included in Equation (2.30) as it is the same for all iterations. For comparing with the conjugate gradient method, let us compute an upper bound for N . From Equation (2.27) it follows that in the worst case $2(\ell-1) = 2^{\nu-1} + 1$. That is, β is bounded by $\beta \leq 2^{\nu-1} - 1$ or $\beta < 2\ell$, which implies that

$$N \leq 4\ell \quad (2.32)$$

Using Equation (2.32) in Equation (2.31), the upper limit for the number of computations is

$$8\ell \log_2 4\ell + 4\ell \quad (2.33)$$

To compare the computational requirements between the two methods (i.e., the solution of normal equations using the conjugate gradient method and the modified conjugate gradient method), let us define R as the ratio N_1/N_2 where N_1 is the number of computations required to solve Equation (2.9) using FFT and the conjugate gradient method, and N_2 is the number of computations required to solve Equation (2.9) using the conjugate gradient method and is given by

$$R = ((8\ell \log_2 4\ell + 4\ell)/(2\ell^2 + 8\ell - 3)) \approx 4 \log_2 4\ell / \ell \quad (2.34)$$

where the approximation is valid for ℓ large. For example, when $\ell = 2^{10}$, $R = .047$, which indicates a considerable reduction in the number of computations.

The estimate given in Equation (2.33) is rather conservative as there are many other simplifications which can be considered. First, the vector \underline{P}_k^i in Equation (2.29) is

$$\underline{p}'_k = \begin{bmatrix} p_k \\ 0 \end{bmatrix}$$

and has zeros. Noting the decomposition (55) of A_{DFT} , the number of computations in determining $A_{DFT} \underline{p}'_k$ may be reduced. Furthermore, \underline{q}'_k in Equation (2.30) need not be determined. Noting these, one can see that an approximate estimate is about half the number given in Equation (2.33). Since the number of computations given in Equation (2.33) corresponds to complex operations, it is clear that the number of real computations required will be the same as in Equation (2.33). The total number of computations required will be $K(8\ell \log_2 4\ell + 4\ell)$, where $K(\leq \ell)$ is the number of iterations required. The number of computations by the proposed approach can be considerably reduced if an approximate solution is already known or if the accuracy requirements are not tight. The Levinson's algorithm requires $(3\ell^2/2)$ fixed operations. In addition, there are other advantages over Levinson's algorithm. These have been discussed elsewhere (14).

In addition to the reduction in the number of computations, accumulated rounding (55) is reduced. An approximate ratio of accumulated rounding error is the same as Equation (2.34). It is well known that the round-off noise problem is a big problem when computing the inverses of dense Toeplitz matrices. Using this method, precision requirements are therefore lower than other methods. The above method indicates a significant potential application in analyzing seismic, speech, and other systems.

It was pointed out earlier that special matrices like circulants can play an important role in filter design applications. In the

following section the relationship between the digital filter design by discrete convolution and by the frequency sampling design is discussed.

2.3 Digital Filter Design by Discrete Convolution and by the Frequency Sampling Technique--A Relationship

In the introduction the discrete convolution was described by the equation

$$\underline{y} = A_{\text{con}} \underline{x} \quad (2.35)$$

In the following we will assume that the matrix A_{con} and the vectors \underline{x} and \underline{y} are real. Using the properties of circulants, Equation (2.35) can be rewritten as

$$\underline{y} = A_{\text{cir}} \underline{x}_1 \quad (2.36)$$

where

$$\underline{x}_1 = \begin{bmatrix} \underline{x} \\ 0 \end{bmatrix} \quad (2.37)$$

and the A_{cir} is constructed from A_{con} . Using Equation (2.20) in Equation (2.36), it follows that

$$A_{\text{DFT}} \underline{y} = D (A_{\text{DFT}} \underline{x}_1) \quad (2.38)$$

where $(A_{\text{DFT}} \underline{x}_1)$ and $(A_{\text{DFT}} \underline{y})$ are the discrete Fourier transform coefficients of the input and output, respectively. Now,

$$d_i = (A_{\text{DFT}} \underline{y})_i / (A_{\text{DFT}} \underline{x}_1)_i \quad i = 0, \dots, m+n \quad (2.39)$$

where the subscript i is introduced to denote the i th entry in the

column. Also, it will be assumed that $d_i \equiv 0$ when $(A_{\text{DFT}} \underline{x}_1)_i = 0$. Also note that in Equation (2.38) D is a diagonal matrix, $D = \text{dia} (d_0, d_1, \dots, d_{m+\ell})$ and the entries in D are given by

$$\begin{bmatrix} d_0 \\ d_1 \\ \vdots \\ d_{\ell+1} \\ \vdots \\ d_{m+\ell} \end{bmatrix} = A_{\text{DFT}} \begin{bmatrix} a_0 \\ a_1 \\ \vdots \\ a_{\ell} \\ 0 \\ \vdots \\ 0 \end{bmatrix} \quad (2.40a)$$

The above set of equations can be expressed in symbolic form as

$$\underline{d} = A_{\text{DFT}} \underline{A}_1 \quad (2.40b)$$

The entries in the vector \underline{A}_1 correspond to the filter weights, and note that there are m zeros on the vector.

In order to have the vector \underline{A}_1 real, certain constraints need to be imposed on d_i 's. When $N \equiv m + \ell + 1$ is even, the conditions are that

$$\begin{aligned} d_i &\text{ is real for } i = 0, (N/2), \\ d_i^* &= d_{N+2-i} \text{ for } i = 1, \dots, ((N/2) - 1) \end{aligned} \quad (2.41a)$$

where $(*)$ indicates the complex conjugate.

When N is odd, the conditions are given by

$$\begin{aligned} d_i &\text{ is real for } i = 0 \\ d_i^* &= d_{N+2-i} \text{ for } i = 1, \dots, (((N-1)/2) - 1) \end{aligned} \quad (2.41b)$$

In addition to the above, additional constraints on d_i 's need to be considered in order to satisfy the zeros in the vector \underline{A}_1 . In the following, two proofs for the constraints in Equation (2.41) are given below.

The first proof can be derived by using the classical result on the discrete Fourier transform of a real sequence (56), which implies that $\{\text{Re}(d_i)\}$ has even symmetry and $\{\text{Im}(d_i)\}$ has odd symmetry. That is,

$$\begin{aligned} \text{Re}(d_i) &= \text{Re}(d_{N-i}) & i &= 0, 1, \dots, N-1 \\ \text{Im}(d_i) &= -\text{Im}(d_{N-i}) & i &= 0, 1, \dots, N-1 \end{aligned} \quad (2.42)$$

From these, Equation (2.41) follows.

The second proof is based upon the idea that the matrix A_{DFT} can be orthogonally transformed into a direct sum of a real matrix and an imaginary matrix (57). That is,

$$A_{\text{DFT}} = Q^T (M_1 \oplus JM_2)Q \quad (2.43)$$

where Q is an orthogonal matrix. Now, from Equation (2.40b), we have

$$Q^T \underline{d} = (M_1 \oplus JM_2) (Q \underline{A}_1) \quad (2.44)$$

Noting that M_1 , M_2 , and $(Q \underline{A}_1)$ are real matrices, it can be seen that the entries in the vector $(Q^T \underline{d})$ are either purely real or purely imaginary. Furthermore, from the special structure of Q , the constraints on d_i 's will follow.

It is clear that the constraints given in Equation (2.41) imply only that the vector \underline{A}_1 is real. Also, the vector \underline{A}_1 contains zeros. This implies that the system of equations in Equation (2.40) is an over-determined system. This system of equations can be solved for \underline{A}_1 by

using the least squares approach (50), or by weighted least squares approach (58). Noting that $(1/\sqrt{N}) A_{\text{DFT}}$ is a unitary matrix, it follows that the least squares approach will give the result that the nonzero entries a_i , $i = 0, 1, \dots, \ell$, in \underline{A}_1 are the first $(\ell+1)$ inverse discrete Fourier transforms of d_k , $k = 0, 1, \dots, m+\ell$.

A special case of the above design is when the input is a digital delta function. That is, $x_0 = 1$ and $x_i = 0$, $i = 1, \dots, m$, in Equation (2.4). For this case, Equation (2.4a) reduces to

$$\begin{bmatrix} y_0 \\ y_1 \\ \cdot \\ \cdot \\ \cdot \\ y_\ell \end{bmatrix} = \begin{bmatrix} a_0 \\ a_1 \\ \cdot \\ \cdot \\ \cdot \\ a_\ell \end{bmatrix} = \underline{a} \quad (2.45)$$

and the d_i 's in Equation (2.39) are given by

$$d_i = (A_{\text{DFT}} \underline{a})_i, \quad i = 0, 1, \dots, \ell \quad (2.46)$$

This implies that the d_i 's can be considered as the points obtained by sampling uniformly at $N = (\ell+1)$ points the given filter characteristics. This is nothing but the filter design by frequency sampling technique (27). The next chapter deals with a direct approach to the frequency sampling filter design, where the unspecified d_i 's are used as design parameters to obtain an optimal or a suboptimal filter.

2.4 Summary

An iterative technique based on circulant matrices and the fast Fourier transforms is presented to solve a system of Toeplitz normal equations. The pros and cons for solving these equations by this method

is discussed. Also, a relationship is derived between the filter designs by direct convolution and by the frequency sampling method.

CHAPTER III

A DIRECT APPROACH TO THE FREQUENCY SAMPLING FILTER DESIGN

3.1 Introduction

Recently there has been a good deal of interest in the finite impulse response filters (FIR), as they can always be realized and are always stable. In addition, they can be designed such that they have linear phase characteristics. There are various techniques available in designing FIR filters. These include the classical Fourier series method (17) (18) (19) (20) (sometimes referred to as the window method), the frequency sampling method (23) through (32), the optimal (in the Chebyshev sense) filter design method (35) (59) through (63), and finally, the statistical methods (44) (45).

Each of the above techniques has its own advantages and disadvantages. These have been discussed earlier in Chapter I. From the literature one can see that there is no simple and direct method to design a FIR filter. In the following a direct approach to frequency sampling design is derived using some of the classical ideas.

3.2 Basic FIR Design Problem

The design of FIR filters involves the selection of $h(kT)$, the filter weights, in the z-domain transfer function,

$$H(z) = \sum_{k=0}^{N-1} h(kT) z^{-k} \quad (3.1)$$

such that $H(z) \Big|_{z=e^{j\omega T}} = H(e^{j\omega T})$ satisfies the given magnitude and/or phase specifications. Hereafter, $T = 1$ for simplicity.

One of the important aspects of FIR filters is that they can be designed to have linear phase characteristics. In the following the discussion is restricted to linear phase FIR filters.

It is well known that the sufficient condition for linear phase is that the weight vector be symmetric about its center, i.e.,

$$h(k) = h(N - k + 1) \quad \text{for all } k \in \{1, \dots, N\} \quad (3.2)$$

Using Equation (3.2) in Equation (3.1), we have

$$H(e^{j\omega}) = \begin{cases} e^{-j\omega(\frac{N-1}{2})} \left[h(\frac{N-1}{2}) + \sum_{k=0}^{(\frac{N-3}{2})} 2h(k) \cos[(\frac{N-1}{2} - k)\omega] \right] & \text{for } N \text{ odd} \\ e^{-j\omega(\frac{N-1}{2})} \left[\sum_{k=0}^{(\frac{N}{2})-1} 2h(k) \cos[(\frac{N-1}{2} - k)\omega] \right] & \text{for } N \text{ even} \end{cases} \quad (3.3a)$$

It is clear from Equation (3.3) that Equation (3.2) implies a linear phase shift corresponding to a delay of $(\frac{N-1}{2})$ samples. It is important to note that for N odd, the phase shift corresponds to an integer number of samples delay, whereas for the case of N even, the phase shift corresponds to an integer plus one-half sample delay.

Before we go into the details of the direct method of design, it is appropriate to review some of the basic equations associated with the frequency sampling method. These are used in the new method of design.

It is well known that the interpolated continuous frequency response of a linear phase filter in Equation (3.1) can be expressed as (see

References (23) (24) (29)):

$$H(e^{j\omega}) = [e^{-j\omega \frac{(N-1)}{2}}] H^*(e^{j\omega}) \quad (3.4)$$

where

$$H^*(e^{j\omega}) = \frac{|H(0)|}{N} \frac{\sin(\omega N/2)}{\sin(\omega/2)} + \sum_{k=1}^{N'} \frac{|H(k)|}{N} \left[\frac{\sin(N((\omega/2) - (\pi k/N)))}{\sin((\omega/2) - (\pi k/N))} + \frac{\sin(N((\omega/2) + (\pi k/N)))}{\sin((\omega/2) + (\pi k/N))} \right] \quad (3.5)$$

with

$$N' = \begin{cases} \frac{N-1}{2} & \text{for } N \text{ odd} \\ \frac{N}{2} - 1 & \text{for } N \text{ even} \end{cases} \quad (3.6)$$

$$H_k \equiv H(k) = \text{DFT}[h(n)]$$

Also, $|H(k)|$ denotes the sampled values of the magnitude response. For design purposes, Equation (3.5) will be used from now on. Note that the linear phase constraints (23) (24) are already incorporated in Equation (3.5).

3.3 Method of Design

A simple direct procedure is presented for the design of finite impulse response filters. This will be done using the following three steps:

1. Frequency sampling techniques.
2. Smoothing techniques.
3. Least squares or a direct solution.

3.3.1 Frequency Sampling Techniques

Since the frequency sampling technique (23) (24) (26) (27) is one of the steps, we will assume that pass, stop, and transition bands can be identified in terms of frequency sample locations ($\omega_k = \frac{2\pi}{N} k$; $k = 0, \dots, N-1$). In the first part low-pass filters will be used as the design problem. Let the first $(\ell - M)$ samples be located in the passband and

$$H^*(e^{j\omega_k}) = |H_k| = 1, \quad k = 0, 1, \dots, (BW - 1), \quad (3.7)$$

where $BW = (\ell - M)$ corresponds to the number of samples in the passband, M is the number of transition samples, and ω_ℓ corresponds to the start of the stopband. Let the transition samples be identified as

$$H^*(e^{j\omega_{\ell-M-b}}) = |H_{\ell-M+b}|, \quad b = 0, \dots, M - 1, \quad (3.8)$$

which are to be determined so as to satisfy the filter specifications.

Let the next $(N' - \ell + 1)$ be assumed to be in the stopband, and

$$H^*(e^{j\omega_k}) = 0 \quad k = \ell, \dots, N' \quad (3.9)$$

where

$$N' = \begin{cases} (N/2) - 1 & \text{for } N \text{ even} \\ ((N-1)/2) & \text{for } N \text{ odd} \end{cases} \quad (3.10)$$

The remaining $H^*(e^{j\omega_k}) = |H(k)|$, $k = N' + 1, \dots, N-1$, are fixed from the symmetry constraints. Figure 1 shows a typical set of specifications for low-pass filters, where $BW = 2$, $M = 3$, and $\ell = 5$. In the above it is clear that the only unknowns are $|H_{\ell-M-b}|$, $b = 0, \dots, M - 1$ and are to be determined such that the maximum side lobe is minimum in some

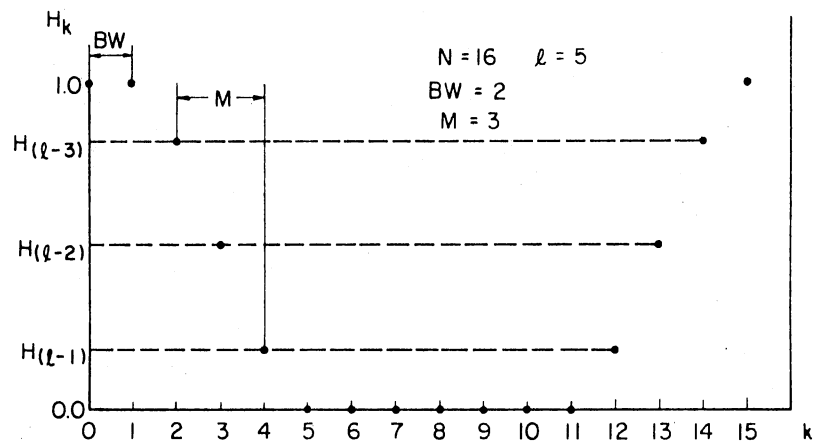


Figure 1. Specifications for a Low-Pass Filter

sense. This is the only criterion to be used in the design and it will be discussed in a later section.

3.3.2 Smoothing Technique

In designing nonrecursive filters, window techniques (17) (18) (19) (20) have been effectively used to reduce the ripples. Some of these window techniques involve the addition of two or more shifted versions of frequency responses to cancel ripples. The same general idea will be used in reducing the ripples.

One of the most important cases of frequency sampling filter design is the case corresponding to one transition sample; that is, $M = 1$ in Equation (3.8). Let us investigate this case first. It is clear that $H^*(e^{j\omega})$ is a function of $H_{\ell-1}$, the unknown transition sample, and can be expressed as

$$H^{*(i)}(e^{j\omega}) = A(\omega) + H_{\ell-1}^{(i)} B(\omega) \quad (3.11)$$

where the superscript i is introduced to denote the fact that $H_{\ell-1}^{(i)}$ can take different values. $A(\omega)$ represents the contribution to $H^*(e^{j\omega})$ by the fixed frequency samples and $B(\omega)$ represents the contribution of the unconstrained frequency sample with magnitude $H_{\ell-1}^{(i)}$. In particular, we will be interested in $H_{\ell-1}^{(i)}$ for $0 \leq H_{\ell-1}^{(i)} \leq 1$. Figure 2 gives the plots of $[H^*(e^{j\omega})]$ for $N = 15$ and $BW = 3$ for various values of $H_{\ell-1}^{(i)}$. Looking at these plots closely, we see that in the stopband

$$[H^{*(i)}(e^{j\omega})] [H^{*(k)}(e^{j\omega})] < 0 \text{ for } \omega \neq \omega_k = \frac{2\pi}{N} k, k = \ell, \dots, N' \quad (3.12a)$$

for

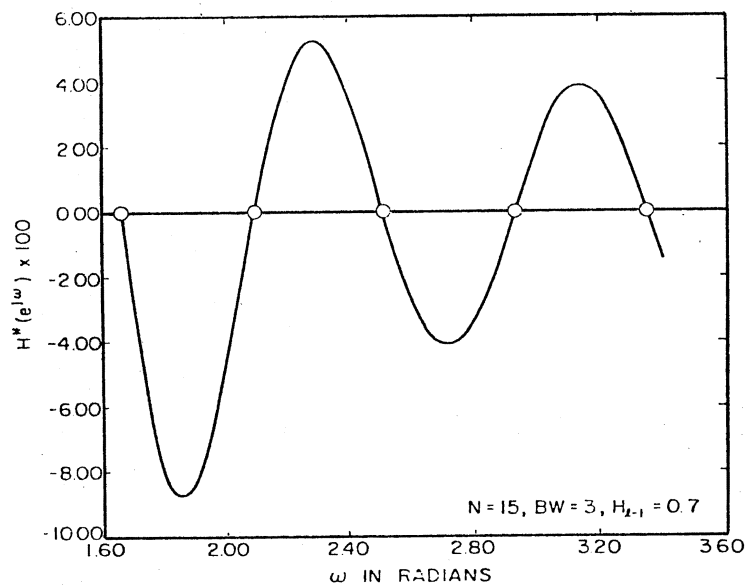
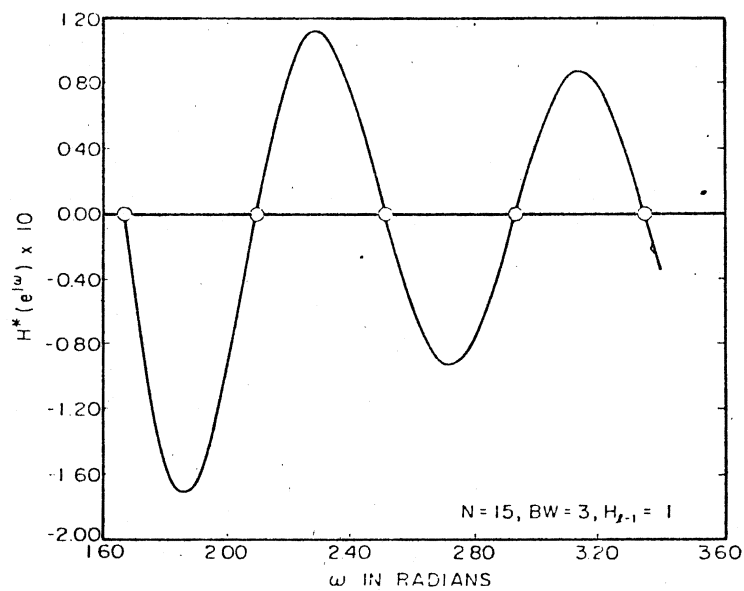


Figure 2. Variation of Stopband Frequency Response as a Function of Transition Sample H_{l-1} (Enlarged Scale)

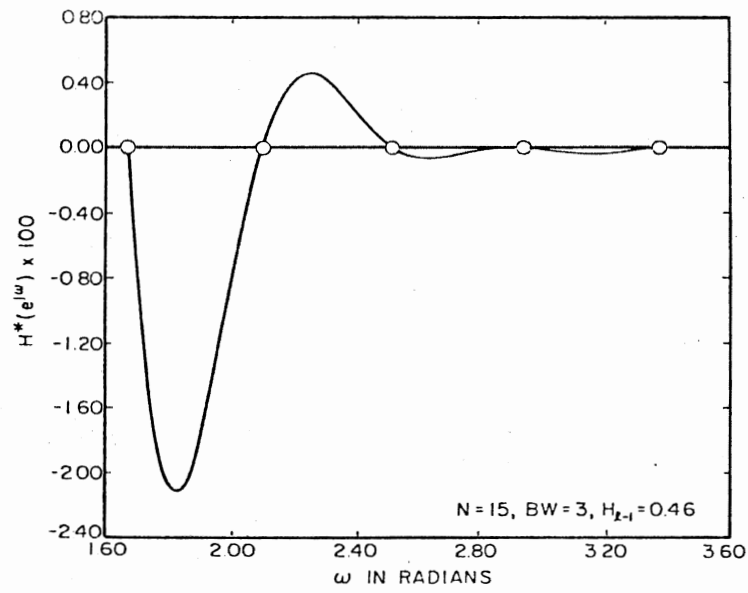
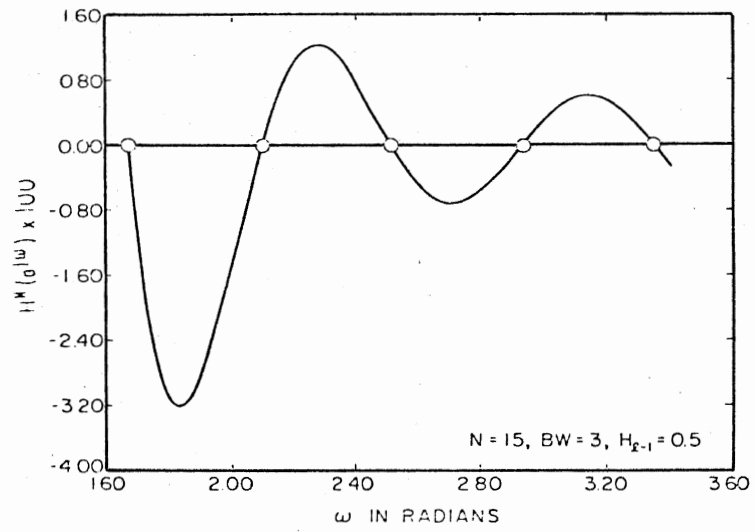


Figure 2. (Continued)

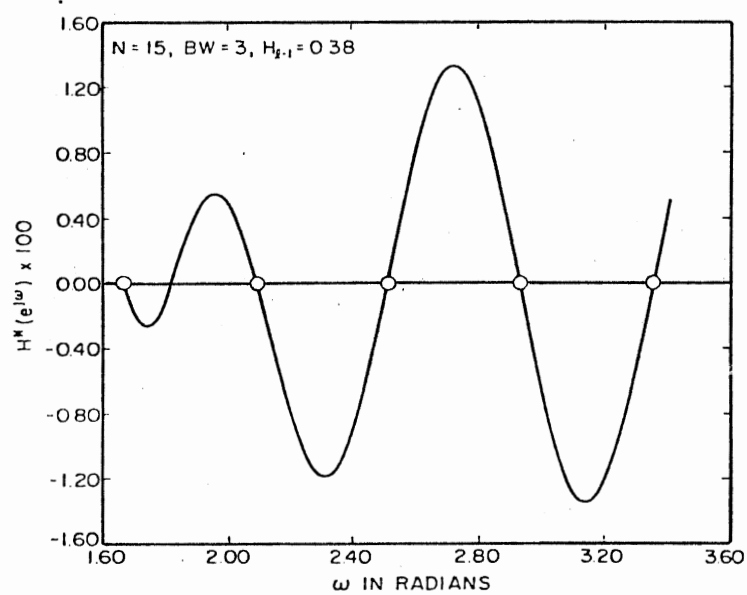
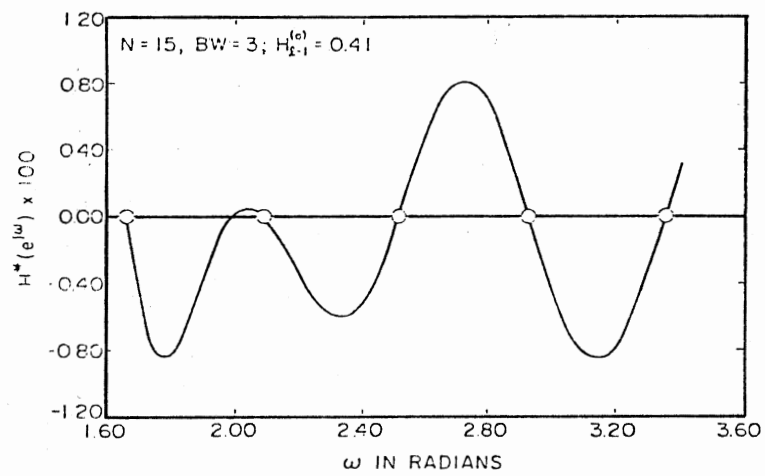
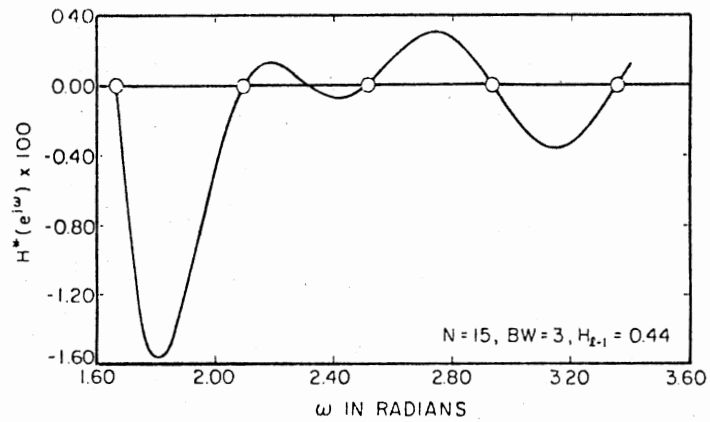


Figure 2. (Continued)

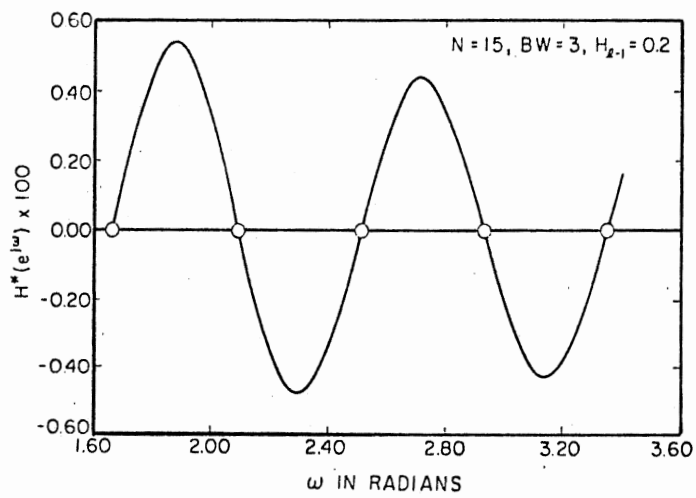
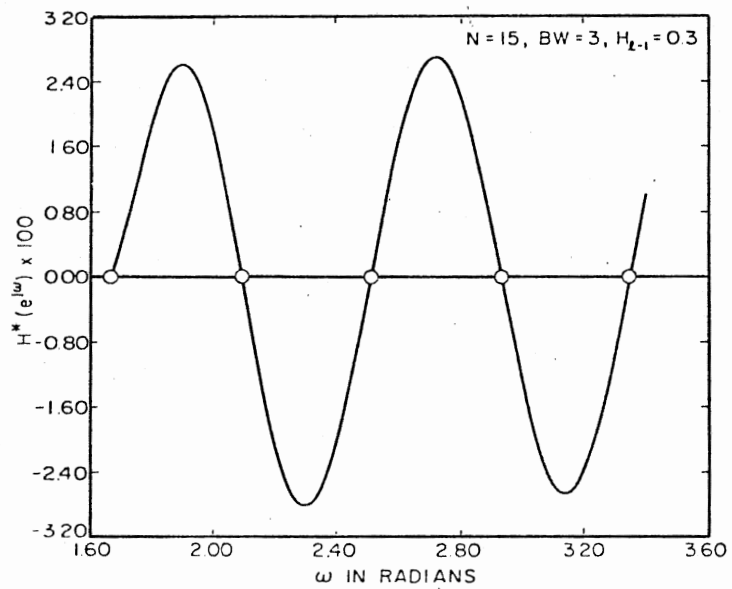


Figure 2. (Continued)

$$H_{\ell-1}^{(i)} > 0.5, H_{\ell-1}^{(k)} < 0.3 \quad (3.12b)$$

From this, by adding the two responses $(H^{*(i)}(e^{j\omega}))$ and $(H^{*(k)}(e^{j\omega}))$, we have ripple size reduction. Figure 3(a) illustrates this point, where $H_{\ell-1}^{(k)} = 0.12$ and $H_{\ell-1}^{(i)} = 0.7$. The plot of

$$H^{*(o)}(e^{j\omega}) = \frac{H^{*(i)}(e^{j\omega}) + H^{*(k)}(e^{j\omega})}{2} \quad (3.13)$$

is also shown in Figure 3(a), where we can see that the ripples have been reduced considerably. The corresponding transition sample is given by

$$H_{\ell-1}^{(o)} = \frac{H_{\ell-1}^{(i)} + H_{\ell-1}^{(k)}}{2} = \frac{0.7 + 0.12}{2} = 0.41 \quad (3.14)$$

From Figure 3(a) it is clear that

$$H^{*(o)}(e^{j\omega}) = \begin{cases} < 0 & \omega_{\ell} < \omega < \omega_{\ell+1} \\ < 0 & \omega_{\ell+1} < \omega < \omega_{\ell+2} \\ > 0 & \omega_{\ell+2} < \omega < \omega_{\ell+3} \end{cases} \quad (3.15)$$

However, the scale in Figure 3(a) is such that the detail in the stop-band response cannot be easily seen. Figure 3(b) shows the same to an enlarged scale. From this, Equation (3.15) can be modified to:

$$H^{*(o)}(e^{j\omega}) = \begin{cases} < 0 & \omega_{\ell} < \omega < \omega_{\ell 0} \\ > 0 & \omega_{\ell 0} < \omega < \omega_{\ell+1} \\ < 0 & \omega_{\ell+1} < \omega < \omega_{\ell+2} \\ > 0 & \omega_{\ell+2} < \omega < \omega_{\ell+3} \end{cases} \quad (3.16)$$

where $\omega_{\ell 0}$ corresponds to the frequency at which $H^{*(o)}(e^{j\omega}) = 0$ between ω_{ℓ} and $\omega_{\ell+1}$. Also, it should be pointed out that in the region

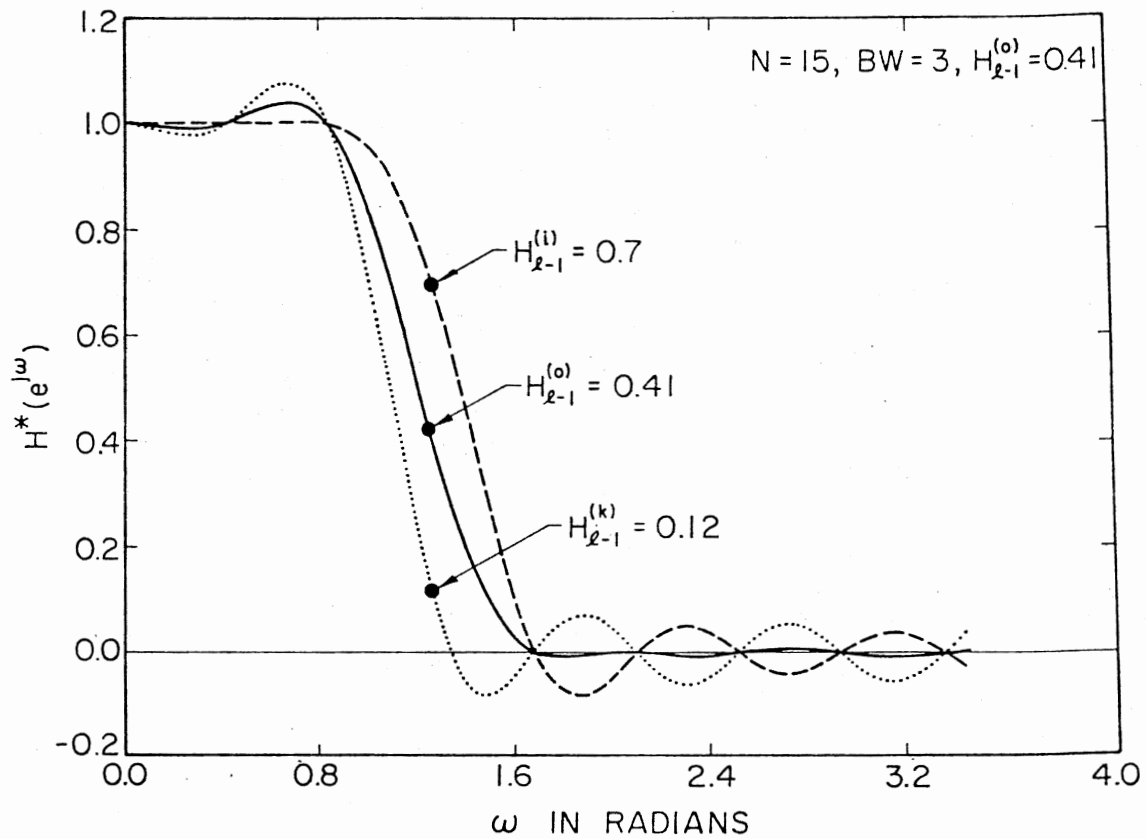


Figure 3(a). Ripple Reduction in the Stopband When Transition Sample is Optimum

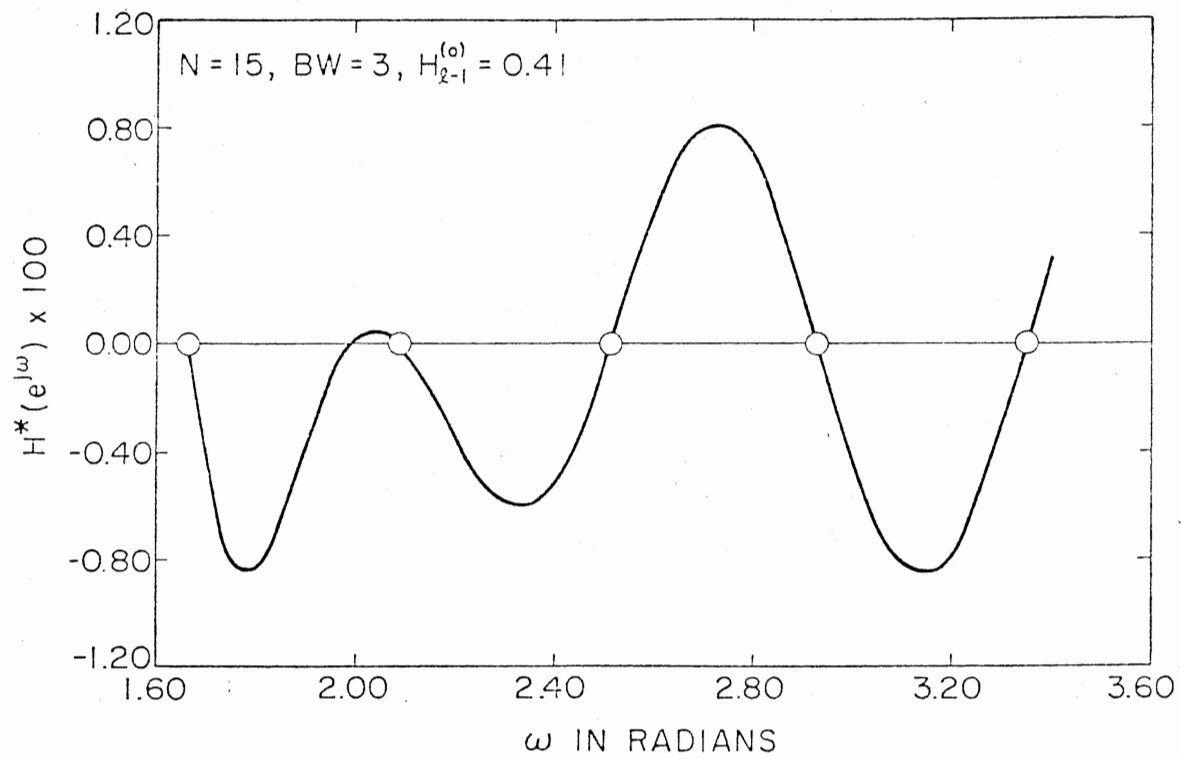


Figure 3(b). Stopband Response When Transition Sample is One

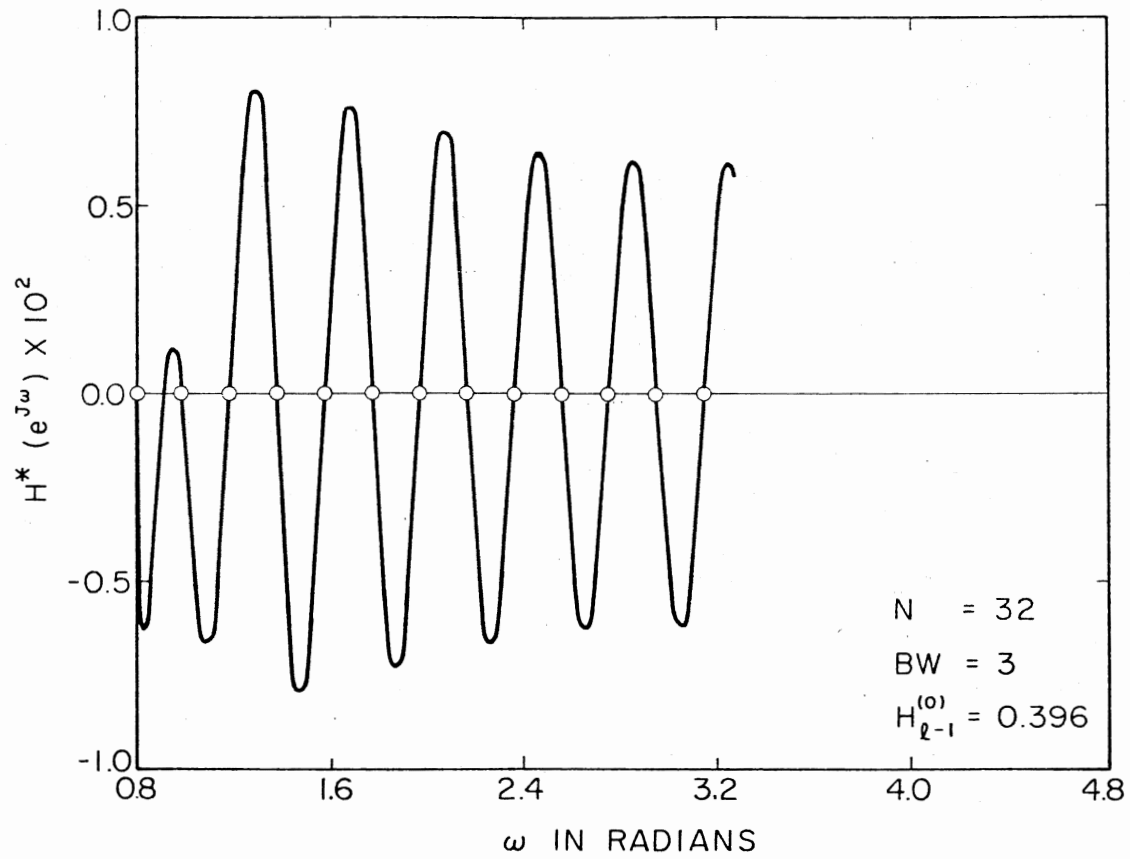


Figure 3(c). Stopband Response When Transition Sample is One (to an Enlarged Scale, N-Even)

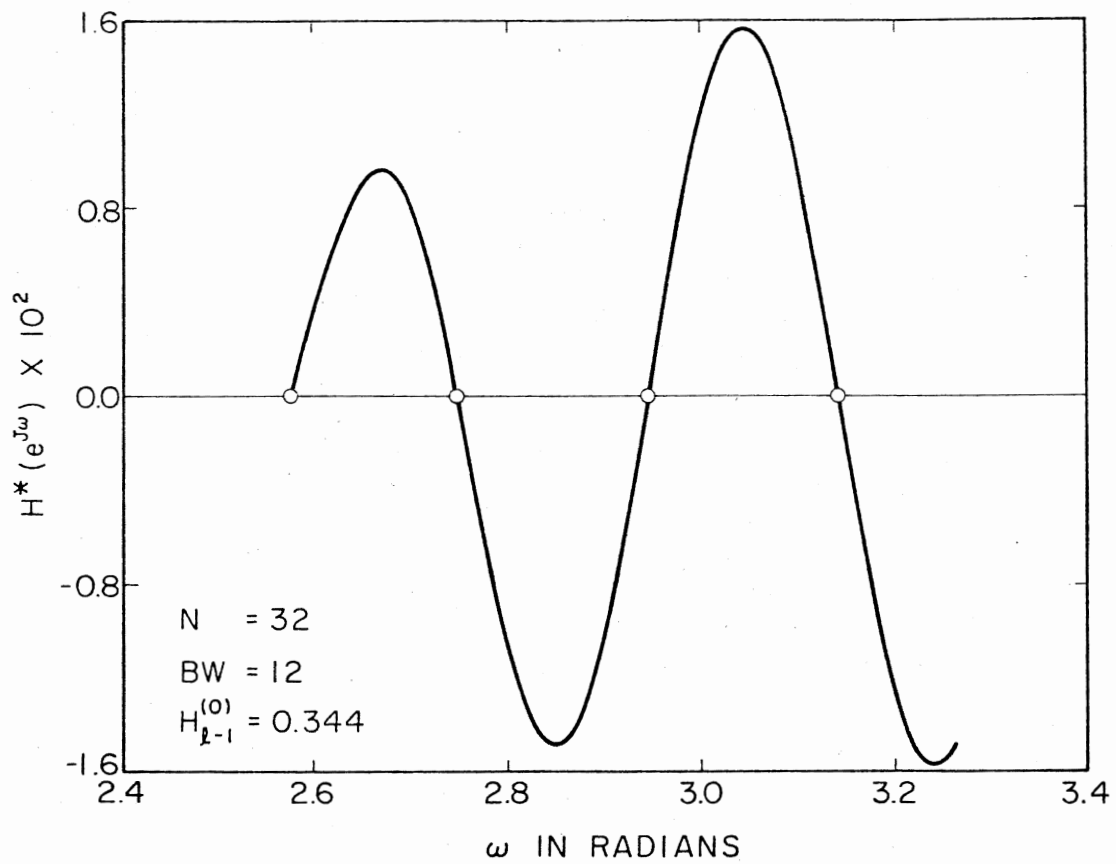


Figure 3(d). Stopband Response for N-Even, M = 1, and for $N/4 < BW < N/2$ (Enlarged Scale)

$\omega_{\ell 0} < \omega < \omega_{\ell+1}$, the peak of the response is small when compared to the other peaks in the stopband. In the rest of the stopband $H^{*(0)}(e^{j\omega})$, in general, alternates. Equations (3.15) and (3.16) are applicable even when N is even and it could be seen from Figure 3(c). In the third step we will make use of Equation (3.16) explicitly. The discussion for more than one transition sample will be presented in a later section.

3.3.3 Least Squares or a Direct Solution

From Figure 3 we see that $H^{*(0)}(e^{j\omega})$ has an almost equi-ripple property in the stopband. It is known that when the transition sample is optimum, the stopband characteristic of such a filter will have minimax characteristics (27). Using these two ideas, we can develop a direct solution to determine the transition sample close to an optimal solution.

In finding the solution, it is important to know the frequencies at which the peaks of $H^{*(0)}(e^{j\omega})$ appear in the stopband. Earlier we have seen that the peak of $H^{*(0)}(e^{j\omega})$, in the range $\omega_{\ell 0} < \omega < \omega_{\ell+1}$, is small and therefore Equation (3.15) could be used instead of Equation (3.16). In addition, we will assume that the peaks occur approximately midway between the sampling frequencies in the stopband. These frequencies are

$$\omega_{\ell+k}^0 = \frac{\omega_{\ell+k} + \omega_{\ell+k+1}}{2}, \quad k = 0, 1, 2, \dots$$

For simplicity we will consider only the first three values in Equation (3.17). Using Equations (3.15) and (3.17) and assuming that the magnitudes of the peaks at $\omega_{\ell+k}^0$ are equal, we can write

$$H^{*(0)}(e^{j\omega_{\ell}^0}) = H^{*(0)}(e^{j\omega_{\ell+1}^0}) \quad (3.18a)$$

$$H^*(o)(e^{j\omega_{\ell+1}^o}) = -H^*(o)(e^{j\omega_{\ell+2}^o}) \quad (3.18b)$$

Now,

$$H^*(o)(e^{j\omega_{\ell}^o}) = a_0 + b_0 H_{\ell-1}^{(o)} \quad (3.19a)$$

$$H^*(o)(e^{j\omega_{\ell+1}^o}) = a_1 + b_1 H_{\ell-1}^{(o)} \quad (3.19b)$$

$$H^*(o)(e^{j\omega_{\ell+2}^o}) = a_2 + b_2 H_{\ell-1}^{(o)} \quad (3.19c)$$

where a_i , $i = 0, 1, 2$ represent the contribution to $H^*(o)(e^{j\omega})$ by the sampled values in the passband, and b_i , $i = 0, 1, 2$ represent the contribution of the unconstrained frequency sample. Substituting Equation (3.19) into Equation (3.18), we have two equations in one unknown. Let this system of equations be written in the form

$$\underline{Y}_1 H_{\ell-1}^{(o)} = \underline{Y}_2 \quad (3.20)$$

where \underline{Y}_1 and \underline{Y}_2 are two-dimensional column vectors. The system in Equation (3.20) is an overdetermined system and can be solved by using the least squares solution (50). That is,

$$H_{\ell-1}^{(o)} = (\underline{Y}_1^T \underline{Y}_1)^{-1} \underline{Y}_1^T \underline{Y}_2 \quad (3.21)$$

where $(\underline{Y}_1^T \underline{Y}_1)$ is a scalar. Using this approach, we have considered the design of a 125th-order and a 256th-order low-pass filter with various values of BW. These are tabulated in Table I, where $H_{\ell-1}^{(R)}$ represents the optimum values obtained by Rabiner and others (27), and $H_{\ell-1}^{(o)}$ are the values obtained by the procedure above.

TABLE I
TRANSITION SAMPLE VALUES

BW	$H_{\ell-1}^{(R)}$	$H_{\ell-1}^{(o)}$	$H_{\ell-1}^{(oc)}$
<u>N = 125</u>			
1	0.42899170	0.43529550	0.42608080
2	0.40867310	0.41466430	0.40406560
3	0.39868774	0.40454840	0.39353060
4	0.39268189	0.39855650	0.38736720
6	0.38579101	0.39181060	0.38049300
8	0.38195801	0.38812720	0.37667780
10	0.37954102	0.38583630	0.39447340
<u>N = 256</u>			
1	0.42891235	0.43520000	0.42604190
5	0.38829956	0.39440000	0.38314000
7	0.38311157	0.38946000	0.37813000
18	0.37368774	0.38102900	0.36967530
66	0.36708985	0.37747100	0.36614250
98	0.36352539	0.37878400	0.36743760

Note that the results are remarkably close for this method, and better results may be obtained by considering the following:

1. Ripple maxima and minima may not appear midway between the stop-band sample frequencies, and therefore a procedure needs to be developed to find the frequencies at which the ripples in the stopband are maximum and minimum.

2. It may be necessary to consider more (or maybe less number of) equations in Equation (3.20). That is, we need to consider more (less) number of $\omega'_{\ell+k}$ in the stopband.

The second consideration does not require additional explanation. However, the first one requires further study.

Earlier it was expressed that when a function is approximated by Fourier series, there will be a considerable error in the vicinity of discontinuity, which is usually referred to as the Gibbs phenomenon (21). The lower bound on the overshoot after discontinuity is approximately 9%. Figure 4 shows a plot of $\beta(t) = [\frac{1}{2} + \frac{1}{\pi} \text{si}(\Omega t)]$, which corresponds to the approximation of a discontinuity at the origin. It is clear that the maxima and minima appear at $\Omega t = \pm k\pi$. However, we are more interested in values of Ωt for which

$$\beta(t) = 1 \quad (3.22)$$

These can be estimated by making use of extensive tables (64) (65) available for $\text{si}(\Omega t)$. Using these tables, we can estimate that the first peak overshoot appears not at the middle but to the left of the middle. To be exact, the peak separates the first ripple by 41.7% to the left and 58.3% to the right. This idea can be used in our estimation, and is discussed in the following.

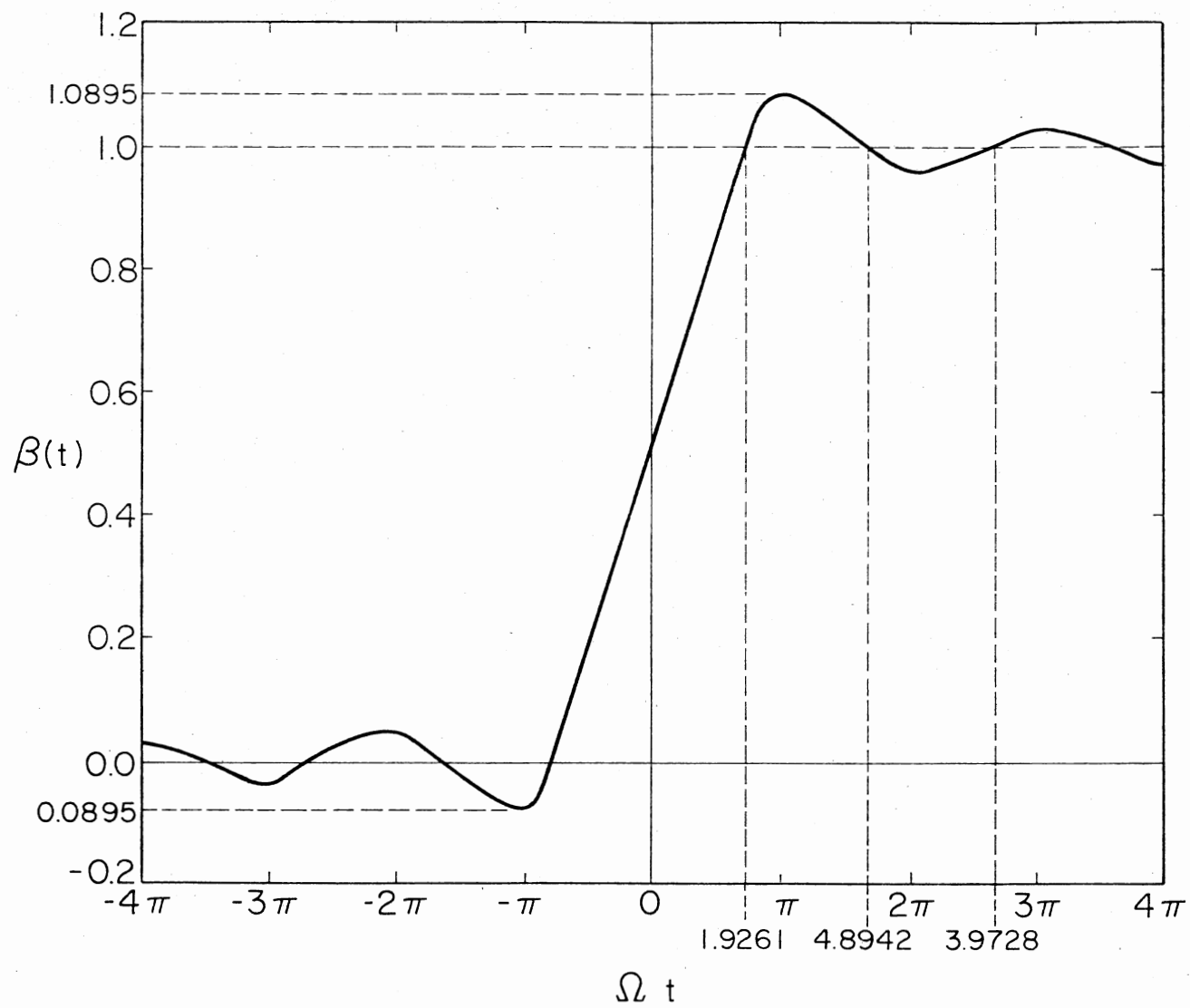


Figure 4. Plot of $\beta(t)$ Around a Step Discontinuity

Using the result above, we can modify Equation (3.17) by

$$\omega_{\ell+k}^{oc} = \omega_{\ell} + c(0.417) \frac{2\pi}{N} + k \frac{2\pi}{N}, k = 0, 1, 2 \quad (3.23)$$

in which a correction factor, c , is introduced. The reasons for this will be discussed in the following.

In Figure 4 we see that $\beta(o) = 0.5$. In our case the transition sample, always less than 0.5, is around 0.4. The effect of this, of course, is that the maximum appears even further left of the middle. An estimate of the correction factor is

$$c \approx \frac{0.4}{0.5} = 0.8 \quad (3.24)$$

Using this in Equation (3.23), we have considered a low-pass filter of order 125 and 256 with various BWs. The values for $H_{\ell-1}^{(o)}$ are obtained and are listed in Table I under the column $H_{\ell-1}^{(oc)}$, where c denotes that a correction has been used. In comparison with the optimum values $H_{\ell-1}^{(R)}$, we see that in most cases the new values $H_{\ell-1}^{(oc)}$ appear to be close to the optimum. Using the above approach, we have designed several low-pass filters for various values of N and BW. The results are tabulated in Table II, where again $H_{\ell-1}^{(R)}$ are the optimal values obtained by Rabiner et al. (27), and the values under the column $H_{\ell-1}^{(De)}$ and $H_{\ell-1}^{(Do)}$ will be discussed later.

When N is even, it can be observed from Table II that the deviation between $H_{\ell-1}^{(R)}$ and $H_{\ell-1}^{(oc)}$ is slightly higher when the number of frequency samples in the passband is close to $N/2$. The reason for this is explained in the following.

It is well known that when N is even, the interpolated frequency response will not be real if the initial set of frequency samples is

TABLE II
OPTIMUM TRANSITION SAMPLE VALUES

BW	$H_{\ell-1}^{(R)}$	$H_{\ell-1}^{(oc)}$	$H_{\ell-1}^{(Do)}$
<u>For N-Odd</u>			
<u>N = 15</u>			
1	0.43378296	0.42920700	0.43346862
2	0.41793823	0.41009000	0.41653264
3	0.41047363	0.40242000	0.40939952
4	0.40405884	0.39880000	0.40405603
5	0.39268189	0.39250000	0.37918409
<u>N = 33</u>			
1	0.42994995	0.42674300	0.42995013
2	0.41042481	0.40537800	0.41042692
3	0.40141601	0.39549600	0.40122466
4	0.39641724	0.39002100	0.39603561
6	0.39161377	0.38470240	0.39097806
8	0.39039917	0.38299130	0.38950116
10	0.39192505	0.38351930	0.39037723
12	0.39420166	0.38619210	0.39312706
14	0.38552246	0.38542000	0.37217282
<u>N = 65</u>			
1	0.42919312	0.42621640	0.42919106
2	0.40903320	0.40433500	0.40903274
3	0.39920654	0.39393290	0.39920496
4	0.39335937	0.38790240	0.39336220
5	0.38950806	0.38400590	0.38950763
6	0.38679809	0.38130680	0.38679813
10	0.38129272	0.37592600	0.38129346
14	0.37946167	0.37412750	0.37946531
18	0.37955322	0.37399500	0.37945672
22	0.38162842	0.37541910	0.38122190

TABLE II (Continued)

BW	$H_{\ell-1}^{(R)}$	$H_{\ell-1}^{(oc)}$	$H_{\ell-1}^{(Do)}$
<u>N = 65 (Cont.)</u>			
26	0.38746948	0.37956000	0.38615039
30	0.38417358	0.38408400	0.37087156
<u>N = 125</u>			
1	0.42899170	0.42608080	0.42899550
2	0.40867310	0.40406560	0.40867287
3	0.39868774	0.39353060	0.39868668
4	0.39268189	0.38736720	0.39268554
6	0.38579101	0.38049300	0.38579451
8	0.38195801	0.37677840	0.38196192
10	0.37954102	0.37447340	0.37954102
18	0.37518311	0.37041350	0.37518569
26	0.37384033	0.36917000	0.37384185
34	0.37371826	0.36902000	0.37372071
42	0.37470093	0.36984000	0.37470245
50	0.37797851	0.37250870	0.37788435
58	0.39086304	0.38307200	0.38983071
59	0.39063110	0.38556700	0.39062951
60	0.38383713	0.38375300	0.37054450

BW	$H_{\ell-1}^{(R)}$	$H_{\ell-1}^{(oc)}$	$H_{\ell-1}^{(De)}$
----	--------------------	---------------------	---------------------

For N-EvenN = 16

1	0.42631836	0.42880000	0.42727875
2	0.40397949	0.40940000	0.40216017
3	0.39454346	0.40157000	0.39109158
4	0.38916626	0.39810400	0.38693690
5	0.38840330	0.39550000	0.40860000

TABLE II (Continued)

BW	$H_{\ell-1}^{(R)}$	$H_{\ell-1}^{(oc)}$	$H_{\ell-1}^{(De)}$
<u>N = 32</u>			
1	0.42856445	0.42678000	0.42830446
2	0.40773926	0.40540000	0.40327667
3	0.39662476	0.39562000	0.39178876
4	0.38925171	0.39020000	0.38557173
6	0.37897949	0.38500000	0.37946214
8	0.36990356	0.38340000	0.37681379
10	0.35928955	0.38400000	0.37563255
12	0.34487915	0.38700000	0.37692103
<u>N = 64</u>			
1	0.42882080	0.42622200	0.42850086
2	0.40830689	0.40424000	0.40341969
3	0.39807129	0.39394900	0.39177515
4	0.39177246	0.38792560	0.38535508
5	0.38742065	0.38403500	0.38139820
6	0.38416748	0.38134260	0.37876661
10	0.37609863	0.37599470	0.37378359
14	0.37089233	0.37424370	0.37206568
18	0.36605225	0.37420320	0.37155465
22	0.35977783	0.37580000	0.37179844
26	0.34813232	0.38000000	0.37268141
<u>N = 128</u>			
1	0.42889404	0.42607840	0.42854521
2	0.40847778	0.40406140	0.40344362
3	0.39838257	0.39352350	0.39175112
4	0.39226685	0.38735920	0.38527050
6	0.38812256	0.38332170	0.38124616
7	0.38281250	0.37837620	0.37661885
10	0.37826538	0.37445240	0.37322903
18	0.37251587	0.37036780	0.36999435

TABLE II (Continued)

BW	$H_{\ell-1}^{(R)}$	$H_{\ell-1}^{(oc)}$	$H_{\ell-1}^{(De)}$
<u>N = 128 (Cont.)</u>			
26	0.36941528	0.36908680	0.36900837
34	0.36686401	0.36887300	0.36874944
42	0.36394653	0.36953970	0.36897358
50	0.35902100	0.37171600	0.36985400
58	0.34273681	0.37958000	0.37206699
<u>N = 256</u>			
1	0.42891235	0.42604190	0.42853700
2	0.40852051	0.40399000	0.40345060
3	0.39646802	0.39341690	0.39174000
4	0.39239502	0.38721000	0.38524750
5	0.38829956	0.38314000	0.38119940
7	0.38311157	0.37813000	0.37654140
10	0.37877197	0.37409000	0.37309460
11	0.37778931	0.37320840	0.37237480
18	0.37368774	0.36967530	0.36967770
34	0.37011490	0.36708280	0.36786230
50	0.36840210	0.36630580	0.36736040
58	0.36773071	0.36617150	0.36724360
66	0.36708985	0.36614250	0.36723540
83	0.36568604	0.36639920	0.36739600
98	0.36352539	0.36743760	0.36787210
106	0.36150513	0.36864000	0.36839050
114	0.35722650	0.37116000	0.36954100

real and symmetric (27). If the impulse response is symmetrical, it can be seen from Figure 5 that the frequency response will not be symmetrical about the $(N/2)$ frequency sample. On account of this, when $BW \leq (N/4)$, the interaction of $\frac{\sin x}{x}$ terms will be smaller and Equation (3.16) still holds good.

On the other hand, when $(N/4) < BW < (N/2)$, the interaction of $\frac{\sin x}{x}$ terms will be predominant and the stopband response will be as shown in Figure 3(d). From this figure it is clear that $H^*(0) e^{j\omega}$ will have the following pattern, that is,

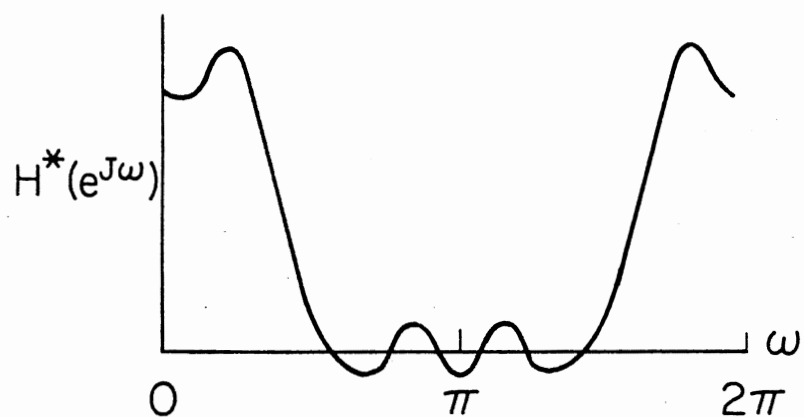
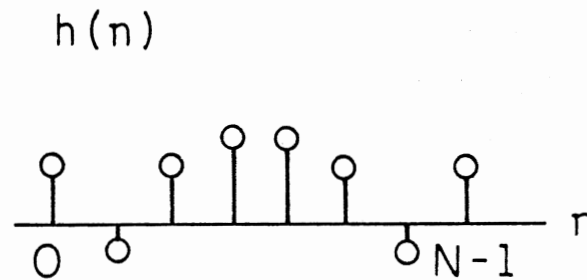
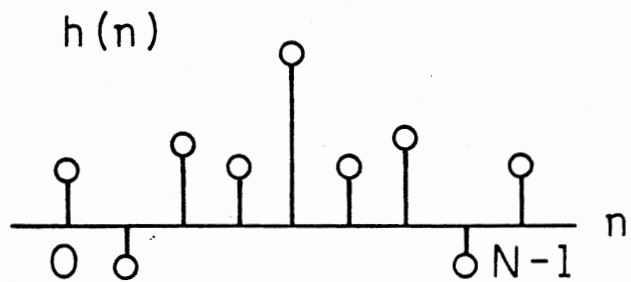
$$H^*(0) e^{j\omega} \begin{cases} > 0 & \omega_{\ell} < \omega < \omega_{\ell+1} \\ < 0 & \omega_{\ell+1} < \omega < \omega_{\ell+2} \\ > 0 & \omega_{\ell+2} < \omega < \omega_{\ell+3} \end{cases} \quad (3.25)$$

Using this, Equation (3.18) can be modified, and is

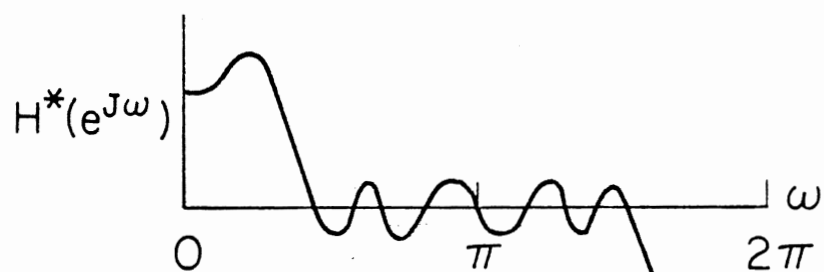
$$\begin{aligned} H^*(0) (e^{j\omega'_{\ell}}) &= -H^*(0) (e^{j\omega'_{\ell+1}}) \\ H^*(0) (e^{j\omega'_{\ell+1}}) &= -H^*(0) (e^{j\omega'_{\ell+2}}) \end{aligned} \quad (3.26)$$

Using Equation (3.19) in Equation (3.26) results in an equation similar to Equation (3.20), which could be solved for $H_{\ell-1}^{(0)}$. Note that in Equation (3.26) ω'_{ℓ} and $\omega'_{\ell+1}$ are given by Equation (3.17). Several low-pass filters are designed for the special cases, $(N/4) < BW < (N/2)$, by the above approach and the results are tabulated in Table III.

From Tables II and III it can be observed that the results are very close to the optimum, and are obtained without making use of search or programming techniques. In order to get an idea about the error involved in our computation, the frequency response of a 32nd-order low-pass filter is plotted for $BW = 10$. Two responses are plotted in



CASE 1 (N-ODD)



CASE 2 (N-EVEN)

Figure 5. Two Cases of Linear Phase Filters

TABLE III
ONE TRANSITION SAMPLE VALUES

BW	$H_{\ell-1}^{(R)}$	$H_{\ell-1}^{(O)}$
<u>N = 256</u>		
114	0.35726560	0.3505166
122	0.34083862	0.3373798
123	0.33485107	0.3287998
124	0.32495117	0.3125050
<u>N = 64</u>		
22	0.35977783	0.3482340
26	0.34813232	0.3374392
<u>N = 128</u>		
50	0.35902100	0.3505377
58	0.34273681	0.3373839

Figure 6 on the same scale for both $H_{\ell-1}^{(R)}$ and $H_{\ell-1}^{(oc)}$. From this figure it can be seen that the deviation between the two responses is hardly noticeable. The above method has a considerable advantage over the existing techniques (27).

In the following a direct solution to find the optimum transition value $H_{\ell-1}^{(De)}$ or $H_{\ell-1}^{(Do)}$ is discussed. This is based on using fewer number of equations in Equation (3.20). Since there is only one unknown $H_{\ell-1}^{(D)}$, we need to consider only one equation. This equation may correspond to one of the following equations (see Equation (3.18)):

$$H_{\ell-1}^{*(D)}(e^{j\omega_{\ell}^D}) = H_{\ell}^{*(D)}(e^{j\omega_{\ell+1}^D}) \quad (3.27a)$$

$$H_{\ell}^{*(D)}(e^{j\omega_{\ell+1}^D}) = -H_{\ell+1}^{*(D)}(e^{j\omega_{\ell+2}^D}) \quad (3.27b)$$

$$H_{\ell}^{*(D)}(e^{j\omega_{\ell}^D}) = -H_{\ell+1}^{*(D)}(e^{j\omega_{\ell+2}^D}) \quad (3.27c)$$

where the superscript D is introduced to denote the direct solution, and the $\omega_{\ell+k}^D$, $\omega_{\ell+k-1}^D < \omega_{\ell+k}^D < \omega_{\ell+k}^D$, $k = 0, 1, 2$ correspond to the frequencies at which the response has a ripple maxima and minima in the stopband.

These frequencies are given later. From the analysis of various optimal responses, it was found that Equation (3.27b) gave better results for N-even and Equation (3.27c) gave better results for N-odd. In the following, Equation (3.27b) is used for N-even and Equation (3.27c) for N-odd. Explicitly,

$$H_{\ell}^{*(De)}(e^{j\omega_{\ell+1}^{De}}) = -H_{\ell+1}^{*(De)}(e^{j\omega_{\ell+2}^{De}}) \quad (3.28a)$$

$$H_{\ell}^{*(Do)}(e^{j\omega_{\ell}^{Do}}) = -H_{\ell+1}^{*(Do)}(e^{j\omega_{\ell+2}^{Do}}) \quad (3.28b)$$

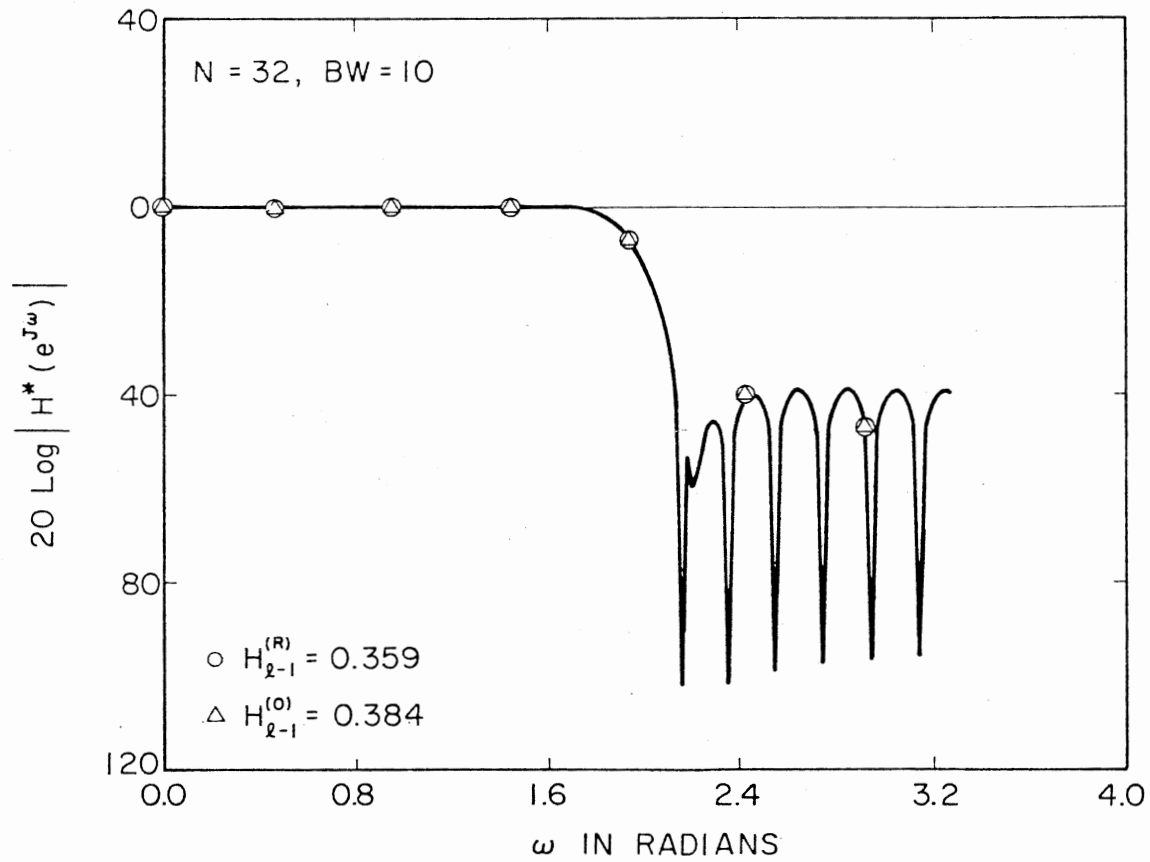


Figure 6. Frequency Response of a Low-Pass Filter for Values of $H_{\ell-1}^{(O)}$ and $H_{\ell-1}^{(R)}$.

where e and o are added to the superscript D to denote the even and odd cases, respectively.

The frequencies $\omega_{\ell+k}^{De}$ and $\omega_{\ell+k}^{Do}$ are determined empirically using $\omega_{\ell+k}^{OC}$ as a guide, and these are

$$\omega_{\ell+1}^{De} = \omega_{\ell+1} + 0.4375 \left(\frac{2\pi}{N} \right) \quad (3.29a)$$

$$\omega_{\ell+2}^{De} = \omega_{\ell+1}^{De} + 0.8749 \left(\frac{2\pi}{N} \right) \quad (3.29b)$$

for N-even and for N-odd,

$$\omega_{\ell}^{Do} = \omega_{\ell} + 0.25 \left(\frac{2\pi}{N} \right) \quad (3.30a)$$

$$\omega_{\ell+2}^{Do} = \omega_{\ell}^{Do} + 2.249 \left(\frac{2\pi}{N} \right) \quad (3.30b)$$

Expressing (see Equation (3.19)):

$$H^*(De) (e^{j\omega_{\ell+k}^{De}}) = a_{ke} + b_{ke} H_{\ell-1}^{(De)}, \quad k = 1, 2 \quad (3.31)$$

$$H^*(Do) (e^{j\omega_{\ell+k}^{Do}}) = a_{ko} + b_{ko} H_{\ell-1}^{(Do)}, \quad k = 0, 2 \quad (3.32)$$

where a_{ke} (a_{ko}) represent the contribution to $H^*(De) (e^{j\omega_{\ell+k}^{De}})$ ($H^*(Do) (e^{j\omega_{\ell+k}^{Do}})$) by the sampled values in the passband and b_{ke} (b_{ko}) represent the contribution of the unconstrained frequency sample. Using Equations (3.29) and (3.31) in Equation (3.28a) results in one equation with unknown as $H_{\ell-1}^{(De)}$. Similar equations can be formed using Equations (3.30) and (3.32) in Equation (3.28) with $H_{\ell-1}^{(Do)}$ as unknown. Obviously, the solution will give the desired results. Several low-pass filters with various values of N and BW are designed and the results for $H_{\ell-1}^{(De)}$ and $H_{\ell-1}^{(Do)}$ are tabulated in Table II. From this table it can be seen that the direct method gives transition sample values close to the optimum values given

in Reference (27). The computational time required to design the low-pass FIR filter with one transition sample by the direct method is negligible when compared to the existing techniques. The results are accurate and they are within the permissible tolerance limits.

Before we consider two and three transition sample low-pass filter designs, we should point out that $\frac{d}{d\omega} H^*(e^{j\omega})$ can be used to compute a value for $H_{\ell-1}$ by equating it to zero near $\omega = \omega_{\ell+1}$ (see Figure 3(b) and 3(c)). The computational time required by this method is more than the above method and therefore is not discussed any further.

3.4 Direct Approach to the Frequency Sampling Filter Design With Two and Three Transition Samples

3.4.1 Two Transition Sample Design

In designing two transition frequency sampling filters, we will make use of some of the same general ideas as in the one-transition type. For this case $M=2$ in Equation (3.8), and the transition samples are located at $\omega_{\ell-2}$ and $\omega_{\ell-1}$. As before, the stopband starts at ω_{ℓ} . The ripple reduction in the two transition sample case can be illustrated by considering two functions:

$$[H^{*(i)}(e^{j\omega})]_p \text{ and } [H^{*(k)}(e^{j\omega})]_{(p+1)} \quad (3.33)$$

where the subscripts p and $(p+1)$ denote the size of BW. Intuitively, we can see that $[H^{*(i)}(e^{j\omega})]_{(p+1)}$ can be approximately obtained by shifting $[H^{*(i)}(e^{j\omega})]_p$ by $\frac{2\pi}{N}$, where N is the order of the filter. Also, from Figure 2, we note that $[H^{*(i)}(e^{j\omega})]_{(p+1)}$ alternates in the stopband for $H_{\ell-1}^{(i)} < 0.3$. From the above it follows that

$$[H^{*(i)}(e^{j\omega})]_p [H^{*(i)}(e^{j\omega})]_{(p+1)} < 0 \quad (3.34a)$$

for

$$\omega_{\ell+k} < \omega < \omega_{\ell+k+1}, \quad k = 0, 1, \dots \quad (3.34b)$$

and for

$$H_{\ell-1}^{(i)}, H_{\ell-2}^{(i)} < 0.3 \quad (3.35)$$

Again, Equation (3.34) gives a clue for ripple reduction. Now, consider two responses $[H^{*(i)}(e^{j\omega})]_p$ and $[H^{*(k)}(e^{j\omega})]_{(p+1)}$ with $H_{\ell-2}^{(i)}, H_{\ell-1}^{(k)} < 0.3$. By adding the two, we have

$$\frac{1}{2} [[H^{*(i)}(e^{j\omega})]_p + [H^{*(k)}(e^{j\omega})]_{p+1}] = [H^{*(o)}(e^{j\omega})]_{p+1} \quad (3.36)$$

where $[H^{*(o)}(e^{j\omega})]_{p+1}$ will have two transition samples $H_{\ell-1}^{(o)}$ and $H_{\ell-2}^{(o)}$, which are given by

$$H_{\ell-2}^{(o)} = \frac{1 + H_{\ell-2}^{(i)}}{2}, \quad H_{\ell-1}^{(o)} = \frac{H_{\ell-1}^{(k)} + 0}{2} \quad (3.37)$$

Figure 7(a) illustrates such an idea for $N = 33$ and $(p+1) = 6$. Figure 7(b) clearly gives the $[H^{*(o)}(e^{j\omega})]_{(p+1)}$ in the stopband to an enlarged scale. From this figure, it can be seen that

$$\begin{aligned}
 &< 0 && \omega_{\ell} < \omega < \omega_{\ell 0} \\
 &> 0 && \omega_{\ell 0} < \omega < \omega_{\ell+1} \\
 [H^{*(o)}(e^{j\omega})]_{(p+1)} = &< 0 && \omega_{\ell+1} < \omega < \omega_{\ell+2} \\
 &> 0 && \omega_{\ell+2} < \omega < \omega_{(\ell+2)0} \\
 &< 0 && \omega_{(\ell+2)0} < \omega < \omega_{\ell+3}
 \end{aligned} \quad (3.38)$$

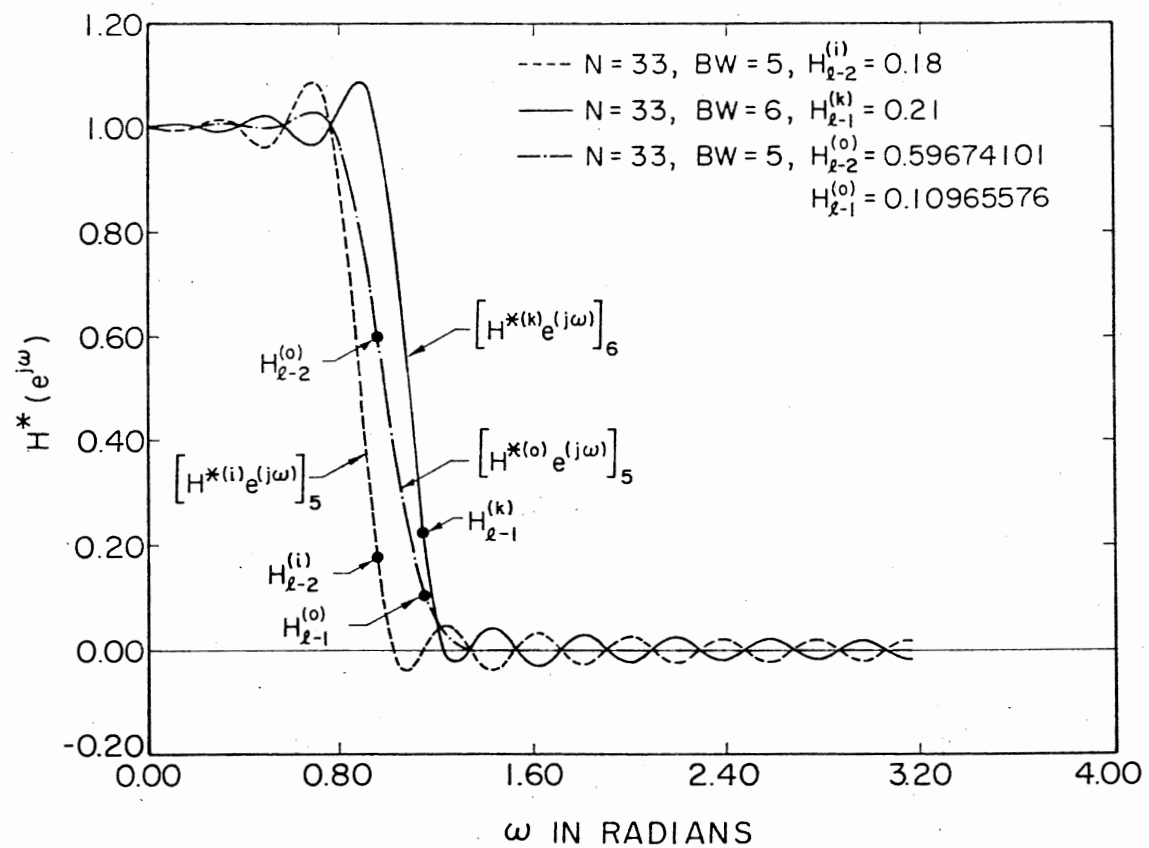


Figure 7(a). Frequency Response for Two Transition Samples

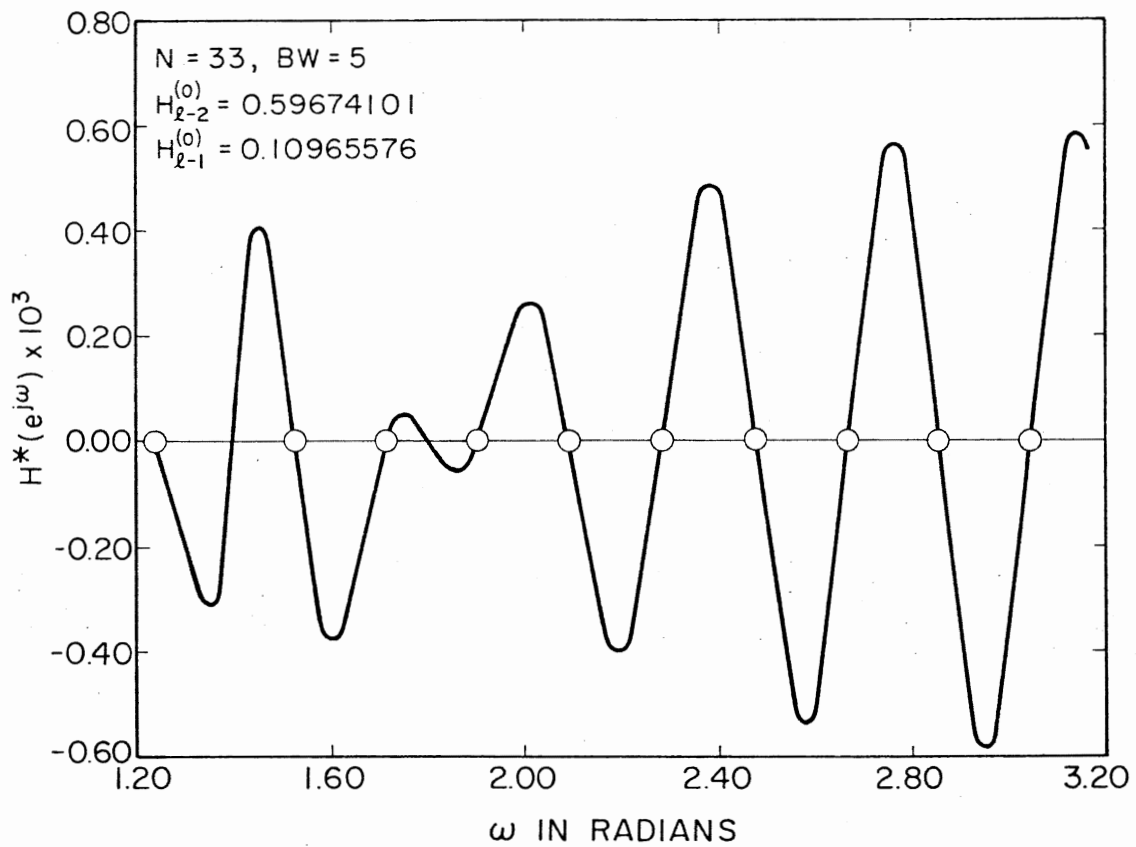


Figure 7(b). Stopband Response for Two Transition Samples (Enlarged Scale)

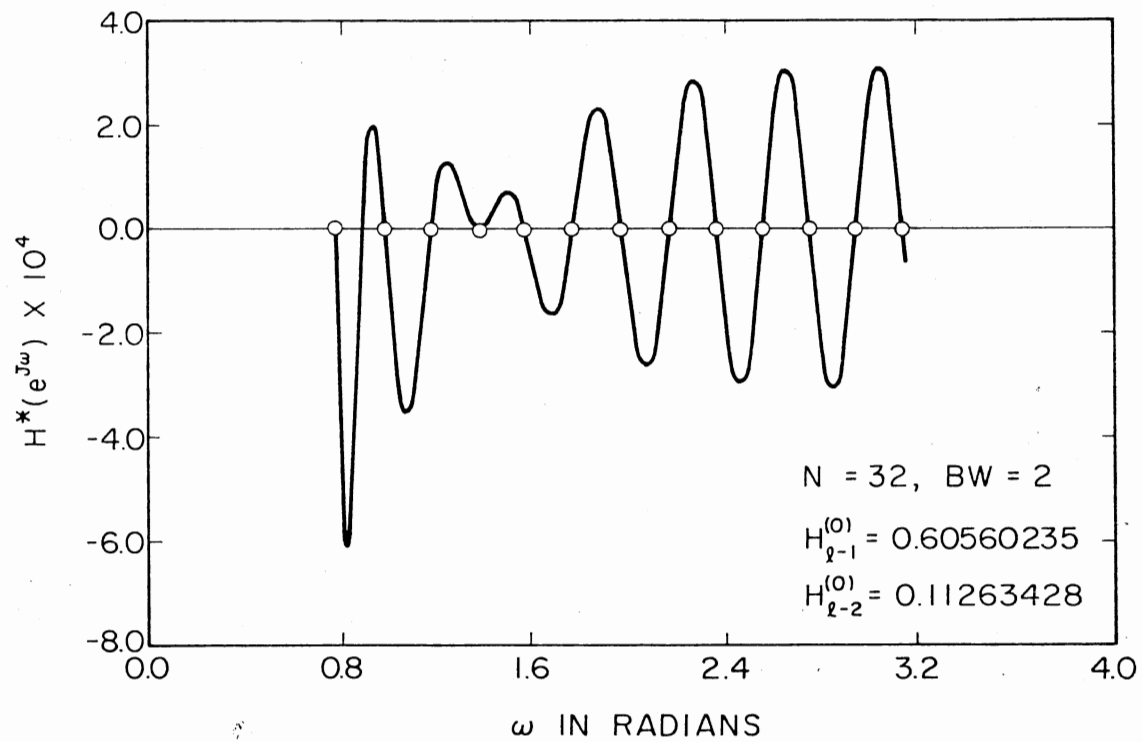


Figure 7(c). Stopband Response for Two Transition Samples
(to an Enlarged Scale, N-Even)

which has a similar pattern as in Equation (3.14). The difference is that in the range $\omega_{\ell 0} < \omega < \omega_{\ell+1}$, the peak is not small. In fact, $[H^{*(0)}(e^{j\omega})]_{(p+1)}$ has three peaks in the range $\omega_{\ell} < \omega < \omega_{\ell+2}$, and the magnitudes of these peaks are approximately equal. For simplicity, we will consider only the first three peaks. Equation (3.38) is the optimal response one would get using the transition sample values $H_{\ell-2}^{(0)}$ and $H_{\ell-1}^{(0)}$. In order to verify Equation (3.38) several responses were studied using the optimal values given in Reference (27) for various values of N and BW . From the results thus obtained, it is observed that Equation (3.38) is true in general for different values of N and BW . For illustrative purposes, a typical stopband response is given in Figure 7(c) for N -even. From this and other simulations it follows that Equation (3.38) is true for any N and forms a basis for the two-transition sample filter design.

Next, let us consider the computation of $H_{(\ell-1)}^{(0)}$ and $H_{(\ell-2)}^{(0)}$. The procedure will be very similar to what was used in the one-transition case. That is, assume that the first three peak ripple magnitudes in the stopband of $[H^{*(0)}(e^{j\omega})]_{p+1}$ are equal. Again, the problem of selecting the location of the frequencies at which the ripple maxima and minima appear should be considered. Using the optimal responses in Figure 7(b) and 7(c) as a guide, the location of the frequencies at which the ripple maxima and minima appear are empirically determined. These are given below.

The first three ripple peaks appear at $\omega_{\ell}^{(D)}$, $\omega_{\ell+1}^{(D)}$, and $\omega_{\ell+2}^{(D)}$, where the superscripts o and e after D are omitted here, as these estimates are valid for both N -odd and N -even. The estimates of these frequencies are given by

$$\omega_{\ell}^{(D)} = \omega_{\ell} + (0.125)\left(\frac{2\pi}{N}\right) \quad (3.39a)$$

$$\omega_{\ell'}^{(D)} = \omega_{\ell}^{(D)} + (0.5)\left(\frac{2\pi}{N}\right) \quad (3.39b)$$

$$\omega_{\ell+1}^{(D)} = \omega_{\ell'}^{(D)} + (0.81)\left(\frac{2\pi}{N}\right) \quad (3.39c)$$

Note that the bounds for these frequencies are given by

$$\omega_{\ell} < \omega_{\ell}^{(D)} < \omega_{\ell'}^{(D)} < \omega_{\ell+1} < \omega_{\ell+1}^{(D)} < \omega_{\ell+2} \quad (3.40)$$

Using Equations (3.38) and (3.39) and assuming that the magnitudes of the peaks are equal, we can write

$$[H^{*(D)}(e^{j\omega_{\ell}^{(D)}})]_{(p+1)} = -[H^{*(D)}(e^{j\omega_{\ell'}^{(D)}})]_{(p+1)} \quad (3.41a)$$

$$[H^{*(D)}(e^{j\omega_{\ell'}^{(D)}})]_{(p+1)} = -[H^{*(D)}(e^{j\omega_{\ell+1}^{(D)}})]_{(p+1)} \quad (3.41b)$$

where Equation (3.41) is valid for both N-even and N-odd. Expressing

$$[H^{*(D)}(e^{j\omega_{\ell}^{(D)}})]_{(p+1)} = c_1 + d_1 H_{\ell-2}^{(D)} + e_1 H_{\ell-1}^{(D)} \quad (3.42a)$$

$$[H^{*(D)}(e^{j\omega_{\ell'}^{(D)}})]_{(p+1)} = c_2 + d_2 H_{\ell-2}^{(D)} + e_2 H_{\ell-1}^{(D)} \quad (3.42b)$$

$$[H^{*(D)}(e^{j\omega_{\ell+1}^{(D)}})]_{(p+1)} = c_3 + d_3 H_{\ell-2}^{(D)} + e_3 H_{\ell-1}^{(D)} \quad (3.42c)$$

where c_i , $i = 1, 2, 3$ represent, respectively, the contributions of

$[H^{*(D)}(e^{j\omega_{\ell}^{(D)}})]_{(p+1)}$, $[H^{*(D)}(e^{j\omega_{\ell'}^{(D)}})]_{(p+1)}$, and $[H^{*(D)}(e^{j\omega_{\ell+1}^{(D)}})]_{(p+1)}$

by the fixed frequency samples; the remaining constants d_1 , d_2 , d_3 ,

e_1 , e_2 , and e_3 are the contributions of the unconstrained frequency sam-

samples with magnitudes $H_{\ell-2}^{(D)}$ and $H_{\ell-1}^{(D)}$. Using Equation (3.40) in Equation (3.39) and rewriting, we have

$$\begin{bmatrix} d_1 + d_2 & e_1 + e_2 \\ d_2 + d_3 & e_2 + e_3 \end{bmatrix} \begin{bmatrix} H_{\ell-2}^{(D)} \\ H_{\ell-1}^{(D)} \end{bmatrix} = \begin{bmatrix} -c_1 - c_2 \\ -c_2 - c_3 \end{bmatrix} \quad (3.43)$$

which can be solved for $H_{\ell-2}^{(D)}$ and $H_{\ell-1}^{(D)}$. Several low-pass filters are designed and the transition sample values $H_{\ell-2}^{(D)}$ and $H_{\ell-1}^{(D)}$ are given in Table IV.

The values listed under columns $H_{(\ell-2)}^{(R)}$ and $H_{(\ell-1)}^{(R)}$ are optimal values derived by Rabiner et al. (27). From this table one can see that the values are remarkably close. Note that search or minimization techniques were not used. It should also be noted that for small N -even and for BW close to $N/2$, the deviation in the transition sample values from the optimum values is due to aliasing effects and due to the nonsymmetrical characteristics of $H^*(e^{j\omega})$. Better transition sample values can be obtained by using new estimates for $\omega_{\ell}^{(D)}$, $\omega_{\ell'}^{(D)}$, and $\omega_{\ell+1}^{(D)}$. For these cases the new estimates are

$$\omega_{\ell}^{(D)} = \omega_{\ell} + 0.3125 \left(\frac{2\pi}{N} \right) \quad (3.42a)$$

$$\omega_{\ell'}^{(D)} = \omega_{\ell}^{(D)} + 0.375 \left(\frac{2\pi}{N} \right) \quad (3.42b)$$

$$\omega_{\ell}^{(D)} = \omega_{\ell'}^{(D)} + 0.50004 \left(\frac{2\pi}{N} \right) \quad (3.42c)$$

With these estimates the new transition sample values are computed for $N = 16$ ($BW = 3, 4$) and $N = 32$ ($BW = 9, 11$). These are given in Table V.

TABLE IV
TWO TRANSITION SAMPLE VALUES

BW	$H_{\ell-2}^{(R)}$	$H_{\ell-1}^{(R)}$	$H_{\ell-2}^{(D)}$	$H_{\ell-1}^{(D)}$
<u>For N-Odd</u>				
<u>N = 15</u>				
1	0.58995418	0.09500122	0.58995337	0.09500232
2	0.59357118	0.10319824	0.59352681	0.10318392
3	0.58594327	0.10083618	0.58395463	0.10084408
4	0.55713120	0.08407593	0.56317058	0.08813473
<u>N = 33</u>				
1	0.58985167	0.09497070	0.58985929	0.09497613
2	0.59743846	0.10585937	0.59537561	0.10441781
3	0.59911696	0.10937500	0.59453670	0.10619281
5	0.59674101	0.10965576	0.59155094	0.10625999
7	0.59417456	0.10902100	0.58929708	0.10568568
9	0.58771575	0.10502930	0.58711423	0.10481077
11	0.58216391	0.10219727	0.58208476	0.10217219
13	0.54712777	0.08137207	0.55326598	0.08536127
<u>N = 65</u>				
1	0.58945943	0.09472656	0.58946148	0.09472834
2	0.59476127	0.10404663	0.59458334	0.10396935
3	0.59577449	0.10720215	0.59338077	0.10557326
4	0.59415763	0.10726929	0.59149978	0.10565666
5	0.59253047	0.10689087	0.58978958	0.10537314
9	0.58845983	0.10548706	0.58550574	0.10412983
13	0.58660485	0.10466309	0.58367202	0.10349931
17	0.58862042	0.10649414	0.58304811	0.10329365
21	0.58894575	0.10701904	0.58311895	0.10336377
25	0.58320831	0.10327148	0.58262735	0.10306064
29	0.54500379	0.08069458	0.55115460	0.08466417

TABLE IV (Continued)

BW	$H_{\ell-2}^{(R)}$	$H_{\ell-1}^{(R)}$	$H_{\ell-2}^{(D)}$	$H_{\ell-1}^{(D)}$
<u>N = 125</u>				
1	0.58933268	0.09464722	0.58934385	0.09465519
2	0.59450024	0.10390015	0.59433964	0.10383172
3	0.59508549	0.10682373	0.59300940	0.10537467
5	0.59187505	0.10668945	0.58916139	0.10505660
7	0.58921869	0.10587158	0.58631764	0.10424669
9	0.58738706	0.10523682	0.58434199	0.10357237
17	0.58358265	0.10372925	0.58051524	0.10211963
25	0.58224835	0.10316772	0.57921683	0.10160304
33	0.58198956	0.10303955	0.57893060	0.10150228
41	0.58245499	0.10313721	0.57399665	0.10172967
49	0.58629534	0.10561523	0.58082174	0.10238399
57	0.57812192	0.10061646	0.57803192	0.10058625
58	0.57121235	0.09663696	0.57126662	0.09667163
59	0.54451285	0.08054886	0.55061195	0.08448141
<u>For N-Even</u>				
<u>N = 32</u>				
1	0.59045212	0.09610596	0.58988240	0.09499410
2	0.60560235	0.11263428	0.59543000	0.10044850
3	0.61192546	0.11931763	0.59460925	0.10623170
5	0.61824023	0.12541540	0.59163184	0.10629000
7	0.62307031	0.12907715	0.58929679	0.10560000
9	0.60685586	0.12068481	0.58670064	0.10457000
11	0.62821502	0.13004150	0.57943200	0.10063924
<u>N = 64</u>				
1	0.58789222	0.09376831	0.58946641	0.09473140
2	0.59421778	0.10411987	0.59459348	0.10397500
3	0.59666158	0.10850220	0.59339614	0.10558140
4	0.59730067	0.11038818	0.59152036	0.10566730

TABLE IV (Continued)

BW	$H_{\ell-2}^{(R)}$	$H_{\ell-1}^{(R)}$	$H_{\ell-2}^{(D)}$	$H_{\ell-1}^{(D)}$
<u>N = 64 (Cont.)</u>				
5	0.59698469	0.11113281	0.58981536	0.10538610
9	0.59088884	0.10936890	0.58555322	0.10415263
13	0.58738641	0.10828857	0.58374478	0.10352740
17	0.58968142	0.11031494	0.58314984	0.10334070
21	0.59249461	0.11254273	0.58322245	0.10340800
25	0.60564501	0.11994629	0.58222502	0.10283880
<u>N = 128</u>				
1	0.58900996	0.09445190	0.58934177	0.09465390
2	0.59379058	0.10349731	0.59433531	0.10382928
3	0.59506081	0.10701294	0.59300277	0.10537113
4	0.59298926	0.10685425	0.59099137	0.10539417
6	0.58953845	0.10596924	0.58759487	0.10463720
9	0.58593906	0.10471191	0.58432116	0.10356242
17	0.58097354	0.10288086	0.58047248	0.10209992
25	0.57812308	0.10182495	0.57914333	0.10156955
33	0.57576437	0.10096436	0.57880629	0.10144500
41	0.57451694	0.10094604	0.57917334	0.10162944
49	0.56922742	0.09865112	0.58043051	0.10220660
57	0.56604486	0.09845581	0.58113628	0.10237700
<u>N = 256</u>				
1	0.58923281	0.09458618	0.58930945	0.09463381
2	0.59425391	0.10375977	0.59426790	0.10374125
3	0.59466635	0.10638569	0.59289944	0.10531596
4	0.59322120	0.10690918	0.59085178	0.10532224
6	0.58998313	0.10612793	0.58738212	0.10453226
9	0.58671387	0.10502319	0.58399667	0.10340100
10	0.58371956	0.10457764	0.58319479	0.10311341
17	0.58217779	0.10323486	0.57982439	0.10180166

TABLE IV (Continued)

BW	$H_{\ell-2}^{(R)}$	$H_{\ell-1}^{(R)}$	$H_{\ell-2}^{(D)}$	$H_{\ell-1}^{(D)}$
N = 256 (Cont.)				
33	0.57708094	0.10212250	0.57719087	0.10071614
49	0.57769495	0.10168457	0.57637271	0.10037250
57	0.57690264	0.10133057	0.57621581	0.10030700
65	0.57627586	0.10109253	0.57617069	0.10029070
81	0.57389784	0.09982910	0.57640019	0.10039707
97	0.56999568	0.09773560	0.57725989	0.10078435
105	0.56641188	0.09583130	0.57818400	0.10120000
113	0.56186695	0.09375000	0.57983000	0.10194000
121	0.54300842	0.08519897	0.58085830	0.10220000
122	0.54292957	0.08584595	0.57934000	0.10737000
123	0.54538271	0.08768921	0.57327400	0.09903600
124	0.56272902	0.09545975	0.56380568	0.09233555

TABLE V
MODIFIED "TRANSITION SAMPLE VALUES"

BW	$H_{(\ell-2)}^{(R)}$	$H_{(\ell-1)}^{(R)}$	$H_{(\ell-2)}^{(D)}$	$H_{(\ell-1)}^{(D)}$
<u>N = 16</u>				
3	0.62855407	0.12827148	0.60605460	0.11495370
4	0.61952704	0.12130127	0.59233985	0.10758616
<u>N = 32</u>				
9	0.60685586	0.12068481	0.60589392	0.11760846
11	0.62821502	0.13004150	0.59691813	0.11259700

From this table we can see that the new transition sample values are slightly closer to the optimal values. In addition, it should be pointed out that these cases are seldom used and are considered here only for completeness.

3.4.2 Three Transition Sample Design

The three transition sample filter design is a simple extension of the two transition sample design. Consider the three functions

$$[H^{*(i)}(e^{j\omega})]_p, [H^{*(k)}(e^{j\omega})]_{p+1}, [H^{*(n)}(e^{j\omega})]_{p+2} \quad (3.44)$$

with transition samples $H_{(\ell-3)}^{(i)}$, $H_{(\ell-2)}^{(k)}$, and $H_{(\ell-1)}^{(n)}$ and with

$$[H^{*(i)}(e^{j\omega})]_p [H^{*(k)}(e^{j\omega})]_{(p+1)} > 0 \quad \omega_{\ell+1} < \omega < \omega_{\ell+k+1} \quad (3.45)$$

$$k = 0, 1, \dots$$

$$[H^{*(k)}(e^{j\omega})]_{(p+1)} [H^{*(n)}(e^{j\omega})]_{(p+2)} < 0 \quad \omega_{\ell+k} < \omega < \omega_{\ell+k+1} \quad (3.46)$$

$$k = 0, 1, \dots$$

As before, by adding three of these responses, we will have ripple reduction. Figure 8(a) illustrates such an idea for $N = 32$ and $p = 2$. Note that other possibilities can also be considered. In Figure 8(a), $[H^{*(o)}(e^{j\omega})]_{(p+2)}$ is obtained from

$$[H^{*(o)}(e^{j\omega})]_{(p+2)} = \frac{1}{5} [3[H^{*(i)}(e^{j\omega})]_p + [H^{*(k)}(e^{j\omega})]_{p+1} + [H^{*(n)}(e^{j\omega})]_{(p+2)}] \quad (3.47)$$

Note the scale factors in each case. Figure 8(b) illustrates the enlarged version of $[H^{*(o)}(e^{j\omega})]_{(p+2)}$ in the stopband. From this figure,

$$< 0 \quad \omega_{\ell} < \omega < \omega_{\ell 0} \quad (3.48a)$$

$$> 0 \quad \omega_{\ell 0} < \omega < \omega_{\ell+1} \quad (3.48b)$$

$$< 0 \quad \omega_{\ell+1} < \omega < \omega_{(\ell+1)0} \quad (3.48c)$$

$$[H^{*(o)}(e^{j\omega})]_{p+2} = > 0 \quad \omega_{(\ell+1)0} < \omega < \omega_{\ell+2} \quad (3.48d)$$

$$< 0 \quad \omega_{\ell+2} < \omega < \omega_{\ell+3} \quad (3.48e)$$

$$> 0 \quad \omega_{\ell+3} < \omega < \omega_{\ell+4} \quad (3.48f)$$

Note again the sign pattern. From Figure 8(b) it is clear that the two peaks in the range $\omega_{\ell+1} < \omega < \omega_{\ell+2}$ are small compared to the other peaks. In our computation we will not use these two peaks. We will use the first, second, fifth, and sixth peaks in the stopband for computing $H_{\ell-i}^{(o)}$, $i = 1, 2, 3$. As before, we can locate the frequencies at which the ripple maxima and minima appear. Equation (3.48) is the optimal response one would obtain by using the transition sample values $H_{(\ell-3)}^{(o)}$,

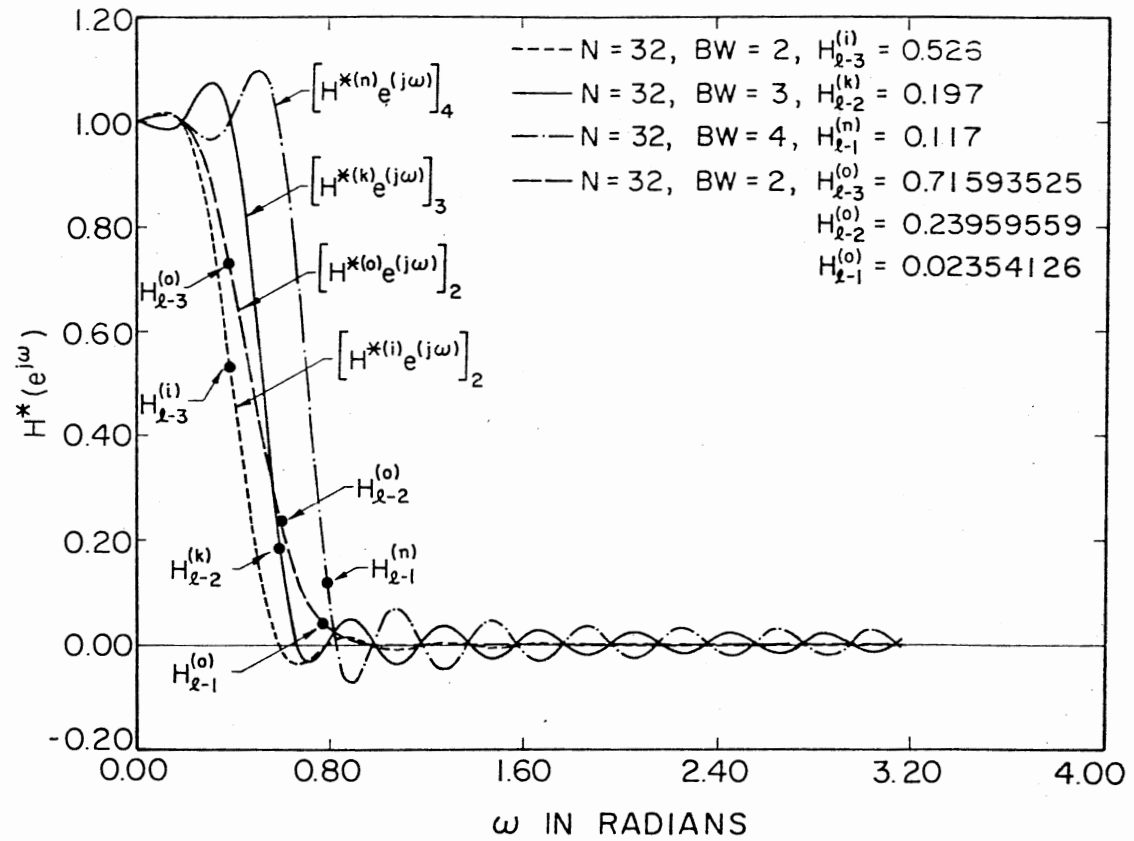


Figure 8(a). Stopband Frequency Response for Three Transition Samples Derived From Figure 1

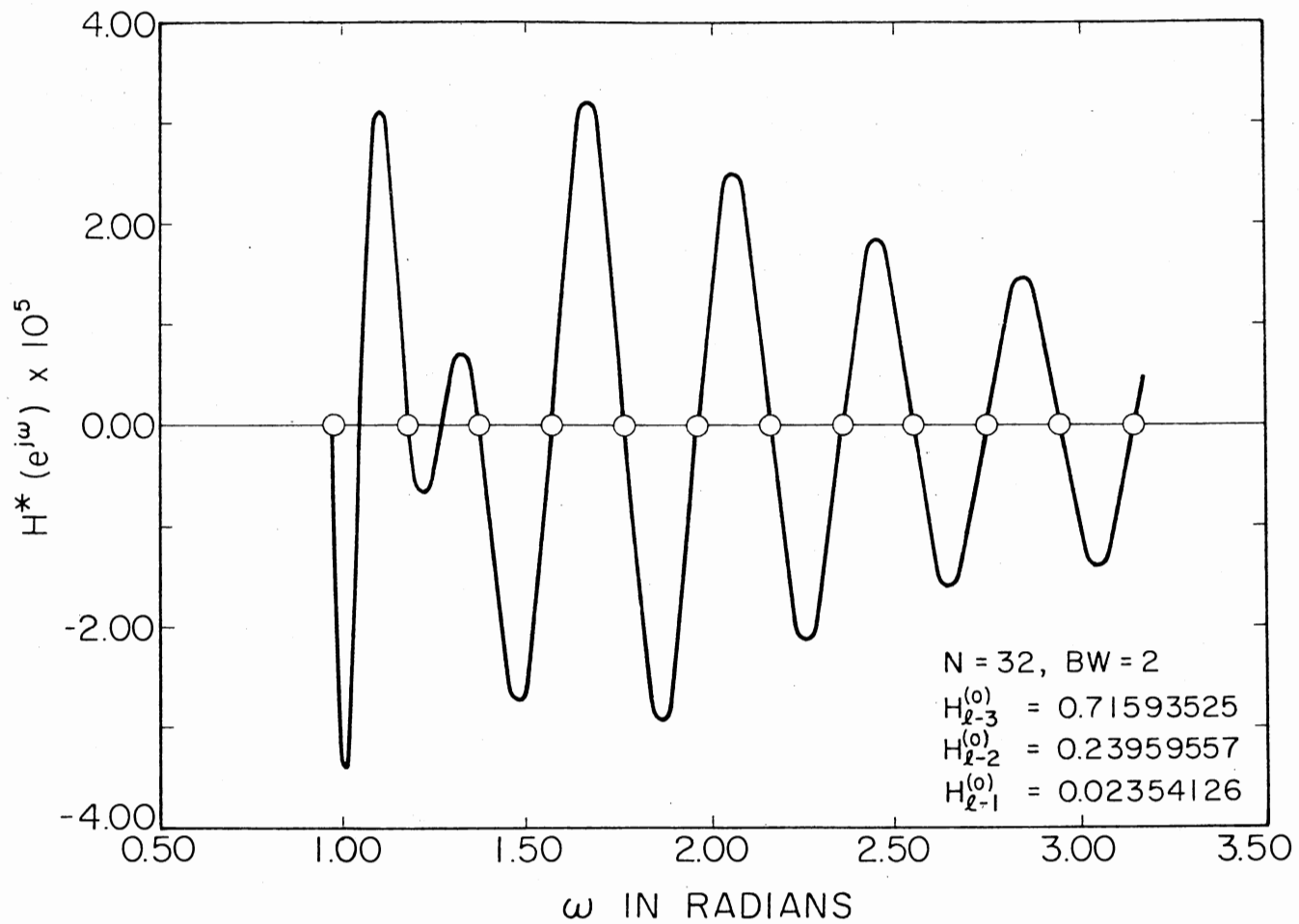


Figure 8(b). Stopband Response for Three Transition Samples (Enlarged Scale)

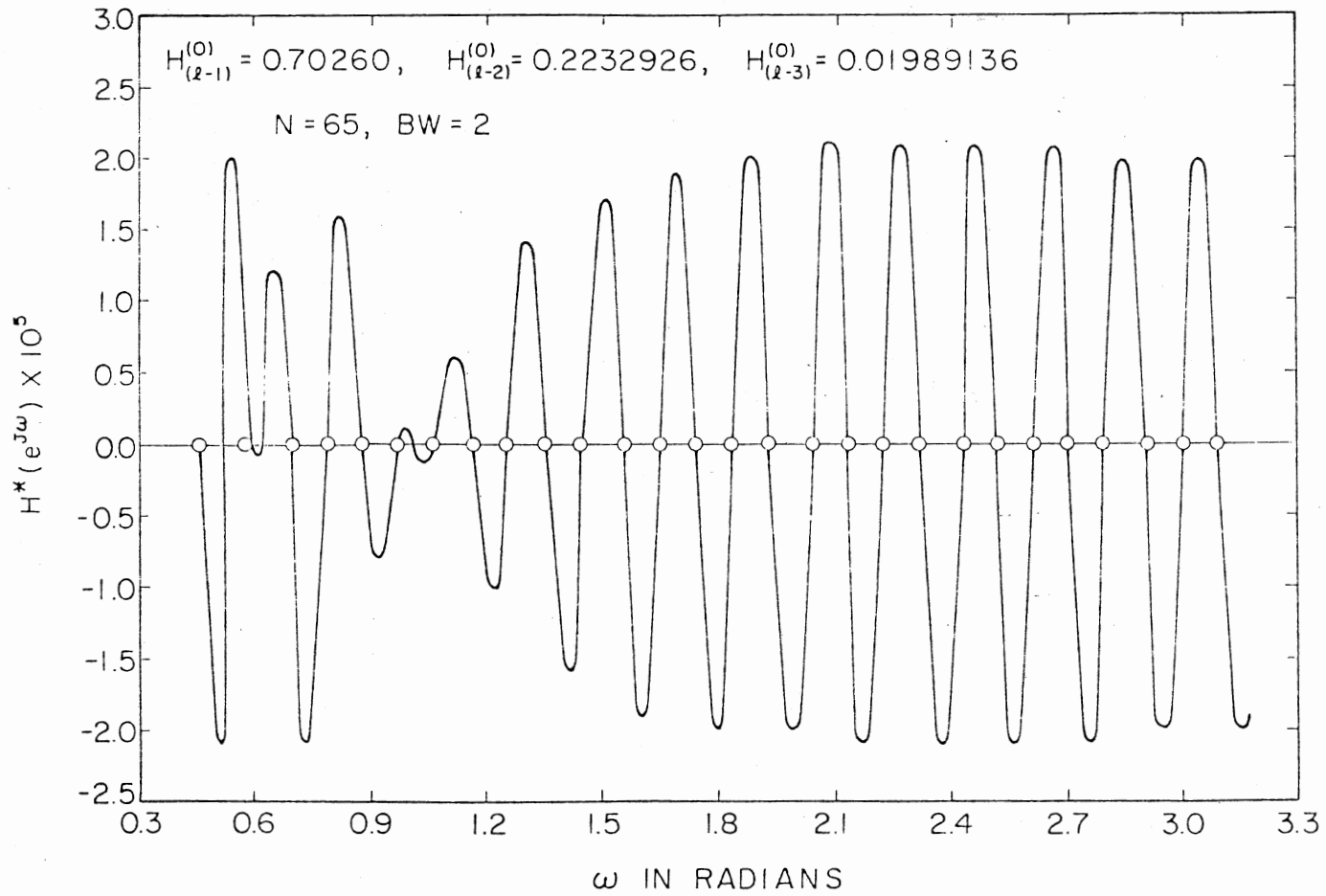


Figure 8(c). Stopband Response for Three Transition Samples (to an Enlarged Scale, N-Even)

$H_{(\ell-2)}^{(o)}$, and $H_{(\ell-1)}^{(o)}$. In order to verify Equation (3.48), several low-pass filters with three transition samples have been simulated using the transition sample values given in Reference (27) and found that, in general, Equation (3.48) is true for N-even. In the following, Equation (3.48) will form a basis for determining the optimum transition values for N-even. The odd case is discussed later.

Next, let us consider the computation of $H_{(\ell-1)}^{(o)}$, $H_{(\ell-2)}^{(o)}$, and $H_{(\ell-3)}^{(o)}$. The procedure will be similar to the two transition case. The first step is to determine the frequencies at which the ripple maxima and minima will appear. Using optimal response in Figure 8(b) as a guide, these frequencies are determined empirically.

Earlier it was pointed out that the first, second, fifth, and sixth peaks in the stopband will be used to determine $H_{\ell-i}^{(o)}$, $i = 1, 2, 3$. Let the frequencies at which these peaks appear be denoted by $\omega_{\ell}^{(De)}$, $\omega_{\ell'}^{(De)}$, $\omega_{\ell+2}^{(De)}$, and $\omega_{\ell+3}^{(De)}$, where the superscript De refers to the direct method of design for the even case. It is clear that the bounds for these frequencies are given by

$$\omega_{\ell} < \omega_{\ell}^{(De)} < \omega_{\ell'}^{(De)} < \omega_{\ell+1} < \omega_{\ell+2}^{(De)} < \omega_{\ell+3} < \omega_{\ell+3}^{(De)} < \omega_{\ell+4} \quad (3.49)$$

The estimates of these frequencies are:

$$\omega_{\ell}^{(De)} = \omega_{\ell} + 0.125 \left(\frac{2\pi}{N} \right) \quad (3.50a)$$

$$\omega_{\ell'}^{(De)} = \omega_{\ell}^{(De)} + 0.4375 \left(\frac{2\pi}{N} \right) \quad (3.50b)$$

$$\omega_{(\ell+2)}^{(De)} = \omega_{\ell'}^{(De)} + 2.0002 \left(\frac{2\pi}{N} \right) \quad (3.50c)$$

$$\omega_{(\ell+3)}^{(De)} = \omega_{(\ell+2)}^{(De)} + 0.9374 \left(\frac{2\pi}{N} \right) \quad (3.50d)$$

Using Equations (3.48) and (3.49) and assuming that the magnitude of the peaks are equal, we can write

$$[H^*(De) (e^{j\omega_{\ell}^{(De)}})]_{(p+2)} = -[H^*(De) (e^{j\omega_{\ell'}^{(De)}})]_{(p+2)} \quad (3.51a)$$

$$[H^*(De) (e^{j\omega_{\ell'}^{(De)}})]_{(p+2)} = -[H^*(De) (e^{j\omega_{(\ell+2)}^{(De)}})]_{(p+2)} \quad (3.51b)$$

$$[H^*(De) (e^{j\omega_{(\ell+3)}^{(De)}})]_{(p+2)} = -[H^*(De) (e^{j\omega_{(\ell+3)}^{(De)}})]_{(p+2)} \quad (3.51c)$$

Expressing

$$[H^*(De) (e^{j\omega_{\ell}^{(De)}})]_{(p+2)} = f_1 + g_1 H_{(\ell-3)}^{(De)} + h_1 H_{(\ell-2)}^{(De)} + i_1 H_{(\ell-1)}^{(De)} \quad (3.52a)$$

$$[H^*(De) (e^{j\omega_{\ell'}^{(De)}})]_{(p+2)} = f_2 + g_2 H_{(\ell-3)}^{(De)} + h_2 H_{(\ell-2)}^{(De)} + i_2 H_{(\ell-1)}^{(De)} \quad (3.52b)$$

$$[H^*(De) (e^{j\omega_{(\ell+2)}^{(De)}})]_{(p+2)} = f_3 + g_3 H_{(\ell-3)}^{(De)} + h_3 H_{(\ell-2)}^{(De)} + i_3 H_{(\ell-1)}^{(De)} \quad (3.52c)$$

$$[H^*(De) (e^{j\omega_{(\ell+3)}^{(De)}})]_{(p+2)} = f_4 + g_4 H_{(\ell-3)}^{(De)} + h_4 H_{(\ell-2)}^{(De)} + i_4 H_{(\ell-1)}^{(De)} \quad (3.52d)$$

where f_j , $j = 1, 2, 3, 4$ represent, respectively, the contribution of

$[H^*(De) (e^{j\omega_{\ell}^{(De)}})]_{(p+2)}$, $[H^*(De) (e^{j\omega_{\ell'}^{(De)}})]_{(p+2)}$, $[H^*(De) (e^{j\omega_{(\ell+2)}^{(De)}})]_{(p+2)}$, and $[H^*(De) (e^{j\omega_{(\ell+3)}^{(De)}})]_{(p+2)}$ by the fixed frequency samples; the remaining constants g_j , h_j , i_j , $j = 1, 2, 3, 4$ are the contributions of the

unconstrained frequency samples. Using Equation (3.52) in Equation (3.51) and rewriting, we have

$$\begin{bmatrix} (g_1 + g_2) & (h_1 + h_2) & (i_1 + i_2) \\ (g_2 + g_3) & (h_2 + h_3) & (i_2 + i_3) \\ (g_3 + g_4) & (h_3 + h_4) & (i_3 + i_4) \end{bmatrix} \begin{bmatrix} H_{(\ell-3)}^{(De)} \\ H_{(\ell-2)}^{(De)} \\ H_{(\ell-1)}^{(De)} \end{bmatrix} = \begin{bmatrix} -f_1 - f_2 \\ -f_2 - f_3 \\ -f_3 - f_4 \end{bmatrix} \quad (3.53)$$

which can be solved for $H_{(\ell-3)}^{(De)}$, $H_{(\ell-2)}^{(De)}$, and $H_{(\ell-1)}^{(De)}$. Several low-pass filters are designed and the transition sample values $H_{(\ell-3)}^{(De)}$, $H_{(\ell-2)}^{(De)}$, and $H_{(\ell-1)}^{(De)}$ are given in Table VI. The values are close to the optimal values.

For comparison purposes, the frequency response of a 256th-order low-pass filter is plotted in Figure 9 using the three transition samples derived above and using the optimal values obtained in Reference (27). From the figure it can be seen that the two responses are remarkably close. The peak ripple in the stopband is approximately the same by both methods and is -87.89 dB. Next, let us consider the odd case.

The procedure for N-odd is very similar to the even case. For $N = 65$, a typical optimal stopband response is plotted in Figure 8(c). This response satisfies the following:

$$[H^*(\omega)(e^{j\omega})]_{(p+2)} = \begin{cases} < 0 & \omega_{\ell} < \omega < \omega_{\ell 0} & (3.54a) \\ > 0 & \omega_{\ell 0} < \omega < \omega_{\ell+1} & (3.54b) \\ > 0 & \omega_{\ell+1} < \omega < \omega_{\ell+2} & (3.54c) \\ < 0 & \omega_{\ell+2} < \omega < \omega_{\ell+3} & (3.54d) \\ > 0 & \omega_{\ell+3} < \omega < \omega_{(\ell+3)_0} & (3.54e) \\ < 0 & \omega_{(\ell+3)_0} < \omega < \omega_{(\ell+4)} & (3.54f) \end{cases}$$

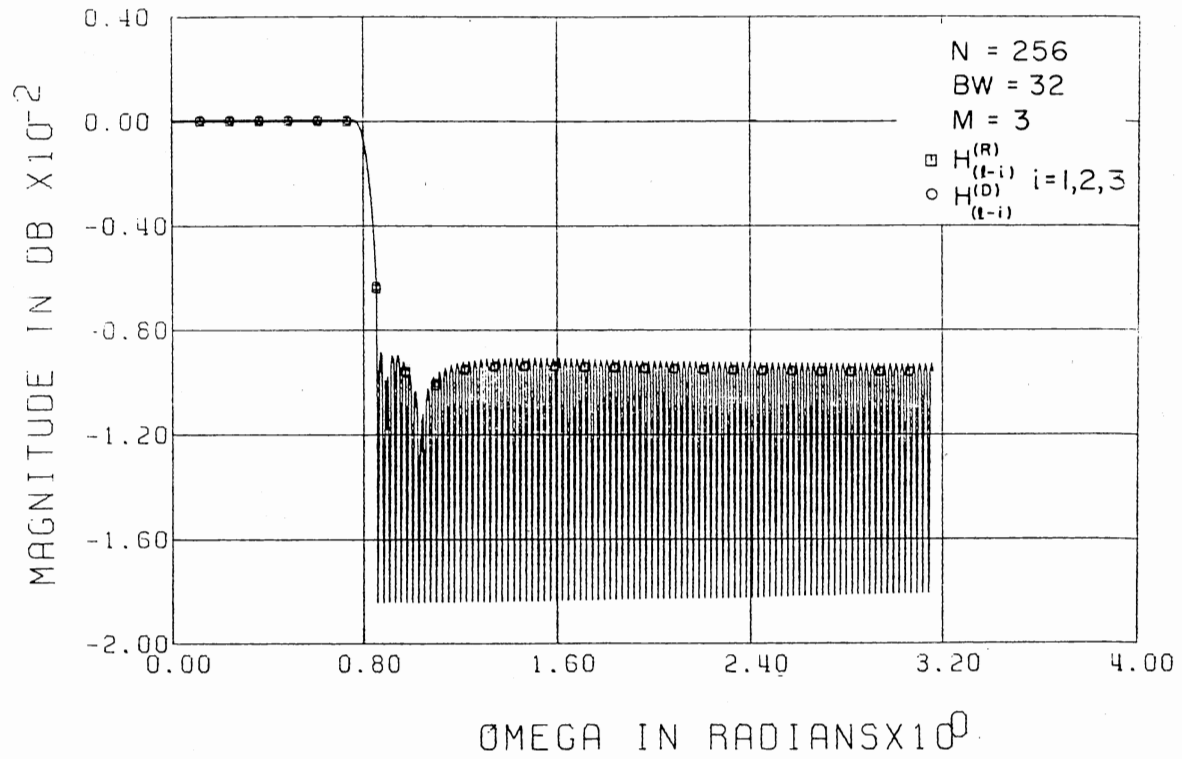


Figure 9. Frequency Response of a Low-Pass Filter

For computational purposes we will use the first four peaks for computing $H_{\ell-i}^{(0)}$, $i = 1, 2, 3$. Let the frequencies at which these peaks appear be denoted by $\omega_{\ell}^{(Do)}$, $\omega_{\ell'}^{(Do)}$, $\omega_{\ell+1}^{(Do)}$, and $\omega_{\ell+2}^{(Do)}$, where the superscript Do refers to the direct method of design for the odd case. It is clear that the bounds for these frequencies are given by

$$\omega_{\ell} < \omega_{\ell}^{(Do)} < \omega_{\ell'}^{(Do)} < \omega_{\ell+1} < \omega_{\ell+1}^{(Do)} < \omega_{\ell+2} < \omega_{\ell+2}^{(Do)} < \omega_{\ell+3} \quad (3.55)$$

The estimates of these frequencies are

$$\omega_{\ell}^{(Do)} = \omega_{\ell} + 0.125 \left(\frac{2\pi}{N}\right) \quad (3.56a)$$

$$\omega_{\ell'}^{(Do)} = \omega_{\ell}^{(Do)} + 0.5 \left(\frac{2\pi}{N}\right) \quad (3.56b)$$

$$\omega_{(\ell+1)}^{(Do)} = \omega_{\ell'}^{(Do)} + 0.875 \left(\frac{2\pi}{N}\right) \quad (3.56c)$$

$$\omega_{(\ell+2)}^{(Do)} = \omega_{(\ell+1)}^{(Do)} + \left(\frac{2\pi}{N}\right) \quad (3.56d)$$

Using Equation (3.54) as a guide and equating the ripple magnitude at the frequencies given in Equation (3.56), and following a procedure similar to the even case, the transition sample values $H_{\ell-i}^{(Do)}$, $i = 1, 2, 3$ can be obtained. Using this procedure, several low-pass filters are designed and the transition sample values are compared with the optimal values given in Reference (27). These are listed in Table VI. From this table it is clear that the results are remarkably close. Note again that the computational time by the direct method is insignificant when compared to a three-dimensional search used in Reference (27).

In the following some of the limitations of the direct method are discussed. The direct method is based on solving a system of equations.

TABLE VI
THREE TRANSITION SAMPLE VALUES

BW	$H_{(\ell-3)}^{(R)}$	$H_{(\ell-2)}^{(R)}$	$H_{(\ell-1)}^{(R)}$	$H_{(\ell-3)}^{(Do)}$	$H_{(\ell-2)}^{(Do)}$	$H_{(\ell-1)}^{(Do)}$
<u>N = 15</u>						
1	0.66897613	0.18457882	0.01455078	0.66882155	0.18440000	0.01454600
2	0.65951526	0.17360713	0.01000977	0.68181400	0.20060000	0.01597000
<u>N = 33</u>						
1	0.67025933	0.18448586	0.01372910	0.67258560	0.18896000	0.01547060
2	0.68914992	0.20723432	0.01668701	0.69820600	0.21982770	0.01995000
4	0.70374222	0.22577646	0.01990967	0.70860100	0.23376600	0.02243000
6	0.70954533	0.23353566	0.02140503	0.70921070	0.23551300	0.02282000
8	0.70362590	0.22815933	0.02062988	0.70637250	0.23297600	0.02335000
10	0.68306885	0.20567451	0.01605835	0.69637200	0.22233600	0.02022000
<u>N = 65</u>						
1	0.67492051	0.19101259	0.01552124	0.67184290	0.18811000	0.01531151
2	0.70260139	0.22329262	0.01989136	0.69710391	0.21860700	0.01971924
3	0.71288030	0.23609223	0.02214966	0.70457718	0.22842020	0.02141220
4	0.71154775	0.23418217	0.02115479	0.70724179	0.23234500	0.02216000
8	0.72436684	0.25203440	0.02576904	0.70823137	0.23521200	0.02285000
12	0.72372888	0.25178881	0.02576904	0.70737982	0.23491870	0.02287000
16	0.71742143	0.24385557	0.02368774	0.70678900	0.23456190	0.02283600

TABLE VI (Continued)

BW	$H_{(\ell-3)}^{(R)}$	$H_{(\ell-2)}^{(R)}$	$H_{(\ell-1)}^{(R)}$	$H_{(\ell-3)}^{(Do)}$	$H_{(\ell-2)}^{(Do)}$	$H_{(\ell-1)}^{(Do)}$
<u>N = 65 (Cont.)</u>						
20	0.69678377	0.22072406	0.01913452	0.70611000	0.23396000	0.02273000
24	0.71008776	0.23899360	0.02396240	0.70240000	0.23004600	0.02195310
<u>N = 125</u>						
1	0.67475127	0.19093541	0.01556396	0.67159870	0.18783840	0.01525950
2	0.70177618	0.22232235	0.01968994	0.69669770	0.21815840	0.01963250
4	0.71788831	0.24380589	0.02420654	0.70654175	0.23160440	0.02202500
6	0.71966323	0.24543860	0.02402344	0.70746866	0.23381200	0.02252000
8	0.71406829	0.23940384	0.02286987	0.70698169	0.23394900	0.02261920
16	0.72206742	0.24955546	0.02507324	0.70454809	0.23238500	0.02244570
24	0.71761565	0.24472233	0.02415771	0.70340232	0.23148400	0.22315800
32	0.72208238	0.24994760	0.02522583	0.70310808	0.23128080	0.02229200
40	0.71850440	0.24590832	0.02439575	0.70345460	0.23164700	0.02236290
48	0.71649557	0.24453094	0.02440186	0.70418956	0.23234100	0.02248340
56	0.68652023	0.21212543	0.01801758	0.69201857	0.21900700	0.01976040
57	0.65248157	0.17459164	0.01030884	0.67843700	0.20430000	0.01681000

TABLE VI (Continued)

BW	$H_{(\ell-3)}^{(R)}$	$H_{(\ell-2)}^{(R)}$	$H_{(\ell-1)}^{(R)}$	$H_{(\ell-3)}^{(De)}$	$H_{(\ell-2)}^{(De)}$	$H_{(\ell-1)}^{(De)}$
<u>N = 16</u>						
1	0.67931499	0.19530278	0.01597290	0.67359061	0.18911630	0.01498357
2	0.70432347	0.22385191	0.01951294	0.70791970	0.23032800	0.02163665
<u>N = 32</u>						
1	0.68302930	0.20052231	0.01735230	0.68169514	0.19867830	0.01686141
2	0.71593525	0.23959557	0.02354126	0.70967033	0.23188635	0.02173876
4	0.73360248	0.26135787	0.02770996	0.72133503	0.24669888	0.02435768
6	0.73796855	0.26670884	0.02871034	0.72104145	0.24173538	0.02440393
8	0.73367810	0.26084303	0.02705688	0.71423699	0.24012310	0.23060395
<u>N = 64</u>						
1	0.67535861	0.19125221	0.01544800	0.68185400	0.19886410	0.01689730
2	0.70507613	0.22634942	0.02057495	0.70991489	0.23209100	0.02179700
3	0.72204262	0.24519492	0.02438354	0.71884417	0.24322318	0.23728355
4	0.72570913	0.25236063	0.02581177	0.72241097	0.24792318	0.02461008
8	0.74181077	0.27213724	0.03010864	0.72496458	0.25203082	0.02549194
12	0.74040381	0.27101526	0.02996826	0.72442204	0.25189000	0.02531811
16	0.74434815	0.27556998	0.03095703	0.72339658	0.25100093	0.02537319
20	0.74029023	0.27059980	0.02975464	0.72106017	0.24865750	0.02992062

TABLE VI (Continued)

BW	$H_{(\lambda-3)}^{(R)}$	$H_{(\lambda-2)}^{(R)}$	$H_{(\lambda-1)}^{(R)}$	$H_{(\lambda-3)}^{(De)}$	$H_{(\lambda-2)}^{(De)}$	$H_{(\lambda-1)}^{(R)}$
<u>N = 128</u>						
1	0.67492092	0.19122512	0.01566772	0.68181580	0.19882005	0.01688900
2	0.70122715	0.22183722	0.01967163	0.70978891	0.23195000	0.02176900
3	0.71450669	0.23824591	0.02271729	0.71863063	0.24298783	0.02367740
5	0.71859482	0.24430176	0.02398071	0.72359944	0.24974480	0.02498128
8	0.72166583	0.24892636	0.02510986	0.72442039	0.25146630	0.02538546
16	0.72460093	0.25347440	0.02633057	0.72316385	0.25080750	0.02524617
24	0.72843530	0.25816799	0.02739258	0.72232893	0.25012100	0.02524380
32	0.72886454	0.25894149	0.02763062	0.72195530	0.24980600	0.02519548
40	0.73824701	0.26996954	0.03014526	0.72180669	0.24968033	0.02517598
48	0.73584086	0.26652967	0.02913208	0.72122605	0.24907448	0.02585913
<u>N = 256</u>						
1	0.67664281	0.19387524	0.01064795	0.68180181	0.19880390	0.01685990
2	0.70144920	0.22197911	0.01963501	0.70974718	0.23190324	0.02176060
3	0.69990539	0.22085960	0.01908569	0.71855956	0.24929095	0.02366216
5	0.71635813	0.24117076	0.02305298	0.72346905	0.24960550	0.02495445
8	0.72164702	0.24843111	0.02479248	0.72420199	0.25123943	0.02534200
9	0.71679420	0.24253562	0.02329712	0.72407159	0.25125770	0.02536440
16	0.71900030	0.24629538	0.02444458	0.72271370	0.25035485	0.02526285
32	0.72307099	0.25163493	0.02577896	0.72099558	0.24886423	0.02505400

TABLE VI (Continued)

BW	$H_{(\ell-3)}^{(R)}$	$H_{(\ell-2)}^{(R)}$	$H_{(\ell-1)}^{(R)}$	$H_{(\ell-3)}^{(De)}$	$H_{(\ell-2)}^{(De)}$	$H_{(\ell-1)}^{(De)}$
N = 256 (Cont.)						
48	0.71550480	0.24359358	0.02421875	0.72036330	0.24828605	0.02492895
56	0.71177494	0.23957232	0.02345581	0.72022679	0.24816250	0.02490849
64	0.71380179	0.24199281	0.02396851	0.72016995	0.24811341	0.02490680
80	0.71103085	0.23926844	0.02351685	0.72026410	0.24821258	0.02499804
96	0.71293931	0.24219392	0.02435913	0.72065320	0.24859501	0.02498000
104	0.71524908	0.24590992	0.02552490	0.72091441	0.24884570	0.02509770
112	0.71857490	0.24926456	0.02607422	0.72064460	0.24852397	0.02496501
120	0.73130690	0.25909273	0.02683105	0.70925127	0.23621000	0.02250350
121	0.72916388	0.25523207	0.02561035	0.70122340	0.22745720	0.02644320
122	0.72456966	0.24778644	0.02344360	0.71057237	0.23806080	0.02349960

In some extreme cases it may not be possible to form the required number of equations. For example, when BW is very near $N/2$, there may not be enough ripple maxima and minima available to form the required number of equations. The magnitude response is symmetrical about $N/2$ ($(N-1)/2$ for N -odd) frequency samples (see Figure 5). Equating ripple maxima and minima beyond π radians will result only in redundant equations. To use the direct method the bounds for BW are given below for N -even and N -odd. From these bounds it is clear that the method is applicable to almost all cases which are used in practice.

$$\text{Bound on BW} \lesssim \begin{cases} ((N+1)/2 - 2M) & \text{for } N\text{-odd} \\ ((N/2) - 2M) & \text{for } N\text{-even} \end{cases}$$

Before proceeding further, we should point out that the designs are given for Type 1 low-pass filter (23) designs. However, these are applicable for Type 2 also. The only difference between Type-1 and Type-2 designs is in the location of the initial frequency sample (23).

Some of the above ideas in designing low-pass filters are extended to bandpass filters and are discussed below.

3.5 Bandpass Filter Design

The bandpass filter, like the low-pass filter case, is specified in terms of frequency sample locations ($\omega_k = \frac{2\pi}{N} k$; $k = 0, \dots, N-1$). A typical set of specifications is shown in Figure 10, where M_1 denotes the number of zero-valued samples prior to first transition sample; $2M$ and BW correspond, respectively, to the number of transition and pass-band frequency samples; and the ℓ th frequency sample corresponds to the edge of the stopband after the passband and transition band. The specifications in Figure 10 correspond to the symmetrical case; that is, the

corresponding transition samples on both sides of the passband are taken as the same. Explicitly,

$$H_{\ell-1} = H_{\ell-2-BW}, \text{ for } M = 1 \quad (3.50a)$$

$$H_{\ell-2} = H_{\ell-3-BW}, H_{\ell-1} = H_{\ell-4-BW}, \text{ for } M = 2 \quad (3.50b)$$

$$H_{\ell-3} = H_{\ell-4-BW}, H_{\ell-2} = H_{\ell-5-BW}, H_{\ell-1} = H_{\ell-6-BW}, \text{ for } M = 3 \quad (3.50c)$$

Even though the nonsymmetrical specification may give a better stopband response, it is not used in practice as it involves twice the number of unknowns, which obviously implies more computational time than the symmetrical case (27). In addition, the additional stopband attenuation is not significant enough to consider the nonsymmetrical case. Therefore, in the following only the symmetrical bandpass filter design is considered.

The design problem is to determine the optimum transition sample values $H_{\ell-i}^{(0)}$. As in the low-pass case, we will consider three cases separately for $M = 1, 2, 3$. There are two methods to design bandpass filters. The first method is based upon rotating the appropriate low-pass frequency samples to the desired center frequency location of the bandpass filter (27). Unfortunately, this approach will result in sub-optimum filters.

The second method of design is based on the direct approach. As before, the method of design is to identify the stopband peaks after the passband and equate their magnitudes at desired locations. Hereafter, the stopband after the passband is referred to as the second stopband. For optimum transition values, the second stopband response has the same general form as in the low-pass case. This is true for $M = 1$,

2, 3. It is clear from Equation (3.50) that $H^*(e^{j\omega})$ is a function of only M variables. By considering $(M+1)$ peaks in the second stopband and equating the magnitudes, we can solve for $H_{\ell-i}$, where i varies from 1 to M . The next problem is obviously the estimation of frequencies at which these peaks appear in the second stopband. This is discussed in the following.

In the initial stages the estimates of these frequencies are taken as the frequency estimates in the low-pass case. The procedure for computing $H_{\ell-i}$ is exactly the same as in the low-pass case. Using this procedure, several bandpass filters are designed. The transition sample values are listed in Tables VII, VIII, and IX under the column(s) $H_{\ell-i}^{(D\ell)}$ where the superscript $D\ell$ indicates that the direct method had been used with low-pass frequency estimates. From this table it can be seen that the results are close. The results can be improved by slightly modifying the frequency estimates. For example, for N -even and $M = 1$, these frequency estimates are

$$\omega_{(\ell+1)}^{(Dem)} = \omega_{(\ell+1)} + 0.4375 \left(\frac{2\pi}{N}\right) \quad (3.51a)$$

$$\omega_{(\ell+2)}^{(Dem)} = \omega_{(\ell+1)}^{(Dem)} + 0.908 \left(\frac{2\pi}{N}\right) \quad (3.51b)$$

where the superscript m is added to De to denote the modification. Using this, new transition sample values are determined and are listed in Table VII under the column(s) $H_{\ell-i}^{(Dm)}$. Note that these are closer to the optimal values in most cases.

For $M = 2$, the modified frequency estimates are

$$\omega_{\ell}^{(Dem)} = \omega_{\ell} + 0.125 \left(\frac{2\pi}{N}\right) \quad (3.52a)$$

TABLE VII

BAND PASS FILTER DESIGN--ONE TRANSITION SAMPLE VALUES

BW	M1	$H_{(\ell-1)}^{(R)}$	$H_{\ell-1}^{(D\ell)}$	$H_{\ell-1}^{(Dm)}$
<u>y = 32</u>				
5	2	0.40270386	0.40667276	0.39465273
5	3	0.39149780	0.40577748	0.39318246
5	4	0.39191895	0.40521567	0.39188286
5	5	0.39454346	0.40512936	0.39077300
6*	2	---	0.33091473	0.32610090
6	3	---	0.33173234	0.32625118
6	4	---	0.33205910	0.32546587
6	5	---	0.33246836	0.32377809
7	2	0.40203247	0.40060789	0.38693788
7	3	0.38943481	0.40037655	0.38569950
7	4	0.38916626	0.40211352	0.38626347
<u>y = 128</u>				
18	20	0.34979248	0.35666284	0.35080178
19	20	0.37623901	0.37888641	0.36897930
20	20	0.35097046	0.35-74142	0.35171492
30	8	0.35111694	0.35998904	0.35368615
13	10	0.38093262	0.38310250	0.37315707
35	2	0.35415039	0.37639695	0.36673980
35	8	0.36517944	0.37624874	0.36645867
35	16	0.36619873	0.37713949	0.36671597
35	20	0.36517944	0.37822934	0.36682640

*The values reported in reference (27) were found to be incorrect through personal discussion with the authors.

TABLE VIII
BAND PASS FILTER DESIGN--TWO TRANSITION SAMPLE VALUES

BW	M1	$H_{\ell-2}^{(R)}$	$H_{\ell-1}^{(R)}$	$H_{\ell-2}^{(D\ell)}$	$H_{\ell-1}^{(D\ell)}$	$H_{\ell-2}^{(Dm)}$	$H_{\ell-1}^{(Dm)}$
<u>N = 32</u>							
3	2	0.61574359	0.11821340	0.60043700	0.10687922	0.61562291	0.11811914
3	3	0.61224050	0.11731567	0.60024400	0.10672362	0.61514781	0.11775416
3	4	0.61825728	0.12105713	0.59981760	0.10643152	0.61427323	0.11714487
3	5	0.62291631	0.12384644	0.59876520	0.10572686	0.61246674	0.11591245
4*	2	---	---	0.48773800	0.06962500	0.52149558	0.08542922
4	3	---	---	0.48862130	0.06995900	0.51908831	0.08438990
4	4	---	---	0.48886600	0.07001174	0.51535416	0.08427197
4	5	---	---	0.48723720	0.06929670	0.50843755	0.07954104
5	2	0.62173523	0.12357788	0.59995400	0.10853550	0.61527529	0.11965490
5	3	0.62286495	0.12523804	0.59861696	0.10766031	0.61313562	0.11822056
5	4	0.62855407	0.12827148	0.59527276	0.10547520	0.60831037	0.11499025
5	5	0.62286495	0.12523804	0.58566614	0.09909300	0.59560601	0.10635950
<u>N = 128</u>							
11	10	0.59676391	0.11203003	0.59293173	0.10698099	0.61413955	0.12083917

TABLE VIII (Continued)

BW	M1	$H_{\ell-2}^{(R)}$	$H_{\ell-1}^{(R)}$	$H_{\ell-2}^{(D\ell)}$	$H_{\ell-1}^{(D\ell)}$	$H_{\ell-2}^{(Dm)}$	$H_{\ell-1}^{(Dm)}$
N = 128 (Cont.)							
16	20	0.55215414	0.09031982	0.55436133	0.09130533	0.58522657	0.10828950
17	20	0.59054608	0.10917969	0.59032336	0.10621975	0.61231700	0.12030180
18	20	0.55425376	0.09111938	0.55693104	0.09231496	0.58736074	0.10918500
28	8	0.55326966	0.09022827	0.56255247	0.09453508	0.59241705	0.11134694
33	2	0.58803040	0.10723877	0.58758180	0.10519906	0.61017280	0.11945610
33	8	0.60405885	0.11864624	0.58776022	0.10530080	0.61024300	0.11949710
33	16	0.59243833	0.11191406	0.58872725	0.10575400	0.61034200	0.11953300
33	20	0.60405885	0.11864624	0.58904313	0.10585391	0.60932847	0.11894700

*The values reported in Reference (27) were found to be incorrect through personal discussion with the authors.

TABLE IX
BAND PASS FILTER DESIGN--THREE TRANSITION SAMPLE VALUES

BW	M1	$H_{(\ell-3)}^{(R)}$	$H_{(\ell-2)}^{(R)}$	$H_{(\ell-1)}^{(R)}$	$H_{(\ell-3)}^{(D\ell)}$	$H_{(\ell-2)}^{(D\ell)}$	$H_{(\ell-1)}^{(D\ell)}$
<u>N = 32</u>							
1	2	0.68572443	0.20360144	0.01790771	0.68098440	0.19782598	0.01668400
1	3	0.68240900	0.19934001	0.01699829	0.67995701	0.19658837	0.01643867
1	4	0.68649875	0.20508501	0.01849976	0.67816095	0.19442841	0.01600690
1	5	0.67931499	0.19530278	0.01597290	0.67450612	0.19003530	0.01527490
2*	2	---	---	---	0.51347724	0.12001553	0.00851332
2	3	---	---	---	0.51017843	0.11770460	0.00818110
2	4	---	---	---	0.50459280	0.11375022	0.00760600
3	2	0.71117572	0.23341023	0.02207642	0.70503567	0.22620200	0.02054300
3	3	0.72135515	0.24743934	0.02587891	0.69990855	0.22006320	0.01925800
3	4	0.70428223	0.22380012	0.01950073	0.70888400	0.23126751	0.02179214
<u>N = 128</u>							
9	10	0.73460394	0.26306832	0.02807617	0.72518960	0.25133060	0.02526000
14	20	0.67233389	0.20640635	0.01867676	0.69253789	0.22374000	0.02093500

TABLE IX (Continued)

BW	M1	$H_{(\ell-3)}^{(R)}$	$H_{(\ell-2)}^{(R)}$	$H_{(\ell-1)}^{(R)}$	$H_{(\ell-3)}^{(D\ell)}$	$H_{(\ell-2)}^{(D\ell)}$	$H_{(\ell-1)}^{(D\ell)}$
N = 128 (Cont.)							
15	20	0.74047619	0.27145008	0.03029785	0.72665649	0.25366280	0.02577300
16	20	0.67549529	0.20830605	0.01875610	0.69646820	0.22698400	0.02143004
26	8	0.68240265	0.21150551	0.01835937	0.70572685	0.23484990	0.02266000
31	2	0.74186481	0.27190412	0.02974243	0.72614637	0.25367596	0.02851741
31	8	0.73722876	0.26787226	0.02946167	0.72609062	0.25361398	0.02583910
31	16	0.74060358	0.27143276	0.03010254	0.72502869	0.25245104	0.02560545
31	20	0.73722876	0.26787226	0.02946167	0.72125372	0.24827766	0.02475732

*The values reported in Reference (27) were found to be incorrect through personal discussion with the authors.

$$\omega_{\ell'}^{(Dem)} = \omega_{\ell}^{(Dem)} + 0.5 \left(\frac{2\pi}{N} \right) \quad (3.52b)$$

$$\omega_{(\ell+1)}^{(Dem)} = \omega_{\ell'}^{(Dem)} + 1.25 \left(\frac{2\pi}{N} \right) \quad (3.52c)$$

Using these, the new transition sample values are computed and are listed in Table VIII under the column $H_{\ell-i}^{(Dm)}$, $i = 1, 2$. Again, the results are closer to the optimum. Table IX gives the transition sample values for three transition sample cases using the low-pass frequency estimates. The values are close enough that the modification is considered unnecessary.

For comparison purposes, a bandpass filter of order 128 is designed using the following specifications: $M1 = 20$, $BW = 16$, and $M = 3$. The transition values used are obtained by direct approach and are given by $H_{(\ell-1)}^{(D\ell)} = 0.02143004$, $H_{(\ell-2)}^{(D\ell)} = 0.226984$, and $H_{(\ell-3)}^{(D\ell)} = 0.6964682$. The corresponding bandpass filter characteristics are plotted in Figure 11. Using the optimal values obtained in Reference (27), the same filter characteristics are plotted in Figure 11. The responses are essentially the same with the maximum peak being -90.8 dB.

From the above discussion it is clear that the direct method of design is simple and accurate. Also, the computation time required by the direct method is negligibly small when compared to the existing technique.

3.6 Ripple Reduction in the Passband

The direct method presented earlier can be considered as an approximation after the discontinuity. However, the same type of idea can be used to get an approximation before the discontinuity; that is, instead of considering the minimum ripple magnitude for the stopband, we can consider the minimum ripple size in the passband. It is clear that the

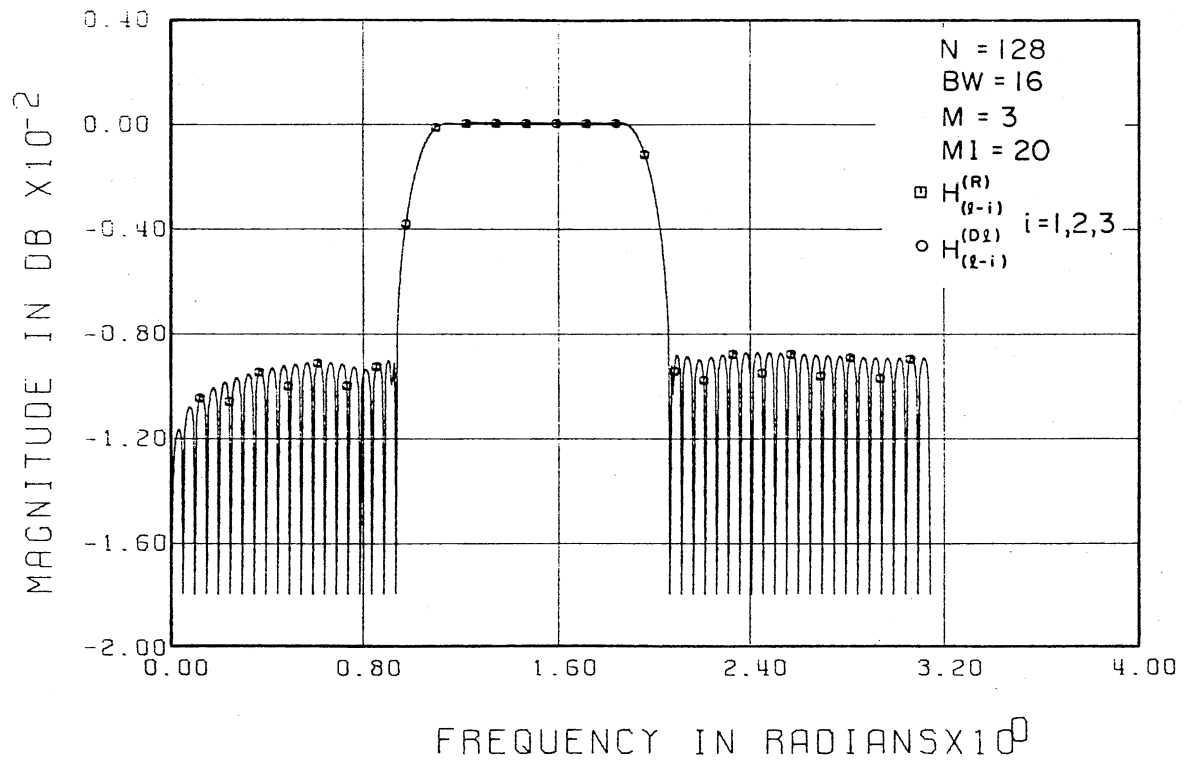


Figure 11. Frequency Response of a Bandpass Filter

design procedure discussed earlier has no control over the ripple size in the passband. In the following a design technique to reduce the ripple size in the passband only is presented for digital low-pass filters. This problem has not been discussed in the literature.

Consider the passband response as a function of the transition samples. Figure 12 shows the passband behavior of $H^*(e^{j\omega})$ for one transition sample, $H'_{\ell-1}$, for $N = 33$ and $BW = 8$. It is clear from this figure that the passband has minimum ripple when $H'_{\ell-1}(0) = 0.66$. The second ripple before the discontinuity is small when compared to the first ripple before the discontinuity. Also, the first and third ripples before the discontinuity have approximately the same ripple size. It should be noted that the same type of behavior appeared in the stopband case. This gives a clue for determining the optimal transition sample value $H'_{\ell-1}(0)$, and is discussed below.

As in the stopband case, the transition sample values can be obtained by equating the ripple sizes. The next step obviously is to find the frequency location at which the ripple peaks appear. For one transition sample case, the first and third peak ripple peaks appear at approximately

$$\omega'_{\ell-2} = \omega_{\ell-2} - 0.125 \left(\frac{2\pi}{N} \right) \quad (3.53a)$$

$$\omega'_{\ell-3} = \omega'_{\ell-2} - 1.499 \left(\frac{2\pi}{N} \right) \quad (3.53b)$$

with

$$\omega_{\ell-4} < \omega'_{\ell-3} < \omega_{\ell-3} < \omega'_{\ell-2} < \omega_{\ell-2} \quad (3.54)$$

The estimates in Equation (3.53) are valid for both N-even and N-odd.

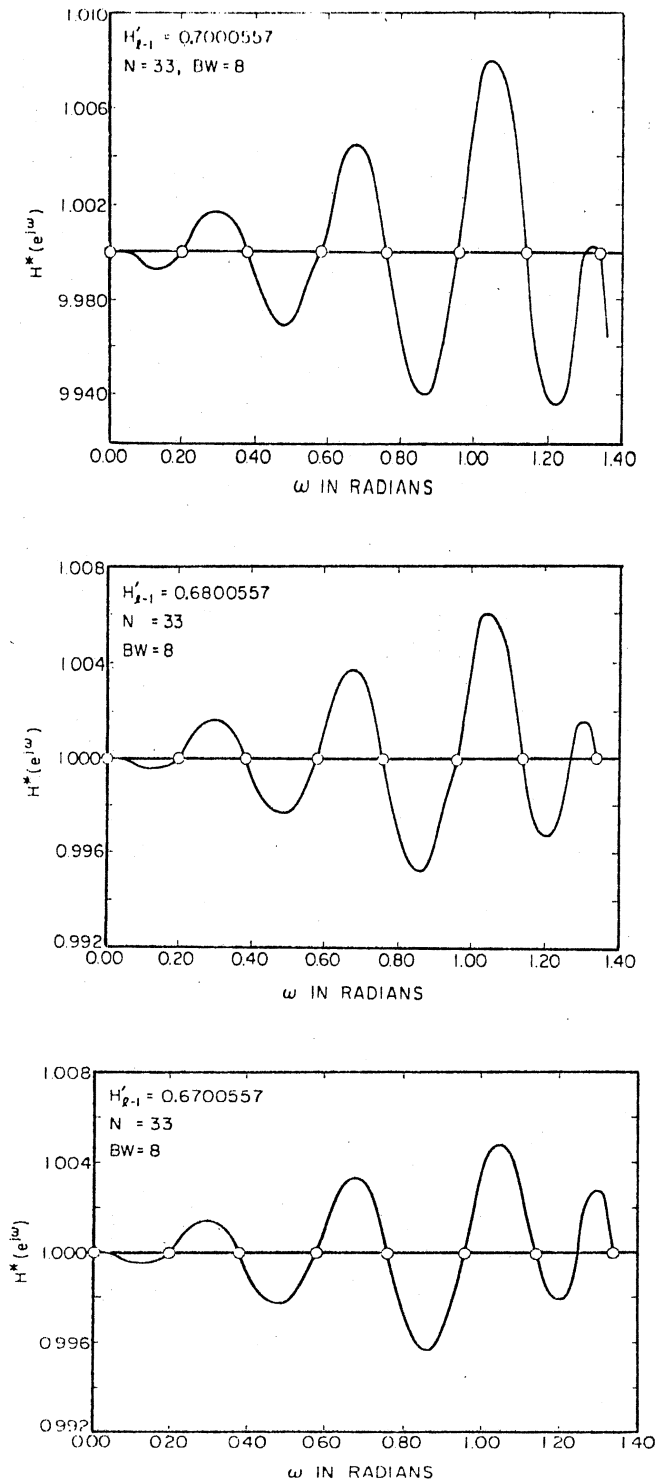


Figure 12. Variation of Passband Response as a Function of Transition Sample

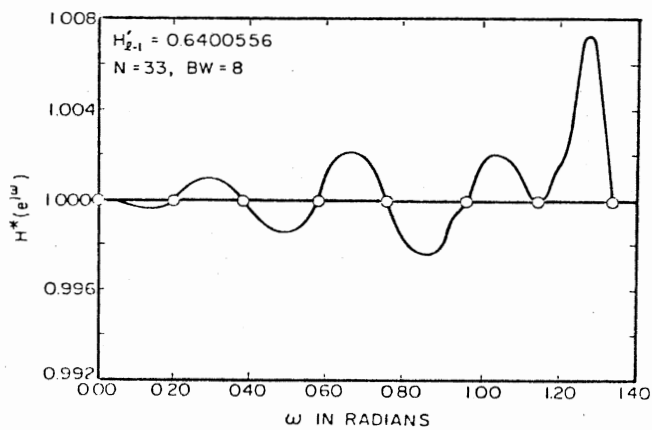
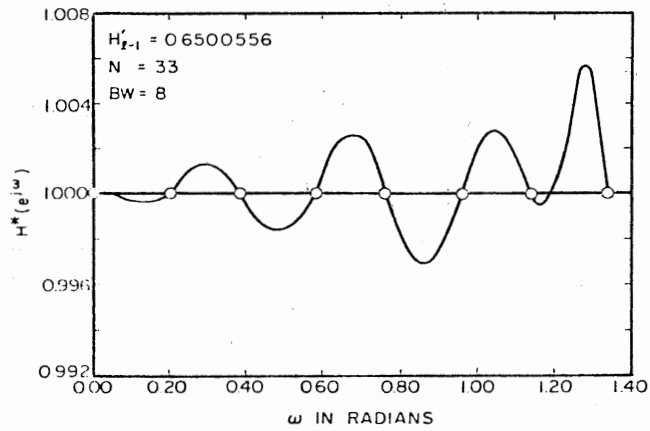
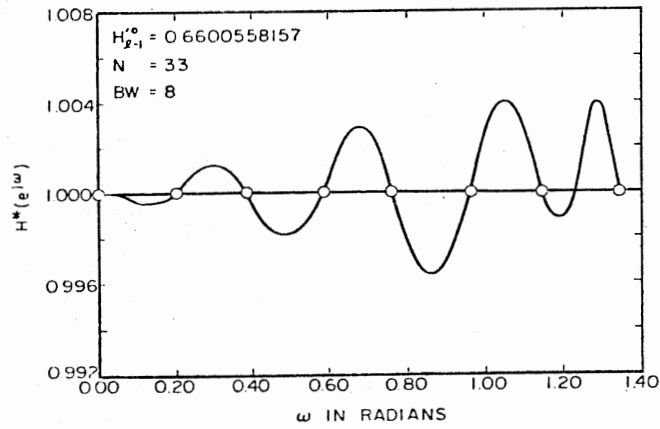


Figure 12. (Continued)

Several low-pass filters are designed for different values of N and BW and the results for $H_{\ell-1}^{(0)}$ are tabulated in Table X. Note that these are applicable for minimum ripple in the passband only.

For the transition samples given in Table X, the responses are plotted and the passband response has the same general form as in Figure 12. It is clear that the same type of approach can be used to determine the transition samples for $M = 2, 3$. However, this is not discussed any further here, as too much ripple reduction in the passband introduces large ripples in the stopband. This is not suitable for most filter designs.

3.7 High-Pass Filter Design

It is clear from Equation (3.2) that $H^*(e^{j\omega}) = 0$ at $\omega = \pi$. Note that Equation (3.2) is valid for symmetrical impulse responses. Unfortunately, $H^*(e^{j\omega}) \neq 0$ for high-pass filters (see Figure 13). Therefore, the digital high-pass filter cannot be designed in the strict sense by the frequency sampling method (23). However, ignoring this problem at $\omega = \pi$, we can design high-pass filters. This is discussed below.

The approach will be similar to the stopband designs discussed earlier. Figure 14 gives the stopband response of a high-pass filter for $N = 32$ and $M = 5$ for different transition sample values, $H_{\ell-1}^{(i)}$. $\omega_{\ell-2}$ represents the frequency sample location at which the stopband ends. When $H_{\ell-1}^{(i)}$ is optimum, i.e., when $H_{\ell-1}^{(i)} = H_{\ell-1}^{(0)}$, it can be seen that $H^*(e^{j\omega})$ have the following pattern:

$$H^*(e^{j\omega}) = \begin{cases} < 0 & \text{for } \omega_{\ell-2} < \omega < \omega_{\ell 0} & (3.55a) \\ > 0 & \text{for } \omega_{\ell 0} < \omega < \omega_{\ell-3} & (3.55b) \\ > 0 & \text{for } \omega_{\ell-3} < \omega < \omega_{\ell-4} & (3.55c) \end{cases}$$

TABLE X
TRANSITION SAMPLE VALUES (PASS BAND)

BW	$H'_{\ell-1}(o)$	BW	$H'_{\ell-1}(o)$
<u>N = 15</u>		<u>y = 125</u>	
3	0.71486779	3	0.70226677
4	0.70023225	4	0.67731154
5	0.70751371	6	0.65921598
6	0.74719605	8	0.65181617
<u>N = 33</u>		10	0.64781659
3	0.70417177	18	0.64163484
4	0.68016281	26	0.63992416
6	0.66429036	34	0.63971341
8	0.66005581	42	0.64076580
10	0.66122499	50	0.64447898
12	0.66893186	58	0.66512434
14	0.69591709	59	0.67516678
15	0.74196609	60	0.69406127
<u>y = 65</u>		61	0.74097346
3	0.70263388	<u>N = 16</u>	
4	0.67784333	3	0.71288805
5	0.66655820	4	0.69599624
6	0.66008166	5	0.69793453
10	0.64947212	6	0.71926600
14	0.64643522	<u>N = 32</u>	
18	0.64616754	3	0.70431012
22	0.64836296	4	0.68037863
26	0.65580988	6	0.66471886
30	0.69441361	8	0.66086783
31	0.74116663	10	0.66287346
		12	0.67300467
		14	0.71278932

TABLE X (Continued)

BW	$H_{\ell-1}^{(0)}$	BW	$H_{\ell-1}^{(0)}$
<u>N = 64</u>		<u>N = 256</u>	
3	0.70264993	3	0.70216474
4	0.67786677	4	0.67716527
5	0.66658918	5	0.66567335
6	0.66012065	7	0.65459750
10	0.64955172	10	0.64740808
14	0.64658215	11	0.64598953
18	0.64644738	18	0.64081390
22	0.64897279	34	0.63743199
26	0.65765446	50	0.63648256
30	0.71154972	58	0.63631395
		66	0.63627973
		80	0.63653672
		106	0.63934134
		114	0.64276615
		122	0.65643695
		123	0.66150116
		124	0.66931056
		125	0.68280665
		126	0.71118831
<u>N = 128</u>			
3	0.70226054		
4	0.67730259		
5	0.66585079		
7	0.65485542		
10	0.64779106		
18	0.64158067		
26	0.63982412		
34	0.63952551		
42	0.64036774		
50	0.64334560		
58	0.65666773		
62	0.71125964		

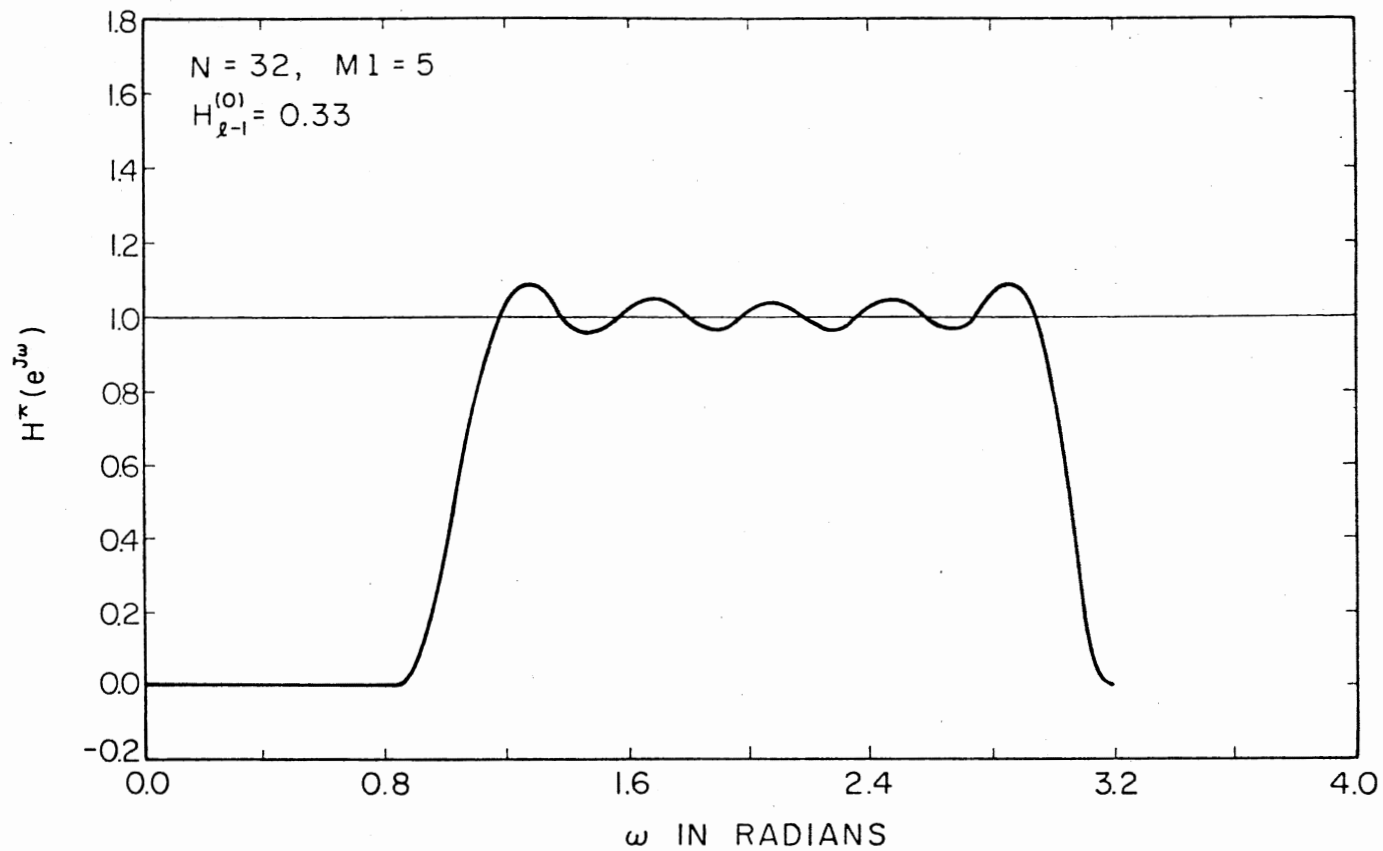


Figure 13. Frequency Response of a High-Pass Filter

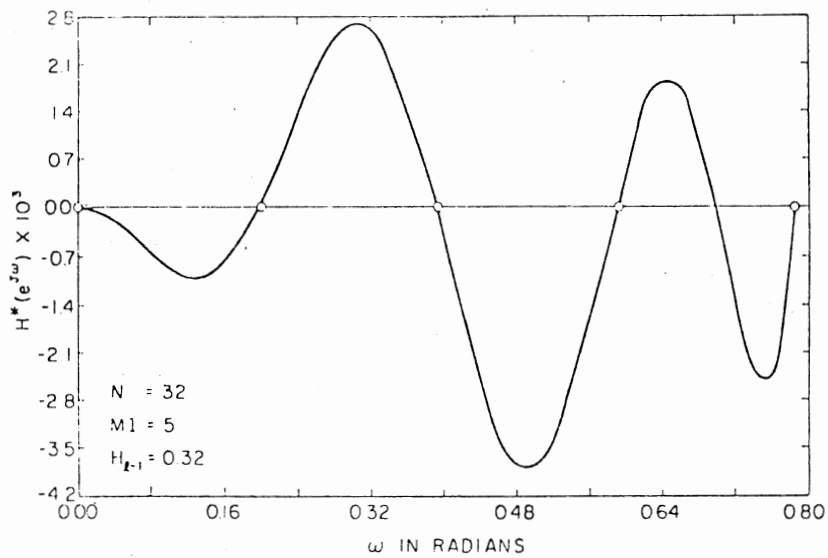
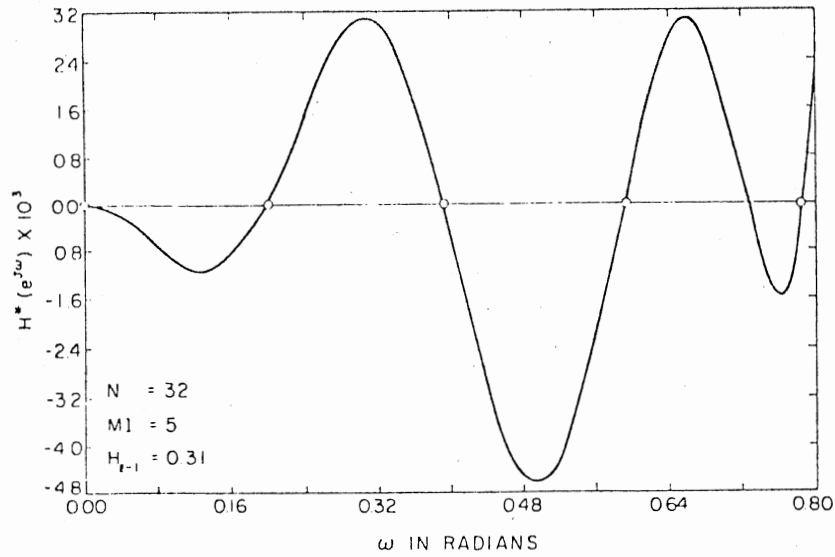


Figure 14. Variation of Stopband Response of a High-Pass Filter as a Function of Transition Sample

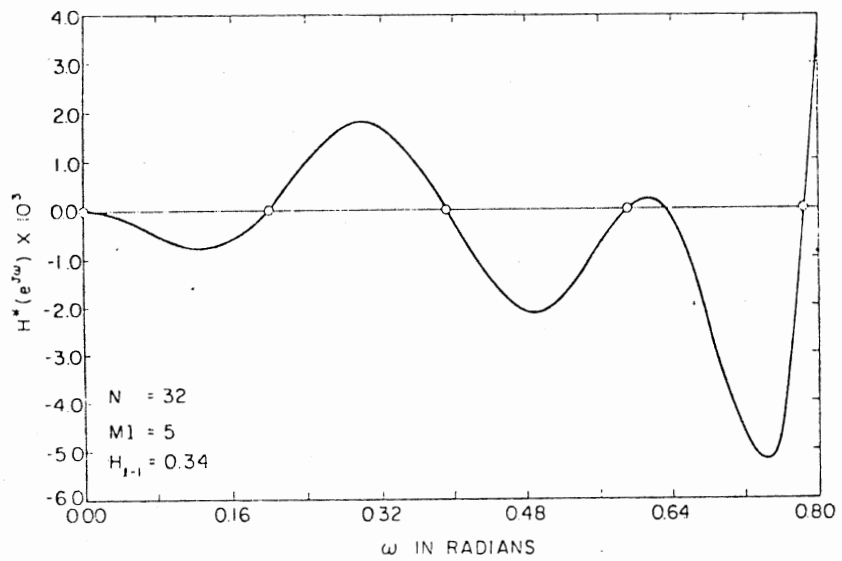
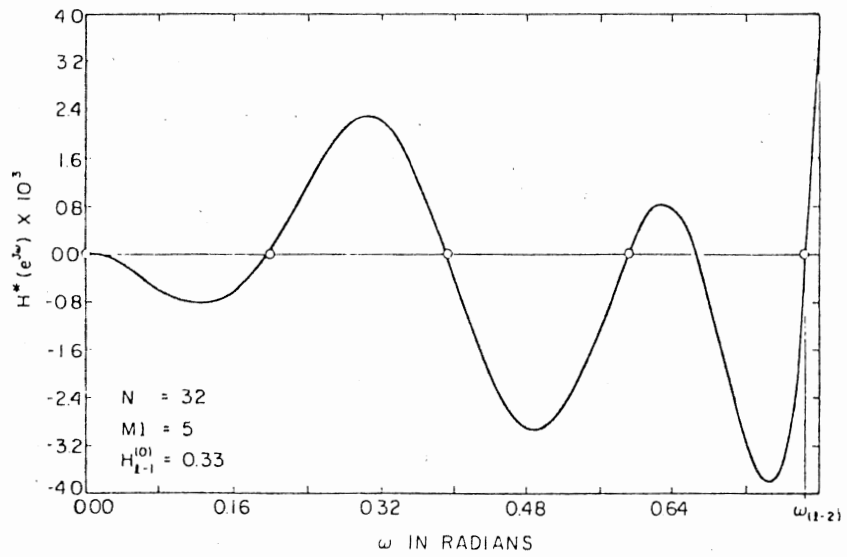


Figure 14. (Continued)

Looking closely at the optimal stopband responses of high-pass and low-pass filters (see Figures 2 and 14), the following observations can be made. Viewing the stopband responses from right to left in the low-pass case and from left to right in the high-pass case, it can be seen that the responses are similar. Equation (3.55) gives a clue for determining $H_{\ell-1}^{(o)}$.

The computation of $H_{\ell-1}^{(o)}$ is based on equating the magnitude of the ripple peaks immediately before the passband--counting from right to left, we will use first and third peaks in the stopband. Again, the problem of selecting the location of the frequencies (say, $\omega'_{\ell 0}$ and $\omega'_{\ell-4}$) at which these peaks appear should be considered. Using the optimal response in Figure 14 as a guide, the location of the frequencies at which the ripple maxima and minima appear are empirically determined. The estimates of these frequencies are given by

$$\omega'_{\ell 0} = \omega_{\ell-2} - 0.375 \left(\frac{2\pi}{N}\right) \quad (3.56a)$$

$$\omega'_{\ell-4} = \omega'_{\ell 0} - 1.3125 \left(\frac{2\pi}{N}\right) \quad (3.56b)$$

Note that the bounds for these frequencies are given by

$$\omega'_{\ell-2} < \omega'_{\ell 0} < \omega_{\ell-3} < \omega'_{\ell-4} < \omega_{\ell-4} \quad (3.57)$$

Using Equation (3.56) in Equation (3.55) and assuming that the magnitudes of the peaks are equal, an equation with $H_{\ell-1}^{(o)}$ as unknown can be obtained. Using this approach, few high-pass filters are designed by the direct approach and the results are tabulated in Table XI. Using the values of $H_{\ell-1}^{(o)}$, stopband responses were plotted and they exhibit the same pattern as in Figure 14.

TABLE XI
HIGH-PASS FILTER DESIGN (ONE TRANSITION SAMPLE VALUES)

M1	$H_{\ell-1}^{(0)}$
<u>y = 32</u>	
3	0.30444908
4	0.32713361
5	0.32957560
<u>y = 128</u>	
6	0.34318804
10	0.35350332
14	0.35738251
18	0.35935215

The same ideas can be extended to design high-pass filters with $M = 2$ and $M = 3$. These are not considered any further as the filters designed by the above approach are not strictly high-pass.

3.8 Summary

This chapter is concerned with the frequency sampling filter design. In designing these filters, the ideas of smoothing techniques and least-squares are used. The direct method of solution is also discussed. The approach presented above is simple and direct, and will not use any search or linear programming techniques. Furthermore, it appears that the proposed method is faster than any other existing technique and the convergence problems need not be considered. Several low-pass bandpass

filters are designed by the direct method and the transition values derived are compared with the optimal values given in the literature. In addition, ripple reduction in the passband along with high-pass filter approximation is discussed.

CHAPTER IV

SUMMARY AND SUGGESTIONS FOR FURTHER STUDY

4.1 Summary

This study deals with the application of the fast Fourier transform (FFT) to the solution of a system of Toeplitz normal equations of the form $\underline{y} = A_{\text{Toe}} \underline{x}$, where A_{Toe} is a symmetric Toeplitz matrix of order ℓ and \underline{x} and \underline{y} are ℓ dimensional vectors. In addition, a direct approach to the frequency sampling digital filter design is presented. Interestingly, a relationship is derived between the filter designs by direct convolution and the frequency sampling method.

The approach to the solution of a system of Toeplitz normal equations is based on using iterative techniques, circulant matrices, and the fast Fourier transform algorithm. The given Toeplitz matrix is converted into a symmetric circulant. An interesting property of a circulant matrix is that the modal matrix of a circulant matrix is the discrete Fourier transform matrix. The iterative technique used in the solution is the conjugate gradient method. The computational requirements are reduced by using the classical fast Fourier transform algorithm.

The computational requirements in the worst case is shown to be $K(8\ell \log_2 4\ell + 4\ell)$, where $K \leq \ell$ and ℓ is the number of equations. There will be a considerable amount of saving in computational time, especially when solving a large number of equations by this method. In addition to the reduction in the number of computations, accumulated rounding is also

reduced. If the approximate solution is known, this method requires fewer number of iterations.

The FIR filters can be effectively designed using frequency sampling techniques. Using the special matrices like the circulants, an interesting relationship is derived between the filter designs by discrete convolution and the frequency sampling method.

The direct approach of FIR filter design involves the use of smoothing techniques and a direct solution. The criteria used is to find the magnitude of the transition samples such that the maximum stopband side lobe is minimum. It is well known that the stopband response will have mini-max characteristics when the transition sample is optimum. The conclusions regarding the behavior of the stopband response are obtained for different values of the transition sample.

Using these ideas a direct solution to determine the transition value is derived. The method is based upon equating the magnitudes of the ripple peaks. The number of peaks considered will depend upon the number of unknown transition sample values. In general, if M denotes the number of transition sample values, $(M + 1)$ ripple peaks in the stopband is normally considered. The frequencies at which the ripple peaks appear are determined empirically using the optimal responses as a guide. Using these frequencies and assuming that the magnitudes of the ripple peaks are the same, the optimum transition sample values are determined.

Using these ideas several low-pass filters are designed and the transition values derived are compared with the optimal values given by Rabiner et al. The transition sample values are near enough to the optimum that these can be used for design purposes. The method does not make use of any search or linear programming techniques. Thus the method

of design is simple and direct. It appears that the direct method of design is faster than any other existing technique and the convergence problems need not be considered.

The direct approach has been extended to design bandpass filters. Again, the transition sample values in the bandpass case are close to the optimal values determined by Rabiner et al. The extension of the direct method of design to the high-pass filters is straightforward. The digital filters designed by the direct method is not strictly high-pass.

The design using the stopband responses to have minimum ripple size as a basis can be viewed as an approximation after the discontinuity. However, the same type of idea is used to get an approximation before the discontinuity. Instead of considering the minimum ripple magnitude in the stopband, the minimum ripple size in the passband is considered. The stopband design has no control over the passband. Several low-pass filters are designed and the transition values are tabulated to have minimum ripple size in the passband. Again, the passband design has no control over the stopband. From the knowledge of the passband and stopband responses, a method for the general filter design could be derived. Further work is necessary in this regard.

The only limitation of this technique is that there should be a minimum number of ripple peaks to form the desired equations, which is not a serious limitation.

4.2 Suggestions for Further Study

Some extensions to the present study are proposed below.

The matrix method presented in Chapter II needs to be studied further. It appears that the matrix approach has significant applications

in the general filter design. The results in Chapter II need to be extended to nonsymmetric Toeplitz matrices.

From Chapter III one can see that the accuracy of the direct method depends on the location of the frequencies at which the ripple maxima and minima appear in the stopband. The empirical formulas developed earlier should further be justified, and the estimates can further be improved by including more terms.

Most of our results were confined to type 1 designs. The same ideas can be extended for type 2 designs. The only difference between the type 1 and type 2 is in the location of the initial frequency sample and the procedure is rather straightforward. The direct approach can perhaps be extended to design digital differentiators.

The direct approach presented in this thesis is for uniform samples. These results need to be extended for nonuniform samples.

Further work is necessary to arrive at a general filter design. The computation of the order of the filter from the given set of specifications is still an open problem. The optimum transition values for stopband and passband should give a clue to determine N , the order of the filter. In addition, these clues could perhaps be used to obtain a general approach.

BIBLIOGRAPHY

- (1) Greenstein, Larry J. "An Introductory Course on Digital Filter Theory." Bell Telephone Laboratories, 1971.
- (2) Levinson, N. "The Wiener RMS (Root Mean Square) Error Criterion in Filter Design and Prediction." J. Math. Phys., Vol. 25, No. 4 (1947), pp. 261-278.
- (3) Robinson, E. A. Statistical Communications and Detection with Special Reference to Digital Data Processing of Radar and Seismic Signals. London: Griffin, 1967.
- (4) Durbin, J. "The Fitting of Time-Series Models." Rev. Int. Inst. Statistics, Vol. 28, No. 3 (1960), pp. 233-243.
- (5) Trench, W. F. "Inversion of Toeplitz Band Matrices." Mathematics of Computation, Vol. 28, No. 128 (1974), pp. 1089-1095.
- (6) Graybill, F. A. Introduction to Matrices with Applications in Statistics. Belmont, Calif.: Wadsworth Publishing Company, Inc., 1969.
- (7) Uppuluri, V. R. R., and J. A. Carpenter. "An Inversion Method for Band Matrices." J. of Mathematical Analysis and Applications, Vol. 31 (1970), pp. 554-558.
- (8) Gilbert, A. "Linear Minimum Squared Estimation on Exponentially Correlated Processes with Applications in Inter-Frame Correlated Video." (Unpub. Ph.D. dissertation, New Mexico State University, 1973.)
- (9) Akakai, H. "Block Toeplitz Matrix Inversion." SIAM Journal of Applied Mathematics, Vol. 26 (1974), pp. 203-212.
- (10) Zohar, S. "Toeplitz Matrix Inversion: The Algorithm of W. F. Trench." J. Assoc. Comput. Mach., Vol. 16, No. 4 (1959), pp. 592-601.
- (11) Cornyn, J. J. "Direct Method for Solving Systems of Linear Equations Involving Nonsingular Block and Scalar Toeplitz or Hankel Matrices." Naval Research Laboratory Memorandum, Report No. NRL-MR-2920, October, 1974.
- (12) Mentz, R. P. "On the Inverse of Some Covariance Matrices of Toeplitz Type." Technical Report, Office of Naval Research Contract No. N00014-67-A-0112-0030. Department of Statistics, Stanford University, Stanford, Calif., July 12, 1972.

- (13) Gray, R. M. "On the Asymptotic Eigenvalue Distribution of Toeplitz Matrices." IEEE Trans. on Information Theory, Vol. IT-18, No. 6 (1972), pp. 725-730.
- (14) Wang, R. J., and S. Treitel. "The Determination of Digital Wiener Filters by Means of Gradient Methods." Geophysics, Vol. 38, (1973), pp. 310-326.
- (15) Rino, C. L. "The Inversion of Covariance Matrices by Finite Fourier Transforms." IEEE Trans. on Information Theory, Vol. IT-16 (March, 1970), pp 230-232.
- (16) Ekstrom, M. P. "An Iterative-Improvement Approach to the Numerical Solution of Vector Toeplitz Systems." IEEE Trans. on Computers, Vol C-23, No. 3 (March, 1974), pp 320-325.
- (17) Kaiser, J. F. "Digital Filters." System Analysis by Digital Computer. New York: John Wiley and Sons, 1966.
- (18) Helms, H. D. "Nonrecursive Digital Filters: Design Methods for Achieving Specifications on Frequency Response." IEEE Trans. Audio Electroacoustics, Vol. Au-16 (September, 1968), pp. 336-342.
- (19) Rossi, C. "Window Functions for Nonrecursive Digital Filters." Electronics Letters, Vol. 3, No. 12 (December, 1967), pp. 559-561.
- (20) Kaiser, J. F. "Nonrecursive Digital Filter Design, Using the I_0 -Sinh Window Function." Proc., 1974 IEEE Int. Symp. on Circuits and Systems. San Francisco, Calif., April, 1974.
- (21) Papoulis, A. The Fourier Integral and Its Applications. New York: McGraw-Hill, 1962, pp. 42-47.
- (22) Blackman, R. B., and J. W. Tukey. The Measurement of Power Spectra. New York: Dover Publications, 1958.
- (23) Rabiner, L., and B. Gold. Theory and Application of Digital Signal Processing. Englewood Cliffs, N. J.: Prentice-Hall, Inc., 1975.
- (24) Oppenheim, A. V., and R. W. Schaffer. Digital Signal Processing. Englewood Cliffs, N. J.: Prentice-Hall, Inc., 1974.
- (25) Martin, M. A. "Digital Filters for Data Processing." Tech. Information Series Report 62-SD484. General Electric Co., Missile and Space Div., 1962.
- (26) Gold, B., and K. Jordan. "A Direct Search Procedure for Designing Finite Duration Impulse Response Filters." IEEE Trans. on Audio and Electroacoustics, Vol. Au-17, No. 1 (March, 1969), pp. 33-36.
- (27) Rabiner, L. R., B. Gold, and C. A. McGonegal. "An Approach to the Approximation Problem for Nonrecursive Digital Filters."

IEEE Trans. on Audio and Electroacoustics, Vol. Au-18, No. 2 (June, 1970), pp. 83-106.

- (28) Rabiner, L. R., and K. Steiglitz. "The Design of Wide-Band Recursive and Nonrecursive Digital Differentiators." IEEE Trans. on Audio and Electroacoustics, Vol. Au-18, No. 2 (June, 1970), pp. 204-209.
- (29) Rabiner, L. R., and R. W. Schafer. "Recursive and Nonrecursive Realization of Digital Filters Designed by Frequency Sampling Techniques." IEEE Trans. on Audio and Electroacoustics, Vol. Au-19, No. 3 (September, 1971), pp. 200-207.
- (30) Rabiner, L. R., and R. W. Schafer. "Correction to Recursive and Nonrecursive Realizations of Digital Filters Designed by Frequency Sampling Techniques." IEEE Trans. on Audio and Electroacoustics, Vol. Au-20, No. 1 (March, 1972), pp. 104-105.
- (31) Rabiner, L. R. "Techniques for Designing Finite-Duration Impulse Response Digital Filters." IEEE Trans. on Communication Technology, Vol. Com-19, No. 2 (1971), pp. 188-195.
- (32) Gold, B., and K. Jordan. "A Note on Digital Filter Synthesis." Proc., IEEE (Lett.), Vol. 56 (October, 1968), pp. 1717-1718.
- (33) Rabiner, L. R. "The Design of Finite Impulse Response Digital Filters Using Linear Programming Techniques." Bell System Tech. J., Vol. 51, No. 6 (July-August, 1972), pp. 280-288.
- (34) Rabiner, L. R. "Linear Program Design of Finite Impulse Response (FIR) Digital Filters." IEEE Trans. on Audio and Electroacoustics, Vol. Au-20, No. 4 (October, 1972), pp. 280-288.
- (35) Hermann, O. "Design of Nonrecursive Digital Filters with Linear Phase." Electronics Letters, Vol. 6, N. 11 (1970), pp. 328-329.
- (36) Hofstetter, E., A. Oppenheim, and J. Siegel. "A New Technique for the Design of Nonrecursive Digital Filters." Proc., Fifth Annual Princeton Conf. on Information Sciences and Systems, 1971, pp. 64-72.
- (37) Hofstetter, E., A. Oppenheim, and J. Siegel. "A New Technique for the Design of Nonrecursive Digital Filters." Proc., Ninth Allerton Conf. on Circuit and System Theory, October, 1971, pp. 789-798.
- (38) Parks, T. W., and J. H. McClellan. "Chebyshev Approximation for Nonrecursive Digital Filters with Linear Phase." IEEE Trans. on Circuit Theory, Vol. CT-19 (March, 1972), pp. 189-194.
- (39) McClellan, H. H., and T. W. Parks. "A Unified Approach to the Design of Optimum FIR Linear Phase Digital Filters." IEEE Trans. Circuit Theory, Vol. CT-20 (November, 1973), pp. 697-701.

- (40) Hill, J. J., R. Linggard, and A. G. J. Holt. "An Analytical Approach to the Design of Nonrecursive Digital Filters." IEEE Trans. on Acoustics, Speech and Signal Processing, Vol. ASSP-23, No. 4 (August, 1975), pp. 383-385.
- (41) Ralphalrazi, V., and Minsoo Suk. "On the Frequency Weighted Least Square Design of Finite Duration Filters." IEEE Trans. on Circuits and Systems, Vol. CAS-22, No. 12 (December, 1975), pp.943-953.
- (42) Leon, B. J., and M. T. McCallig. "Design of Nonrecursive Digital Filters to Meet Maximum and Minimum Frequency Response Constraints." Intl. Conf. on Speech, Acoustics and Signal Processing, Philadelphia, 1976.
- (43) Leon, B. J., and M. T. McCallig. "Design of Nonrecursive Digital Filters to Meet Maximum and Minimum Frequency Response Constraints." Conference Record, 1976 IEEE Intl. Conf. on Acoustics, Speech and Signal Processing, April 12-14, 1976.
- (44) Farden, D. C., and L. L. Scharf. "Statistical Design of Nonrecursive Digital Filters." IEEE Trans. on Acoustics, Speech and Signal Processing, Vol. ASSP-22 (June, 1974), pp. 188-195.
- (45) Butler, P. "Comments on Statistical Design of Nonrecursive Digital Filters." IEEE Trans. on Acoustics, Speech, and Signal Processing, Vol. ASSP-23 (June, 1975), pp. 494-495.
- (46) Whittle, P. "On the Fitting of Multivariate Autoregressions, and the Approximate Factorization of a Spectral Density Matrix." Biometrika, Vol. 50 (March, 1963), pp. 129-134.
- (47) Helstrom, C. W. "Image Restoration by the Method of Least Squares." J. Opt. Soc. Amer., Vol. 37 (March, 1967), pp. 297-303.
- (48) Tao, K. "On the Direct Calculation of MMSE of Linear Realizable Estimator by Toeplitz Form Method." IEEE Trans. Information Theory, Vol. 17 (January, 1971), pp. 95-97.
- (49) Hunt, B. R. "A Matrix Theory Proof of the Discrete Convolution Theorem." IEEE Trans. on Audio and Electroacoustics, Vol. Au-19, No. 4 (December, 1971), pp. 285-288.
- (50) Penrose, R. "A Generalized Inverse for Matrices." Proc., Cambridge Phil. Soc., 51 (July, 1955), pp. 406-413.
- (51) Wang, R. J. "The Determination of Optimum Gate Lengths of Time Varying Wiener Filtering." Geophysics, Vol. 34 (1969), pp. 683-695.
- (52) Cooley, J. W., and J. W. Tukey. "An Algorithm for the Machine Calculation of Fourier Series." Mathematics of Computation, Vol. 19 (1965), pp. 297-301.

- (53) Hestenes, M. R. "The Conjugate Gradient Method for Solving Linear Systems." Proc., Symposia in Applied Mathematics, Vol VI. New York: McGraw-Hill Book Co., Inc., 1956.
- (54) Hamburger, H. L., and M. E. Grimshaw (Ed.). Linear Transformation in N-Dimensional Vector Space. Cambridge: Cambridge University Press, 1951, pp. 94-96.
- (55) Gentlemen, W. M. "Matrix Multiplication of Fast Fourier Transforms." BSTJ, Vol. 47 (1968), pp. 1092-1102.
- (56) Brigham, E. O. The Fast Fourier Transform. Englewood Cliffs, N. J.: Prentice-Hall, 1975.
- (57) Yarlagadda, R. "A Note on the Eigenvectors of DFT Matrices." IEEE Trans. on Acoustics, Speech, and Signal Processing, Vol. ASSP-25, No. 6 (December, 1977), pp. 586-589.
- (58) Anderson, N. "A Generalization of the Method of Averages for Over Determined Linear Systems." Mathematics of Computation, Vol. 29, No. 130 (1975), pp. 607-614.
- (59) Rabiner, L. R., J. H. McClellan, and T. W. Parks. "FIR Digital Filter Design Techniques Using Weighted Chebyshev Approximation." Proc., IEEE, Vol. 63 (April, 1975), pp. 595-610.
- (60) Hermann, O., and H. W. Schuessler. "Design of Nonrecursive Digital Filters with Minimum Phase." Electronics Letters, Vol. 6, No. 11 (1970), pp. 329-330.
- (61) Hermann, O., and H. W. Schuessler. "On the Design of Selective Nonrecursive Digital Filters." IEEE Arden House Workshop, Harriman, New York, January, 1970.
- (62) Helms, H. D. "Digital Filters with Equiripple or Minimax Responses." IEEE Trans. on Audio and Electroacoustics, Vol. Au-19, No. 1 (1971), pp. 87-94.
- (63) Parks, T. W., and J. H. McClellan. "Chebyshev Approximation for Nonrecursive Digital Filters with Linear Phase." IEEE Trans. Circuit Theory, Vol. CT-19 (March, 1972), pp. 189-194.
- (64) Lown, A. N. "Tables of Sine, Cosine and Exponential Integrals, Vol. I." Federal Works Agency, Work Projects Administration for the City of New York, 1940.
- (65) Jahnke, L., F. Emde, and F. Losch. Tables of Higher Functions. New York: McGraw-Hill, 1960, pp. 17-25.

APPENDIX A

COMPUTATION OF FREQUENCY RESPONSE OF FIR FILTERS

This program determines the values of the frequency response of Type 1 linear phase filters at different frequency locations using Equation (3.5) given in Chapter III. Input data includes, the order of the filter y , the number of passband frequency sample values IZ , and the transition sample values T_1 , T_2 , and T_3 . The scaling factors are evaluated in sub-routine scale, and the frequency response is plotted using the plot routine PLT20A.

```

$JOB TIME=10,PAGES=10,NOSUBCHK,LIBLIST
C
C THIS PROGRAM IS USED TO DERIVE THE FREQUENCY RESPONSE OF A LOW-PASS
C BY USING THE DIRECT APPROACH TO FREQUENCY SAMPLING METHOD. THE
C FOLLOWING PARAMETERS ARE USED AS INPUT.
C PARAMETERS IS USED AS INPUT.
C
C      IZ IS THE NUMBER OF PASS BAND FREQUENCY SAMPLES.
C
C      Y DENOTES THE ORDER OF THE FILTER.
C
C      T1 IS THE FIRST OPTIMUM TRANSITION SAMPLE VALUE.
C
C      T2 IS THE SECOND OPTIMUM TRANSITION SAMPLE VALUE.
C
C      T3 IS THE THIRD OPTIMUM TRANSITION SAMPLE VALUE.
C
C      EPS IS USED WHEN FINDING THE LIMITING VALUE OF A FUNCTION.
C
C      M1 IS THE FIRST SAMPLED TRANSITION VALUE.
C
C      M2 IS THE SECOND SAMPLED TRANSITION SAMPLE VALUE.
C
C      M3 IS THE THIRD TRANSITION SAMPLE VALUE.
C
C      K4 DENOTES THE NUMBER OF POINTS IN BETWEEN THE SAMPLED VALUES
C
1  IMPLICIT REAL *8(A-H,J-Z)
2  REAL X1(800),Y1(800),X2(800),Y2(500),VMIN,VMAX,XMIN,XMAX
   I,YMIN,YMAX
3  IZ=2
4  IOUT =6
5  Y=125.
6  T1=C.7017761800
7  T2=C.2223223500
8  T3=0.0196899400
9  K4=4
10 EPS=1.E-8
11 M1= IZ
12 M2= IZ+1
13 M3= M2+1
C
C X REPRESENTS THE FREQUENCY IN RADIANS. STARTING FREQUENCY IS SET TO
C ZERO.
C
14 X=0.00
15 I=1
16 PI=3.141592654
17 XX=PI
C
C COMPUTE THE START OF THE STOP BAND.
C
18 XY=(2.*PI*DFLOAT(IZ+3))/Y
19 GO TO 50
C
C INCREMENT THE FREQUENCY.
C
20 X=X+(2.*PI)/(Y*DFLOAT(K4))
C
C COMPUTE THE MAGNITUDE BY THE FIRST FREQUENCY SAMPLE.

```

```

21  C 50 R76=DSIN(X*Y/2.)
22      R77=DSIN(X/2.)
23      R5=R76
24      IF (CABS(R76).LE.EPS.AND.DABS(R77).LE.EPS) R76=(Y/2.)*DCOS(X*Y/2.)
25      IF (CABS(R5).LE.EPS.AND.DABS(R77).LE.EPS) R77=(0.500)*DCOS(X/2.)
26      R78=(1./Y)*(R76/R77)

C
C COMPUTE THE MAGNITUDE BY THE OTHER FREQUENCY SAMPLES.
C
27      KR=1
28      R72=0.00
29      GO TO 20
30  10  KR=KR+1
31  20  X3=(PI*DFLOAT(KR))/Y
32      X4=(X/2.)-X3
33      X5=(X/2.)+X3
34      X6=Y*X4
35      X7=Y*X5
36      R79=DSIN(X6)
37      R80=DSIN(X4)
38      RR=R79
39      IF (DABS(R79).LE.EPS.AND.DABS(R80).LE.EPS) R79=(Y/2.)*DCOS(X6)
40      IF (DABS(RR).LE.EPS.AND.DABS(R80).LE.EPS) R80=(0.500)*DCOS(X4)
41      R81=(1./Y)*(R79/R80)
42      IF (KR.EQ.M1) R81=R81*T1
43      IF (KR.EQ.M2) R81=R81*T2
44      IF (KR.EQ.M3) R81=R81*T3
45      R72=R81+R72
46      R82=DSIN(X7)
47      R83=DSIN(X5)
48      RY=R82
49      IF (DABS(R82).LE.EPS.AND.DABS(R83).LE.EPS) R82=(Y/2.)*DCOS(X7)
50      IF (DABS(RY).LE.EPS.AND.DABS(R83).LE.EPS) R83=(0.500)*DCOS(X5)
51      R84=(1./Y)*(R82/R83)
52      IF (KR.EQ.M1) R84=R84*T1
53      IF (KR.EQ.M2) R84=R84*T2
54      IF (KR.EQ.M3) R84=R84*T3
55      R72=R72+R84
56      IF (KR.LE.(LZ+1)) GO TO 10
57      R72=R72+R78

C
C STORE THE FREQUENCIES FROM ZERO TO PI RADIAN.
C
58      X1(I)=X

C
C STORE THE CORRESPONDING MAGNITUDES.
C
59      Y1(I)=R72
60      I=I+1

C
C TERMINATE THE PROGRAM WHEN THE FREQUENCY IS PI RADIAN.
C
61      IF (X.LE.XX) GO TO 49
62      IL=I-1
63      LI=0
64      DO 200 J=1,IL
65      WRITE (IOUT,105) X1(J),Y1(J)
66  105  FORMAT(5X,E20.10,5X,E20.10)
67      IF (X1(J).GE.XY) GO TO 209

```



```

68      GO TO 200
69      209  LI=LI+1
70      X2(LI)=X1(J)
71      Y2(LI)=Y1(J)
72      200  CONTINUE
       C
       C
73      CALL SCAXIS(X1,IL,VMIN,VMAX,XMIN,XMAX,10)
74      CALL SCAXIS(Y1,IL,VMIN,VMAX,YMIN,YMAX,10)
75      CALL PLT20A(X1,Y1,IL,XMAX,XMIN,YMAX,YMIN)
76      LR=LI
77      DO 89 JJ=1,LR
78      WRITE(IOUT,105) X2(JJ),Y2(JJ)
79      89   CONTINUE
       C
       C USE THE PLOT ROUTINE TO PLOT THE STOP BAND RESPONSE.
       C
80      CALL SCAXIS(X2,LR,VMIN,VMAX,XMIN,XMAX,10)
81      CALL SCAXIS(Y2,LR,VMIN,VMAX,YMIN,YMAX,10)
82      CALL PLT20A(X2,Y2,LR,XMAX,XMIN,YMAX,YMIN)
83      STOP
84      END

85      SUBROUTINE SCAXIS (V,NV,VMIN,VMAX,SMIN,SMAX,NG )
       C
       C .....
       C
       C . THIS IS A ROUTINE WHICH WILL SELECT A SCALE FOR DATA TO BE
       C . PLOTTED. THE USER MAY EITHER SUPPLY THE DATA TO BE SCALED
       C . OR THE MINIMUM AND MAXIMUM DATA VALUES. IN ADDITION, THE
       C . V : THE VECTOR OF DATA TO BE SCALED.
       C .
       C . NV : THE NUMBER OF POINTS IN V TO BE SCALED. IF NV IS
       C . ZERO, THEN THE ROUTINE ASSUMES THAT VMIN AND VMAX
       C . NOT TO BE SEARCHED.
       C . CONTAIN THE MINIMUM AND MAXIMUM OF THE DATA AND V IS
       C . VMIN : THE MINIMUM DATA VALUE
       C . VMAX : THE MAXIMUM DATA VALUE
       C . SMIN : THE SCALED MINIMUM VALUE. SMIN .LE. VMIN
       C . SMAX : THE SCALED MAXIMUM VALUE. SMAX .GE. VMAX
       C . NG : THE NUMBER OF INCREMENTS TO APPEAR ON THE SCALED AXIS
       C .
       C . IN ADDITION, AN INTEGER ARRAY CALLED "ALLOW" CONTAINS THE
       C . ALLOWABLE SCALING VALUES. THESE MAY BE CHANGED TO GIVE A
       C . DIFFERENT SET OF VALUES BY SPECIFYING NEW VALUES AND PLACING
       C . THEM IN A COMMON ARRAY CALLED /ALLOW/ ( MAXIMUM OF 20
       C . VALUES ).
       C .
       C .....
       C
86      DIMENSION V(1)
87      INTEGER ALLOW(9) / 1, 2, 3, 4, 5, 6, 7, 8, 9 /, NA / 9 /
       C*** SEARCH FOR VMIN AND VMAX IF NEEDED
       C***
88      IF ( NV .EQ. 0 ) GO TO 20
89      VMIN = V(1)
90      VMAX = V(1)
91      DO 10 I = 2, NV
92      VMIN = AMINI ( VMIN, V(I) )

```

```

SCAX 1
SCAX 2
SCAX 3
SCAX 4
SCAX 5
SCAX 6
SCAX 7
SCAX 11
SCAX 10
SCAX 12
SCAX 13
SCAX 15
SCAX 14
SCAX 16
SCAX 17
SCAX 18
SCAX 19
SCAX 20
SCAX 21
SCAX 22
SCAX 23
SCAX 24
SCAX 25
SCAX 26
SCAX 27
SCAX 28
SCAX 29
SCAX 30
SCAX 31
SCAX 32
SCAX 33
SCAX 34
SCAX 35
SCAX 36
SCAX 37
SCAX 38
SCAX 39

```

```

93          VMAX = AMAX1 ( VMAX, V(I) )          SCAX 40
94      10      CONTINUE                          SCAX 41
C***          SCALE ( VMAX - VMIN ) / NG TO HAVE THE SAME NUMBER OF SCAX 42
C***          DIGITS AS THE ENTRIES IN ALLOW      SCAX 43
C***          SCAX 44
C***          SCAX 45
95      20          ND = IFIX ( 1.01 + ALOG10 ( FLOAT(ALLOW(1) ) ) ) SCAX 46
96          VINC = ( VMAX - VMIN ) / NG          SCAX 47
97          A = ALOG10 ( VINC )                  SCAX 48
98          I = A                                SCAX 49
99          IF ( A .LT. 0.0 ) I = I - 1          SCAX 50
100         SCALE = 10.0 ** ( ND - 1 - I )       SCAX 51
101         VINC = VINC * SCALE                  SCAX 52
C***          SCAX 53
C***          FIND AN ELEMENT IN ALLOW THAT IS GREATER THAN OR EQUAL TO VINC SCAX 54
C***          SCAX 55
102         DD 30 I = 1, NA                      SCAX 56
103             A = ALLOW(I)                     SCAX 57
104             IF ( A .GE. VINC ) GO TO 50       SCAX 58
105         30      CONTINUE                      SCAX 59
106         40          I = 1                    SCAX 60
107             A = ALLOW(I)                     SCAX 61
108             SCALE = SCALE / 10.0            SCAX 62
C***          SCAX 63
C***          THE SMALLEST ALLOWABLE INCREMENT IS NOW A / SCALE. SCAX 64
C***          NOW PICK SMIN AND SMAX SUCH THAT ZERO WILL BE ONE SCAX 65
C***          OF THE INCREMENT VALUES         SCAX 66
C***          SCAX 67
109         50          VINC = A / SCALE          SCAX 68
110             A = VMIN / VINC                  SCAX 69
111             J = A                            SCAX 70
112             IF ( A .LT. 0.0 ) J = J - 1      SCAX 71
113             SMIN = J * VINC                  SCAX 72
114             SMAX = SMIN + VINC * NG         SCAX 73
115             IF ( SMAX .GE. VMAX ) GO TO 60   SCAX 74
C***          SCAX 75
C***          VINC IS TOO SMALL TO FIT THE ADJUSTED RANGE. INCREASE IT. SCAX 76
C***          SCAX 77
116             IF ( I .EQ. NA ) GO TO 40       SCAX 78
117             I = I + 1                        SCAX 79
118             A = ALLOW(I)                     SCAX 80
119             GO TO 50                          SCAX 81
C***          SCAX 82
120         60      RETURN                        SCAX 83
121         END                                  SCAX 84

$ENTRY
122     SUBROUTINE PLT20A ( X, Y, KI, XMAX, XMIN, YMAX, YMIN )    PLOT 1
C          PLOT 2
C          ..... PLOT 3
C          . PLOT 4
C          . SUBROUTINE TO PRODUCE A PRINTER PLOT OF X VRS. Y . PLOT 5
C          . X AND Y ARE ROUNDED ( NOT TRUNCATED ) TO THE NEAREST . PLOT 6
C          . INTEGERS BEFORE PLOTTING. GRID SIZE IS 10 X 10. . PLOT 7
C          . PLOT 8
C          . X : ARRAY OF X COORDINATES . PLOT 9
C          . Y : ARRAY OF Y COORDINATES . PLOT 10
C          . KI : NUMBER OF POINTS IN X AND Y . PLOT 11
C          . XMAX : MAXIMUM X VALUE . PLOT 12
C          . XMIN : MINIMUM X VALUE . PLOT 13

```

C	.	IF XMAX = XMIN, X WILL BE SEARCHED TO FIND THE MINIMUM	.PLOT	14
C	.	AND MAXIMUM VALUES.	.PLOT	15
C	.	YMAX : MAXIMUM Y VALUE	.PLOT	16
C	.	YMIN : MINIMUM Y VALUE	.PLOT	17
C	.	IF YMAX = YMIN, Y WILL BE SEARCHED TO FIND THE MINIMUM	.PLOT	18
C	.	AND MAXIMUM VALUES.	.PLOT	19
C	.		.PLOT	20
CPLOT	21
C	.		.PLOT	22
123		DIMENSION X(1), Y(1)	.PLOT	23
124		CCAMCN / PGINTS / IFX(101), ZX(11)	.PLOT	24
125		DATA IBLNK, ISTAR / 1H , 1H* /	.PLOT	25
126		DATA IYMAX / 50 /, J1 / 1 /	.PLOT	26
127		LINE = 5	.PLOT	27
128		XL = XMAX	.PLOT	28
129		YL = YMAX	.PLOT	29
130		XS = XMIN	.PLOT	30
131		YS = YMIN	.PLOT	31
132		IF (XMAX .NE. XMIN) GO TO 20	.PLOT	32
133		XL = X(1)	.PLOT	33
134		XS = X(1)	.PLOT	34
135		DO 10 N = 2, KI	.PLOT	35
136		XL = AMAX1 (X(N), XL)	.PLOT	36
137		XS = AMIN1 (X(N), XS)	.PLOT	37
138	10	CONTINUE	.PLOT	38
139	20	IF (YMAX .NE. YMIN) GO TO 40	.PLOT	39
140		YL = Y(1)	.PLOT	40
141		YS = Y(1)	.PLOT	41
142		DO 30 N = 2, KI	.PLOT	42
143		YL = AMAX1 (Y(N), YL)	.PLOT	43
144		YS = AMIN1 (Y(N), YS)	.PLOT	44
145	30	CONTINUE	.PLOT	45
146	40	XSCALE = (XL - XS) * 0.51	.PLOT	46
147		YSCALE = (YL - YS) / FLOAT (IYMAX)	.PLOT	47
148		PRINT 200	.PLOT	48
149		PRINT 210	.PLOT	49
150		LL = IYMAX	.PLOT	50
151		GO TO 60	.PLOT	51
152	50	LL = LL - 1	.PLOT	52
153	60	DO 70 I = 1, 101	.PLOT	53
154		IFX(I) = IBLNK	.PLOT	54
155	70	CONTINUE	.PLOT	55
156		DO 90 I = J1, KI	.PLOT	56
157		IF (X(I) .GT. XL .OR. X(I) .LT. XS) GO TO 90	.PLOT	57
158		IF (Y(I) .GT. YL .OR. Y(I) .LT. YS) GO TO 90	.PLOT	58
159		IY = (Y(I) - YS) / YSCALE + 0.5	.PLOT	59
160		IF (IY - LL) 90, 80, 90	.PLOT	60
161	80	IX = (X(I) - XS) / XSCALE + 0.5	.PLOT	61
162		II = IX + 1	.PLOT	62
163		IFX(II) = ISTAR	.PLOT	63
164	90	CONTINUE	.PLOT	64
165		ZY = FLOAT (LL) * YSCALE + YS	.PLOT	65
166		IF (LINE .EQ. 5) PRINT 220, ZY, (IFX(I), I = 1, 101)	.PLOT	66
167		IF (LINE .NE. 5) PRINT 240, (IFX(I), I = 1, 101)	.PLOT	67
168		LINE = LINE + 1	.PLOT	68
169		IF (LINE .GT. 5) LINE = 1	.PLOT	69
170		IF (LL .NE. 0) GO TO 50	.PLOT	70
171		PRINT 210	.PLOT	71
172		DO 100 K = 1, 11	.PLOT	72
173		ZX(K) = 10. * FLOAT (K - 1) * XSCALE + XS	.PLOT	73

```
174      CONTINUE
175      PRINT 230, ( ZX(K), K = 1, 11 )
176      PRINT 220
177      RETURN
178      200 FORMAT ( 1H1 )
179      210 FORMAT ( 15X, 20 ( 5H1... ), 1H1 )
180      220 FORMAT ( 1H, 1PE10.3, 2X, 2+-1+, 1D1A1, 1H1 )
181      230 FORMAT ( 9X, 11 ( 2X, F8.3 ) )
182      240 FORMAT ( 1+X, 1H, 10I31, 1H1 )
183      END
184      PLOT 74
185      PLOT 75
186      PLOT 76
187      PLOT 77
188      PLOT 78
189      PLOT 79
190      PLOT 80
191      PLOT 81
192      PLOT 82
```

APPENDIX B

COMPUTATION OF TRANSITION SAMPLE VALUES

The program computes the transition sample values using the direct approach discussed in Chapter III. Input data includes, the order of the filter y , and the number of passband frequency sample values I_Z , and the total number of transition sample values N_2 . In addition to the above, for the bandpass and high-pass cases an additional parameter M_1 (i.e., the zero valued frequency samples just before the first transition sample) is also required. The output of the program includes the transition sample values along with R_{72} , R_{73} , which represents contributions to the frequency response by the fixed and unknown transition sample values, respectively.

```

$JOB TIME=10,PAGES=10,NDSUBCHK,LIBLIST
C BAND PASS FILTER DESIGN.
C THIS PROGRAM USES THE DIRECT APPROACH TO FREQUENCY SAMPLING FILTER
C DESIGN PRESENTED IN CHAPTER THREE TO COMPUTE THE TRANSITION SAMPLE
C VALUES. THE FOLLOWING PARAMETERS ARE USED AS INPUT.
C
C Y=ORDER OF THE FILTER.
C IZ=NUMBER OF PASS BAND FREQUENCY SAMPLES.
C M1=TOTAL NUMBER OF ZERO VALUED FREQUENCY SAMPLES BEFORE THE FIRST
C TRANSITION SAMPLE VALUE
1 IMPLICIT REAL*8(A-H,O-Z)
2 DIMENSION R1(4),R2(4),T1(+),T2(4),P3(3),P1(3,3),P2(3,3),
3 LZ(3,3),IL(3),IM(3),P7(3),Ps(3)
4 Y=123
5 M2=3
6 DO 333 M1=16,20,4
7 LZ=31
8 M2=M1+1
9 M3=M2+1
10 M4=M3+IZ+1
11 M5=M4+1
12 M6=M5+1
13 M7=M6+1
14 PI=3.141592654
C
C USE THE FIRST FREQUENCY ESTIMATE.
14 X=(2.00*PI*DFLOAT(M7))/Y+(2.00*PI/Y)*0.125
15 KL=C
16 I=0
C
17 62 KR=M1
18 R72=0.00
19 R73=0.00
20 R74=0.00
21 R75=0.00
C
C COMPUTE THE CONTRIBUTION BY THE FIXED FREQUENCY SAMPLES.
C
22 GO TO 20
23 10 KR=KR+1
24 20 X3=(PI*DFLOAT(KR))/Y
25 X4=(X/2.00)-X3
26 X5=(X/2.00)+X3
27 X6=Y*X4
28 X7=Y*X5
29 IF(KR.EQ.M1.OR.KR.EQ.M6) GO TO 60
30 IF(KR.EQ.M2.OR.KR.EQ.M5) GO TO 63
31 IF(KR.EQ.M3.OR.KR.EQ.M4) GO TO 64
32 R79=DSIN(X6)
33 R80=DSIN(X4)
34 R81=(1.00/Y)*(R79/R80)
35 R72=R72+R81
36 R82=DSIN(X7)
37 R83=DSIN(X5)
38 R84=(1.00/Y)*(R82/R83)
39 R72=R72+R84
40 GO TO 61
C
C CONTRIBUTION BY THE FIRST AND THE LAST TRANSITION SAMPLES.
C

```

```

41 60 R90=DSIN(X6)
42 R91=DSIN(X4)
43 R92=(1.00/Y)*(R90/R91)
44 R73=R73+R92
45 R93=DSIN(X7)
46 R94=DSIN(X5)
47 S4=R93
48 R95=(1.00/Y)*(R93/R94)
49 R73=R73+R95
50 GO TO 61

C
C
C
CONTRIBUTION BY THE SECOND AND THE LAST BUT ONE TRANSITION SAMPLES.
51 63 R96=DSIN(X6)
52 R97=DSIN(X4)
53 R98=(1.00/Y)*(R96/R97)
54 R74=R74+R98
55 R99=DSIN(X7)
56 R100=DSIN(X5)
57 R101=(1./Y)*(R99/R100)
58 R74=R74+R101
59 GO TO 61

C
C
C
CONTRIBUTION BY THE THIRD AND THE LAST BUT TWO TRANSITION SAMPLES
60 64 S96=DSIN(X6)
61 S97=DSIN(X4)
62 S98=(1.00/Y)*(S96/S97)
63 R75=R75+S98
64 S99=DSIN(X7)
65 S100=DSIN(X5)
66 S101=(1.00/Y)*(S99/S100)
67 R75=R75+S101
68 61 IF(KR.EQ.46) GO TO 600
69 GO TO 10
70 600 I=I+1
71 R1(I)=R73
72 R2(I)=R74
73 T1(I)=R75
74 T2(I)=R72
75 WRITE(6,88) R72,R73,R74,R75
76 88 FORMAT(1H,5X,4HR72=,D20.10,5X,4HR73=,D20.10,5X,5X,4HR74=,D20.10,
12X,4HR75=,D20.10)
77 KL=KL+1
78 WRITE(6,89)X

C
C
C
USE THE SECOND FREQUENCY ESTIMATE.
79 IF(KL.EQ.1) X=X+(2.00*PI/Y)*0.4375

C
C
C
USE THE THIRD FREQUENCY ESTIMATE.
80 USE THE THIRD FREQUENCY ESTIMATE.
IF(KL.EQ.2) X=X+(2.00*PI/Y)*2.0002

C
C
C
USE THE FOURTH FREQUENCY ESTIMATE.
81 IF(KL.EQ.3) X=X+(2.00*PI/Y)*0.9374
82 89 FORMAT(/////5X,2HX=,D20.10)
83 IF(KL.LT.4) GO TO 62
84 I=1

```

```

C
C      EQUATE THE RIPPLE VALUES.
C
85 601 P3(I)=-T2(I)-T2(I+1)
86     J=1
87     P(I,J)=P1(I)+P1(I+1)
88     P(I,J+1)=P2(I)+P2(I+1)
89     P(I,J+2)=T1(I)+T1(I+1)
90     IF(1.E0.(KL-1))GO TO 103
91     I=I+1
92     GO TO 601
93 103 NN=KL-1
94     WRITE(6,6+1) (P3(I),I=1,NN)
95     WRITE(6,641)((P(I,J),J=1,N2),I=1,NN)
96 641 FORMAT(1H ,4D20.10)
C
C      COMPUTATION OF TRANSITION SAMPLE VALUES.
C
97     CALL TRANS(P,P1,NN,N2)
98     WRITE(6,651)
99 651 FORMAT(/,5X,'TRANSPOSE')
100    WRITE(6,641)((P1(I,J),J=1,NN),I=1,N2)
101    CALL MULT(P1,P,P2,N2,NN,N2)
102    WRITE(6,651)
103 661 FORMAT(/,5X,'PRODUCT OF P AND TRANSPOSE')
104    WRITE(6,641)((P2(I,J),J=1,N2),I=1,N2)
105    NR=N2*N2
106    CALL PACK(1,N2,NR,Z,P2)
107    CALL MINV(2,N2,DET,IL,IM)
108    CALL PACK(2,N2,NR,Z,P2)
109    WRITE(6,671)
110 671 FORMAT(/,5X,'MATRIX INVERSE')
111    WRITE(6,641)((P2(I,J),J=1,N2),I=1,N2)
112    CALL MULT(P1,P3,P7,N2,NN,1)
113    WRITE(6,641) (P7(I),I=1,N2)
114    CALL MULT(P2,P7,P8,N2,N2,1)
115    WRITE(6,691)
116 691 FORMAT(1H ,5X,'UNKNOWN TRANSITION SAMPLE' )
117    WRITE(6,641) (P8(I),I=1,N2)
118    WRITE(6,689) IZ,M1
119 689  FORMAT(1H ,5X,3HIZ=,I5,5X,3HMI=,I5)
120 333 CONTINUE
121     STOP
122     END

123     SUBROUTINE MULT(A,B,C,M,L,N)
124     IMPLICIT REAL*8(A-H,O-Z)
125     DIMENSION A(M,L),B(L,N),C(M,N)
126     DO 20 I=1,M
127     DO 20 J=1,N
128     SUM=0.00
129     DO 10 K=1,L
130     PRD=A(I,K)*B(K,J)
131     SUM=SUM+PRD
132 10 CONTINUE
133     C(I,J)=SUM
134 20 CONTINUE
135     RETURN
136     END

```



```

137 SUBROUTINE TRANS(A,B,M,N)
138 IMPLICIT REAL*8(A-H,O-Z)
139 DIMENSION A(M,N),B(N,M)
140 DO 16 I=1,M
141 DO 16 J=1,N
142 B(J,I)=A(I,J)
143 16 CONTINUE
144 RETURN
145 END

C
C ..... MINV 10
C ..... MINV 20
C ..... MINV 30
C SUBROUTINE MINV MINV 40
C ..... MINV 50
C PURPOSE MINV 60
C INVERT A MATRIX MINV 70
C ..... MINV 80
C USAGE MINV 90
C CALL MINV(A,N,D,L,M) MINV 100
C ..... MINV 110
C DESCRIPTION OF PARAMETERS MINV 120
C A - INPUT MATRIX, DESTROYED IN COMPUTATION AND REPLACED BY MINV 130
C RESULTANT INVERSE. MINV 140
C N - ORDER OF MATRIX A MINV 150
C D - RESULTANT DETERMINANT MINV 160
C L - WORK VECTOR OF LENGTH N MINV 170
C M - WORK VECTOR OF LENGTH N MINV 180
C ..... MINV 190
C REMARKS MINV 200
C MATRIX A MUST BE A GENERAL MATRIX MINV 210
C ..... MINV 220
C SUBROUTINES AND FUNCTION SUBPROGRAMS REQUIRED MINV 230
C NJNE MINV 240
C ..... MINV 250
C METHOD MINV 260
C THE STANDARD GAUSS-JORDAN METHOD IS USED. THE DETERMINANT MINV 270
C IS ALSO CALCULATED. A DETERMINANT OF ZERO INDICATES THAT MINV 280
C THE MATRIX IS SINGULAR. MINV 290
C ..... MINV 300
C ..... MINV 310
C ..... MINV 320

146 SUBROUTINE MINV(A,N,D,L,M) MINV 330
147 DIMENSION A(L),L(L),M(L) MINV 340
148 DOUBLE PRECISION A,D,BIGA,HOLD
149 DOUBLE PRECISION DABS

C
C ..... MINV 350
C ..... MINV 360
C ..... MINV 370
C IF A DOUBLE PRECISION VERSION OF THIS ROUTINE IS DESIRED, THE MINV 380
C IN COLUMN 1 SHOULD BE REMOVED FROM THE DOUBLE PRECISION MINV 390
C STATEMENT WHICH FOLLOWS. MINV 400
C ..... MINV 410
C DOUBLE PRECISION A,D,BIGA,HOLD MINV 420
C ..... MINV 430
C THE C MUST ALSO BE REMOVED FROM DOUBLE PRECISION STATEMENTS MINV 440
C APPEARING IN OTHER ROUTINES USED IN CONJUNCTION WITH THIS MINV 450
C ROUTINE. MINV 460
C ..... MINV 470
C THE DOUBLE PRECISION VERSION OF THIS SUBROUTINE MUST ALSO MINV 480

```

C	CONTAIN DOUBLE PRECISION FORTRAN FUNCTIONS. ABS IN STATEMENT	MINV 490
C	10 MUST BE CHANGED TO DABS.	MINV 500
C		MINV 510
C	MINV 520
C		MINV 530
C	SEARCH FOR LARGEST ELEMENT	MINV 540
C		MINV 550
150	D=1.0	MINV 560
151	NK=-N	MINV 570
152	DO 30 K=1,N	MINV 580
153	NK=NK+N	MINV 590
154	L(K)=K	MINV 600
155	M(K)=K	MINV 610
156	KK=NK+K	MINV 620
157	BIGA=A(KK)	MINV 630
158	DO 20 J=K,N	MINV 640
159	IZ=N*(J-1)	MINV 650
160	DO 20 I=K,N	MINV 660
161	IJ=IZ+I	MINV 670
162	10 IF(CABS(BIGA)-CABS(A(IJ))) 15,20,20	
163	15 BIGA=A(IJ)	MINV 690
164	L(K)=I	MINV 700
165	M(K)=J	MINV 710
166	20 CONTINUE	MINV 720
C		MINV 730
C	INTERCHANGE ROWS	MINV 740
C		MINV 750
167	J=L(K)	MINV 760
168	IF(J-K) 35,35,25	MINV 770
169	25 KI=K-N	MINV 780
170	DO 30 I=1,N	MINV 790
171	KI=KI+N	MINV 800
172	HOLD=-A(KI)	MINV 810
173	JI=KI-K+J	MINV 820
174	A(KI)=A(JI)	MINV 830
175	30 A(JI)=HOLD	MINV 840
C		MINV 850
C	INTERCHANGE COLUMNS	MINV 860
C		MINV 870
176	35 I=M(K)	MINV 880
177	IF(I-K) 45,45,38	MINV 890
178	38 JP=N*(I-1)	MINV 900
179	DO 40 J=1,N	MINV 910
180	JK=NK+J	MINV 920
181	JJ=JP+J	MINV 930
182	HOLD=-A(JK)	MINV 940
183	A(JK)=A(JJ)	MINV 950
184	40 A(JJ)=HOLD	MINV 960
C		MINV 970
C	DIVIDE COLUMN BY MINUS PIVOT (VALUE OF PIVOT ELEMENT IS	MINV 980
C	CONTAINED IN BIGA)	MINV 990
C		MINV1000
185	45 IF(BIGA) 48,46,48	MINV1010
186	46 D=0.0	MINV1020
187	RETURN	MINV1030
188	48 DO 55 I=1,N	MINV1040
189	IF(I-K) 50,55,50	MINV1050
190	50 IK=NK+I	MINV1060
191	A(IK)=A(IK)/(-BIGA)	MINV1070
192	55 CONTINUE	MINV1080

	C		MINV1090
	C	REDUCE MATRIX	MINV1100
	C		MINV1110
193		DO 65 I=1,N	MINV1120
194		IK=KK+1	MINV1130
195		HOLD=A(IK)	MINV1140
196		IJ=I-N	MINV1150
197		DO 65 J=1,N	MINV1160
198		IJ=IJ+N	MINV1170
199		IF(I-K) 60,65,60	MINV1180
200	60	IF(J-K) 62,65,62	MINV1190
201	62	KJ=IJ-I+K	MINV1200
202		A(IJ)=HOLD+A(KJ)+A(IJ)	MINV1210
203	65	CONTINUE	MINV1220
	C		MINV1230
	C	DIVIDE ROW BY PIVOT	MINV1240
	C		MINV1250
204		KJ=K-N	MINV1260
205		DO 75 J=1,N	MINV1270
206		KJ=KJ+N	MINV1280
207		IF(J-K) 70,75,70	MINV1290
208	70	A(KJ)=A(KJ)/BIGA	MINV1300
209	75	CONTINUE	MINV1310
	C		MINV1320
	C	PRODUCT OF PIVOTS	MINV1330
	C		MINV1340
210		D=D*BIGA	MINV1350
	C		MINV1360
	C	REPLACE PIVOT BY RECIPROCAL	MINV1370
	C		MINV1380
211		A(KK)=1.0/BIGA	MINV1390
212	80	CONTINUE	MINV1400
	C		MINV1410
	C	-FINAL ROW AND COLUMN INTERCHANGE	MINV1420
	C		MINV1430
213		K=N	MINV1440
214	100	K=(K-1)	MINV1450
215		IF(K) 150,150,105	MINV1460
216	105	I=L(K)	MINV1470
217		IF(I-K) 120,120,108	MINV1480
218	108	JQ=N*(K-1)	MINV1490
219		JR=N*(I-1)	MINV1500
220		DO 110 J=1,N	MINV1510
221		JK=JQ+J	MINV1520
222		HJL=A(JK)	MINV1530
223		JT=JR+J	MINV1540
224		A(JK)=-A(JI)	MINV1550
225	110	A(JI)=HOLD	MINV1560
226	120	J=M(K)	MINV1570
227		IF(J-K) 100,100,125	MINV1580
228	125	KI=K-N	MINV1590
229		DO 130 I=1,N	MINV1600
230		KI=KI+N	MINV1610
231		HOLD=A(KI)	MINV1620
232		JI=KI-K+J	MINV1630
233		A(KI)=-A(JI)	MINV1640
234	130	A(JI)=HOLD	MINV1650
235		GO TO 100	MINV1660
236	150	RETURN	MINV1670
237		END	MINV1680

```

238     SUBROUTINE PACK(ICODE,N,N2,A,B)
239     IMPLICIT REAL*8(A-H,O-Z)
240     DIMENSION A(N2),B(N,N)
241     IF (ICODE.EQ.1) GO TO 20
      C   CREATE MATRIX B FROM ARRAY A
242     I=1
243     J=1
244     DO 10 K=1,N2
245     B(I,J)=A(K)
246     I=I+1
247     IF(I.LE.N) GO TO 10
      J=J+1
248     I=1
249     10  CONTINUE
250     GO TO 30
251     C   CREATE ARRAY A FROM MATRIX B
252     20  K=1
253     DO 25 J=1,N
254     DO 25 I=1,N
255     A(K)=B(I,J)
256     K=K+1
257     25  CONTINUE
258     30  RETURN
259     END

```

```

$JOB TIME=10,PAGES=10,NDSUBCHK,LIBLIST
C
C THIS PROGRAM USES THE DIRECT APPROACH TO FREQUENCY SAMPLING FILTER
C DESIGN PRESENTED IN CHAPTER THREE TO COMPUTE THE TRANSITION SAMPLE
C VALUES. THE FOLLOWING PARAMETERS ARE USED AS INPUT.
C LOWPASS FILTER DESIGN - ONE TRANSITION (PASS BAND)
C Y-ORDER OF THE FILTER.
C IZ-NUMBER OF PASS BAND FREQUENCY SAMPLES.
C M-TOTAL NUMBER OF DIFFERENT PASSBAND FREQUENCY SAMPLES.
1 IMPLICIT REAL*8(A-H,O-Z)
2 DIMENSION R1(2),R2(2),R3(1),R4(1),X1(2),ILIST(40)
3 M=1
4 Y=256.
5 LL=2
6 READ(5,600) (ILIST(I),I=1,M )
7 600 FORMAT(16I5)
8 DO 300 JJ=1,M
9 II=ILIST(JJ)
10 IZ=II
11 K3=II+1
12 PI=3.141592654
13 I=K3+1
14 Y1=((2.*PI*I)/Y)
15 KL=0
16 WRITE(6,641 ) II
17 641 FORMAT(1H ,5X,3HI(=,I5)
18 Y2=((2.*PI*(I+1))/Y)
19 Y4=Y2-Y1
20 II=II-1
21 Y1=(2.*PI*DFLOAT(II))/Y
C
C USE THE FIRST FREQUENCY ESTIMATE.
22 X=Y1-[0.125]*((2.*PI)/Y)
23 19 KL=KL+1
C
C COMPUTE THE CONTRIBUTION OF THE FIRST FREQUENCY SAMPLE.
24 R77=(1./Y)*((DSIN(X*Y/2.))/(DSIN(X/2.)))
25 R72=0.0
26 KR=1
27 GO TO 20
C
C COMPUTE THE CONTRIBUTION BY THE REMAINING FIXED FREQUENCY SAMPLES.
28 10 KR=KR +1
29 20 X3=(PI*DFLOAT(KR))/Y
30 X4=(X/2.)-X3
31 X5=(X/2.)+X3
32 X6=Y*X4
33 X7=Y*X5
34 IF(KR.GT.(IZ-1)) GO TO 39
35 R70=(1./Y)*(DSIN(X6)/DSIN(X4))
36 R72=R70+R72
37 R70=(1./Y)*(DSIN(X7)/DSIN(X5))
38 R72=R72+R70
39 IF((KR+1).LE.IZ) GO TO 10
C
C COMPUTE THE CONTRIBUTION BY THE FIRST TRANSITION SAMPLE.
C

```

```

40 39 R73=(1./Y)*(DSIN(X6)/DSIN(X4))
41 R75=(1./Y)*(DSIN(X7)/DSIN(X5))
42 R7+=R75+R73
43 R72=R77+R72
44 WRITE(6,33) R72,R74
45 33 FORMAT(1H ,5X,4HR72=,D20.10,5X,4HR74=,D20.10)
46 R1(KL)=R72
47 R2(KL)=R74
48 X1(KL)=X
C
C USE THE SECOND FREQUENCY ESTIMATE.
C
49 IF(KL.EQ.1) X=X-1.499997205*(2.*PI/Y)
50 IF(KL.LT.LL) GO TO 19
51 WRITE(6,302) (X1(JL),JL=1,KL)
52 302 FORMAT(///,5X,2HX=,D20.10,5X,2HX=,D20.10)
53 I=1
C
C EQUATE THE RIPPLE VALUES.
C
54 6C R3(I)=R1(I+1)-R1(I)
55 R4(I)=R2(I)-R2(I+1)
56 WRITE(6,6) R3(I),R4(I)
57 6 FORMAT(//,5X,3HR3=,D20.10,5X,3HR4=,D20.10)
C
C COMPUTE THE TRANSITION SAMPLE VALUE
58 R8=R3(I)/R4(I)
59 WRITE(6,69)
60 69 FORMAT(1H ,5X,'UNKNOWN TRANSITION SAMPLE' )
61 WRITE(6,7) R8
62 7 FORMAT(//,5X,3HR8=,D20.10)
63 300 CONTINUE
64 STOP
65 END

```

```

5 JOB TIME=10,PAGES=10,NOSUBCHK,LIBLIST
C THIS PROGRAM USES THE DIRECT APPROACH TO FREQUENCY SAMPLING FILTER
C DESIGN PRESENTED IN CHAPTER THREE TO COMPUTE THE TRANSITION SAMPLE
C VALUES. THE FOLLOWING PARAMETERS ARE USED AS INPUT.
C LOW PASS FILTER DESIGN - TWO TRANSITION SAMPLES
C Y-ORDER OF THE FILTER.
C IZ-NUMBER OF PASS BAND FREQUENCY SAMPLES.
C M-TOTAL NUMBER OF DIFFERENT PASSBAND FREQUENCY SAMPLES.
1 IMPLICIT REAL*8(A-H,O-Z)
2 DIMENSION R1(3),R2(3),S(3),R3(2),R4(2,2),R5(2,2),R6(2,2),R7(2)
   L,R8(2),Z(2,2),EEMAT(2,2),IL(2),I4(2),A1(4),ILIST(40)
3 LL=3
4 N2=2
5 M=1
6 Y=32.
7 READ(5,600) (ILIST(I),I=1,4)
8 600 FORMAT(16I5)
9 DO 300 JJ=L,M
10 II=ILIST(JJ)
11 IZ=II
12 K3=II+2
13 PI=3.141592654
14 I=K3
15 Y1=((2.*PI*I)/Y)
16 KL=C
17 WRITE(6,641) II
18 641 FORMAT(1H,5X,3HII=,I5)
19 Y2=((2.*PI*(I+1))/Y)
20 Y4=Y2-Y1
C
C USE THE FIRST FREQUENCY ESTIMATE.
C
21 X=Y1+(2.*C)/16.00)*Y4
22 19 KL=KL+1
C
C COMPUTE THE CONTRIBUTION OF THE FIRST FREQUENCY SAMPLE.
C
23 R77=(1./Y)*((DSIN(X*Y/2.))/(DSIN(X/2.)))
24 R72=0.0
25 KR=1
26 GO TO 20
C
C COMPUTE THE CONTRIBUTION BY THE REMAINING FIXED FREQUENCY SAMPLES.
C
27 10 KR=KR +1
28 20 X3=(PI*DFLOAT(KR))/Y
29 X4=(X/2.)-X3
30 X5=(X/2.)+X3
31 X6=Y*X4
32 X7=Y*X5
33 S3=(PI*DFLOAT(KR+1))/Y
34 S4=(X/2.)-S3
35 S5=(X/2.)+S3
36 S6=Y*S4
37 S7=Y*S5
38 IF(KR.GT.(IZ-1)) GO TO 39
39 R70=(1./Y)*(DSIN(X6)/DSIN(X4))
40 R72=R70+R72
41 R70=(1./Y)*(DSIN(X7)/DSIN(X5))
42 R72=R72+R70

```

```

43      IF((KR+1).LE.12) GO TO 10
      C
      C      COMPUTE THE CONTRIBUTION BY THE FIRST TRANSITION SAMPLE.
      C
44      39      R73=(1./Y)*(DSIN(X6)/DSIN(X4))
45              R75=(1./Y)*(DSIN(X7)/DSIN(X5))
46              R74=R75+R73
47              R72=R77+R72
      C
      C      CONTRIBUTION BY THE SECOND TRANSITION SAMPLE.
      C
48              S76=(1./Y)*(DSIN(S6)/DSIN(S4))
49              S77=(1./Y)*(DSIN(S7)/DSIN(S5))
50              S78=S76+S77
51      WRITE(6,33) R72,R74,S78
52      33      FORMAT(1H ,5X,4HR72=,D20.10,5X,4HR74=,D20.10,5X,4HS78=,D20.10)
53              R1(KL)=R72
54              R2(KL)=R74
55              S(KL)=S78
56              X1(KL)=X
      C
      C      USE THE SECOND FREQUENCY ESTIMATE.
      C
57      IF(KL.EQ.1) X=X+(2.00*PI/Y)*0.50
      C
      C      USE THE THIRD FREQUENCY ESTIMATE.
      C
58      IF(KL.EQ.2) X=X+(2.00*PI/Y)*0.8125
59      IF(KL.LT.LL) GO TO 19
60      WRITE(6,32) (X1(JL),JL=1,KL)
61      302      FORMAT(///,5X,2HX=,D20.10,5X,2HX=,D20.10,5X,2HX=,D20.10)
62              I=1
      C
      C      EQUATE THE RIPPLE VALUES.
      C
63      60      R3(I)=-R1(I)-R1(I+1)
64              J=1
65              R4(I,J)=R2(I )+R2(I+1)
66              R4(I,J+1)=S(I)+S(I+1)
67              IF(I.EQ.(KL-1)) GO TO 103
68              I=I +1
69              GO TO 60
70      103      NN=KL-1
71              WRITE(6,64) (R3(I),I=1,NN)
72              WRITE(6,64)((R4(I,J),J=1,N2),I=1,NN)
73      64      FORMAT(1H ,4D20.10)
      C
      C      COMPUTE THE TRANSITION SAMPLE VALUES.
74      CALL TRANS(R4,R5,NN,N2)
75      WRITE(6,65)
76      65      FORMAT(///,5X,'TRANSPOSE')
77              WRITE(6,64) ((R5(I,J),J=1,NN),I=1,N2)
78      CALL MULT(R5,R4,R6,N2,NN,N2)
79      WRITE(6,66)
80      66      FORMAT(///,5X,'PRODUCT OF R4 AND TRANSPOSE')
81              WRITE(6,64) ((R6(I,J),J=1,N2),I=1,N2)
82              NR=N2*N2
83              CALL PACK(1,N2,NR,Z,R6)
84              CALL MINV(Z,N2,DET,IL,IM)
85              CALL PACK(2,N2,NR,Z,R6)

```



```
86      WRITE(6,67)
87 67    FORMAT(///,5X,'MATRIX INVERSE')
88      WRITE(6,64) ((R6(I,J),J=1,N2),I=1,N2)
89      CALL MULT(R5,R3,R7,N2,N2,1)
90      WRITE(6,64) (R7(I),I=1,N2)
91      CALL MULT(R6,R7,R3,N2,N2,1)
92      WRITE(6,69)
93 69    FORMAT(1H,5X,'UNKNOWN TRANSITION SAMPLE')
94      WRITE(6,64) (R6(I),I=1,N2)
95 300   CONTINUE
96 301   WRITE(6,303) X
97 303   FORMAT(1M,5X,2HX=,D20.10)
98      STOP
99      END
```

```

$JOB TIME=10,PAGES=10,NUSUBCK,K,LIBLIST
C
C THIS PROGRAM USES THE DIRECT APPROACH TO FREQUENCY SAMPLING FILTER
C DESIGN PRESENTED IN CHAPTER THREE TO COMPUTE THE TRANSITION SAMPLE
C VALUES. THE FOLLOWING PARAMETERS ARE USED AS INPUT.
C LOWPASS FILTER DESIGN - THREE TRANSITION SAMPLES
C Y=ORDER OF THE FILTER.
C IZ=NUMBER OF PASS-BAND FREQUENCY SAMPLES.
C M=TOTAL NUMBER OF DIFFERENT PASSBAND FREQUENCY SAMPLES.
1 IMPLICIT REAL*8(A--Z)
2 DIMENSION R1(4),R2(4),B(4),T(4),R3(3),R4(3,3),R5(3,3),R6(3,3),
  IR7(3),P6(3),Z(3,3),BFMAT(3,3),IL(3),IM(3),X1(5),ILIST(40)
3 LL=4
4 N2=3
5 Y=256.
6 M=1
7 INP=5
8 READ(INP,600) (ILIST(I),I=1,M)
9 600  FORMAT(10I5)
10 DO 300 JJ=1,M
11 II=ILIST(JJ)
12 IZ=II
13 K3=II+3
14 PI=3.141592654
15 I=K3
16 Y1=((2.*PI*I)/Y)
17 KL=0
18 WRITE(6,641) II
19 641  FORMAT(1H,5X,3HII=,I5)
20 Y2=((2.*PI*(I+1))/Y)
21 Y4=Y2-Y1
C
C USE THE FIRST FREQUENCY ESTIMATE.
C
22 X=Y1+(2.00/16.00)*Y4
23 19  KL=KL+1
C
C COMPUTE THE CONTRIBUTION OF THE FIRST FREQUENCY SAMPLE.
C
24 R77=(1./Y)*((DSIN(X*Y/2.))/(DSIN(X/2.)))
25 R72=0.0
26 KR=1
27 GO TO 20
C
C COMPUTE THE CONTRIBUTION BY THE REMAINING FIXED FREQUENCY SAMPLES.
28 10  KR=KR +1
29 20  X3=(PI*DFLOAT(KR))/Y
30 X4=(X/2.)-X3
31 X5=(X/2.)+X3
32 X6=Y*X4
33 X7=Y*X5
34 S3=(PI*DFLOAT(KR+1))/Y
35 S4=(X/2.)-S3
36 S5=(X/2.)+S3
37 S6=Y*S4
38 S7=Y*S5
39 Q3=(PI*DFLOAT(KR+2))/Y
40 Q4=(X/2.00)-Q3
41 Q5=(X/2.00)+Q3

```

```

42      Q6=Y*Q4
43      Q7=Y*Q5
44      IF(KR.LT.(I2-1)) GO TO 39
45      R70=(1./Y)*(DSIN(X6)/DSIN(X4))
46      R72=R70+R72
47      R70=(1./Y)*(DSIN(X7)/DSIN(X5))
48      R72=R72+R70
49      IF((KR+1).LE.I2) GO TO 10
      C
      C
      C
50 39    R73=(1./Y)*(DSIN(X6)/DSIN(X4))
51      R75=(1./Y)*(DSIN(X7)/DSIN(X5))
52      R74=R75+R73
53      R72=R72+R74
      C
      C
      C
54      S76=(1./Y)*(DSIN(S6)/DSIN(S4))
55      S77=(1./Y)*(DSIN(S7)/DSIN(S5))
56      S78=S76+S77
      C
      C
      C
57      Q73=(1.00/Y)*(DSIN(Q6)/DSIN(Q4))
58      Q75=(1.00/Y)*(DSIN(Q7)/DSIN(Q5))
59      Q74=Q75+Q73
60      WRITE(6,33) R72,R74,S78,Q74
61 33    FORMAT(1F,5X,4HR72=,D20.10,5X,4HR74=,D20.10,5X,4HS78=,D20.10,5X,
14HQ74=,D20.10)
62      R1(KL)=R72
63      R2(KL)=R74
64      S(KL)=S78
65      T(KL)=Q74
66      X1(KL)=X
      C
      C
      C
67      IF(KL.EQ.1) X=X+(2.00*PI/Y)*0.43750003500
      C
      C
      C
68      IF(KL.EQ.2) X=X+(2.00*PI/Y)*2.0000000200
      C
      C
      C
69      IF(KL.EQ.3) X=X+(2.00*PI/Y)*0.937499997200
70      IF(KL.LT.LL) GO TO 19
71      WRITE(6,302) (X1(JL),JL=1,KL)
72 302   FORMAT(///,5X,2HX=,D20.10,5X,2HX=,D20.10,5X,2HX=,D20.10,5X,2HX=,
1D20.10)
73      I=1
      C
      C
      C
74 60    R3(I)=-R1(I)-R1(I+1)
75      J=1
76      R4(I,J)=R2(I)+R2(I+1)
77      R4(I,J+1)=S(I)+S(I+1)
78      R4(I,J+2)=T(I)+T(I+1)

```

```

79      IF(I.EQ.(NL-1)) GO TO 103
80      I=I+1
81      GO TO 90
82      103  NN=NL-1
83      WRITE(6,64) (R3(I),I=1,NN)
84      WRITE(6,64) ((C4(I,J),J=1,N2),I=1,NN)
85      64   FORMAT(1H ,4D20.10)
      C
      C   COMPUTE THE TRANSITION SAMPLE VALUES.
      C
86      CALL TRANS(R4,R5,N1,N2)
87      WRITE(6,65)
88      65   FORMAT(///,5X,'TRANSPOSE')
89      WRITE(6,64) ((R5(I,J),J=1,NN),I=1,N2)
90      CALL MULT(R5,R4,R6,N2,NN,N2)
91      WRITE(6,65)
92      66   FORMAT(///,5X,'PRODUCT OF P4 AND TRANSPOSE')
93      WRITE(6,64) ((R6(I,J),J=1,N2),I=1,N2)
94      NR=N2*N2
95      CALL PACK(1,N2,NR,Z,R6)
96      CALL MINV(Z,N2,DET,(L,I4))
97      CALL PACK(2,N2,NR,Z,R6)
98      WRITE(6,67)
99      67   FORMAT(///,5X,'MATRIX INVERSE')
100     WRITE(6,64) ((R6(I,J),J=1,N2),I=1,N2)
101     CALL MULT(R5,R3,R7,N2,NN,1)
102     WRITE(6,64) (R7(I),I=1,N2)
103     CALL MULT(R6,R7,R8,N2,N2,1)
104     WRITE(6,69)
105     69   FORMAT(1H ,5X,'UNKNOWN TRANSITION SAMPLE' )
106     WRITE(6,64) (R8(I),I=1,N2)
107     300  CONTINUE
108     301  WRITE(6,303) X
109     303  FORMAT(1H ,5X,2HX=.D20.10)
110     STOP
111     END

```

VITA 2

B. N. Sureshbabu

Candidate for the Degree of
Doctor of Philosophy

Thesis: A DIRECT APPROACH TO FREQUENCY SAMPLING FILTER DESIGN

Major Field: Electrical Engineering

Biographical:

Personal: Born in Bangalore, India, December 29, 1949, the son of Mr. and Mrs. B. S. Narayanadas.

Education: Received the high school diploma from Government High School for boys, Bangalore, India, in March, 1963; received the Bachelor of Engineering degree in Electrical Engineering from Bangalore University, 1970; received the Master of Engineering from Bangalore University, 1972, with a major in Electrical Engineering; completed requirements for the Doctor of Philosophy degree at Oklahoma State University with a major in Electrical Engineering, May, 1978.

Professional Experience: Development Engineer, motor factory, research and development, N.G.E.F. Ltd., Bangalore, India, from December, 1971, to August, 1974; teaching assistant, School of Electrical Engineering, Oklahoma State University, 1975-1977; Electrical Engineer/Scientist, Collins Radio, Richardson, Texas, summer, 1975.

Professional Organizations: Student Member of Institute of Electrical and Electronic Engineers.